SAPHYRE

Contract No. FP7-ICT-248001

Adaptive and Robust Signal Processing in Multi-User and Multi-Cellular Environments (initial)

D3.1a

Contractual date:	M12
Actual date:	M13
Authors:	Martin Haardt, Zuleita Ka Ming Ho, Eduard Jorswieck, Eleftherios Karipidis, Jacek Kibilda, Jianhui Li, Johannes Lindblom, Christian Scheunert, Jan Sýkora, David Gesbert, Erik G. Larsson, Jianshu Zhang
Participants:	TUD, CTU, ECM, LiU, TUIL, WRC
Work package:	WP3
Security:	Public
Nature:	Report
Version:	1.0
Number of pages:	125

Keywords

Spectrum Sharing, Infrastructure Sharing, SAPHYRE Gain, Interference Channel, Relay.

Executive Summary

This document describes the signal processing techniques being developed within the Task 3.1. New physical layer techniques have been designed for resource sharing schemes to further improve the spectral efficiency, enhance the coverage, increase the user satisfaction and lead to an increased revenue for operators as well as decreased capital and operating expenditures. Four reference scenarios are first defined, of which the Topology A (interference channel, spectrum sharing among multiple operators) and Topology C (interference relay channel and two-way relaying, both spectrum and infrastructure sharing among multiple operators) are investigated in more detail within this deliverable. Concerning the interference channel, different cases are studied, including the achievable rate region developed for the generalized K-user multiple input single output (MISO) interference channel, the interference alignment precoding techniques for sum rate optimization in the multiple input multiple output (MIMO) interference channels and the distributed beamforming algorithm for the two-user multiple input single output (MISO) interference channel that is approximately Pareto-optimal. For schemes assisted via amplify and forward MIMO relays, two categories are presented. On one side, linear precoding algorithms for sum rate maximization and the resource allocation for mean square error minimization in the (uni-directional) interference relay channel are studied. On the other side, sub-optimal relaying strategies are developed for the multiple input multiple output (MIMO) two-way relaying channels. Furthermore, the required information information exchange is also addressed. Moreover, we demonstrate for each scenario the sharing gain or SAPHYRE gain, which is defined as the system rate of the simultaneous sharing scenario compared to the time-shared use of the spectrum and infrastructure by the operators (time division case, in this case, the operators and users are multiplexed in the time domain).

Contents

Notation

Abbreviations

AF	amplify and forward
ANOMAX	algebraic norm maximization
AQM	Active Queue Management
BD	block diagonalization
BS	base station
CBS	Commit Burst Size
CIR	Commit Information Rate
CoZF	coordinated zero-forcing
CSI	channel state information
DCM	dual channel matching
DFT	discrete Fourier transform
EBS	Excessive Burst Size
EIR	Excessive Information Rate
EVC	Ethernet Virtual Circuit
FlexCoBF	flexible coordinated beamforming
IC	interference channel
ICIC	Inter-Cell Interference Coordination
IETF	Internet Engineering Task Force
IRC	interference relay channel
LTE	Long Term Evolution
MIMO	multiple input multiple output
MISO	multiple input single output
MMSE	minimum mean square error
MR	maximum ratio
MRC	maximum ratio combing
NBS	Nash bargaining solution
NE	Nash equilibrium
P2P	point to point
PIR	Peak Information Rate
PO	Pareto optimal
QoS	Quality of Service
RBD	regularized block diagonalization
RC	relay channel
RED	Random Early Detection
SINR	signal-to-interference-plus-noise ratio

SLA	Service Level Agreement
SNR	signal-to-noise ratio
SR	sum rate
srTCM	single rate Three Color Marker
SVD	singular value decomposition
TCP	Transmission Control Protocol
TDMA	time division multiple access
trTCM	dual rate Three Color Marker
TSW2CM	Time Sliding Window Two Color Marker
TSW3CM	Time Sliding Window Three Color Marker
TWR	two-way relaying
UT	user terminal
VLAN	Virtual LAN
ZF	zero forcing

Mathematical Notation

$\mathbb{C}$	set of complex numbers
$\mathbb{R}$	set of real numbers
$\mathbb{Z}$	set of integers
$\mathcal{CN}$	complex normal distribution
$\mathrm{tr}\{\cdot\}$	trace of a matrix
$\mathrm{rank}\{\cdot\}$	rank of a matrix
$\mathcal{R}\{\cdot\}$	range (span) of a matrix
$\mathcal{N}\{\cdot\}$	nullspace of a matrix
$\mathbf{\Pi_Z}$	orthogonal projection onto the range of $\mathbf{Z}$
$\mathbf{\Pi_Z^\perp}$	orthogonal projection onto the orthogonal complement of the range of $\mathbf{Z}$
$\mathbf{I}$	identity matrix
$\mathbb{E}\{\cdot\}$	expectation operator

1 Introduction

In current wireless communication systems, the radio spectrum and the infrastructure are typically used such that interference is avoided by exclusive allocation of frequency bands and employment of base stations. SAPHYRE will demonstrate how equal-priority resource sharing in wireless networks improves the spectral efficiency, enhances coverage, increases user satisfaction, leads to increased revenue for operators, and decreases capital and operating expenditures.

The physical resources which are shared can be divided into two classes, namely spectrum and infrastructure. These are shared with respect to a set of 'players', consisting of operators and users. Each player has a set of private information, e.g., operators have their business models and their revenue strategies, users have their private interests and their partly private state information including traffic, mobility, channel parameters. These goals and parameters are usually not revealed to others.

The spectrum sharing is performed with respect to a set of constraints. These constraints are divided into two areas, namely regulatory and environmental constraints. They can partly overlap as in the case of spectrum masks and power constraints which are both regulatory and environmental. The main difference between these two areas is that regulatory constraints contain fairness and social welfare or legal issues whereas environmental constraints contain fundamental limitations imposed by physics.

The resource sharing problems are interdisciplinary and require regulatory and political bodies, business and market experts, and technical input from communication and network engineers. The ongoing discussion about spectrum commons is led mainly from a regulatory and market point of view. However, advances in communication systems (e.g., multi-antenna systems, multi-carrier transmission techniques, adaptive receivers, software defined radio, interference cancellation) are recognized already to have a very strong impact since they enable the efficient and concurrent use of spectrum.

From a communications engineering point of view, different types of orthogonality in frequency, time, space of coding domain have been used for resource allocation depending on the type of interference: For users in one cell operated by one operator (intracell interference) TDMA combined with FDMA (used in GSM systems) or CDMA (combined with TDMA/FDMA in 3G systems) is applied to separate their signals at the receivers. For different sectors or cells, the intercell interference is controlled by applying different frequency reuse factors [1]. Fractional and adaptive

frequency reuse is discussed in LTE and WiMAX [2]. Very recently, techniques for separating transmissions from different operators (inter-operator interference) without orthogonal resource allocation have been developed: First flexible resource sharing approaches have been developed and results indicate that the overall efficiency of the system can be improved by sharing different resources in the network between several operators [3, 4]. Sharing of spectrum or infrastructure ends up in creating interference on the physical layer. Therefore, interest in physical and MAC layer optimization for resource sharing has increased recently.

This report deals with the design and performance analysis of adaptive and robust signal processing algorithms to exploit the additional degrees of freedom in multi-user and multi-cellular environments. Furthermore, it is important to:

- define a performance metric,
- show the gain (loss) with respect to the chosen performance metric as compared to a non-sharing scenario,
- point out conditions when a significant gain can be achieved for the chosen scenario (topology), and
- illustrate the order of magnitude of this gain.

This sharing gain, namely the SAPHYRE gain, can be defined as the performance comparison in terms of various performance metrics (e.g., the system sum-rate, the achievable rate region, etc.). In this deliverable, we define two types of SAPHYRE gains in terms of system rate of the simultaneous sharing scenario compared to the time-shared use of the spectrum and infrastructure by the operators (time division case, in this case, the operators and users are multiplexed in the time domain). The absolute SAPHYRE gain is defined as

$$\Xi_{\mathrm{A}} = \sum_{k=1}^{K} U_k - \frac{1}{K} \sum_{k=1}^{K} U_k^{\mathrm{SU}}, \tag{1.1}$$

and the fractional SAPHYRE gain is defined as

$$\Xi_{\mathrm{F}} = \frac{\sum_{k=1}^{K} U_k}{\frac{1}{K} \sum_{k=1}^{K} U_k^{\mathrm{SU}}}, \tag{1.2}$$

where $k \in \{1, 2, \cdots, K\}$ is the index of the users. The utility function of the kth user in the sharing scenario and the time division case are denoted by U_k and U_k^{SU}, respectively.

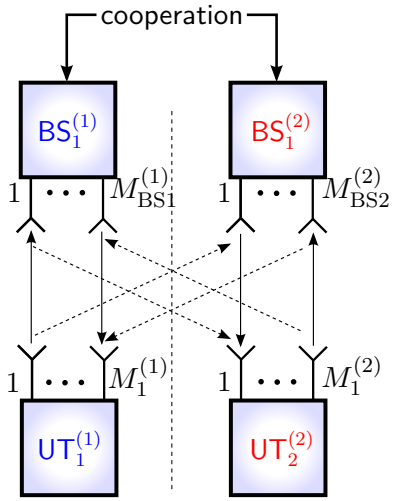

Figure 1.1: Topology A: Spectrum sharing, no infrastructure sharing.

1.1 Reference Scenarios

Within SAPYHRE it is important to have unified reference scenarios for a comparative analysis of the system performance by the various developed solutions and algorithms. The scenarios/topologies developed and applied in this work package are described in the following.

Topology A. Figure 1.1 shows the first topology that is investigated in WP3. Different operators share the same spectrum. BSs and UTs have single or multiple antennas. There is cooperation between BSs. Physical layer techniques for this topologies are described in Chapters 3 and 4.

Topology B. Figure 1.2 shows another topology for WP3. The UTs belonging to different operators share the BS. They could use the same spectrum or different frequencies.

Topology C. Figure 1.3 demonstrates the generic topology with a relay. The spectrum and relay are shared between entities (e.g., UTs, BSs) of different operators. The particular sets of this topology with specific variants/parameterizations are investigated in Chapter 5.

Topology D. Figure 1.4 shows a topology where the BS and the relay are shared between multiple operators.

For further details, please refer to the SAPYHRE deliverable D3.3a.

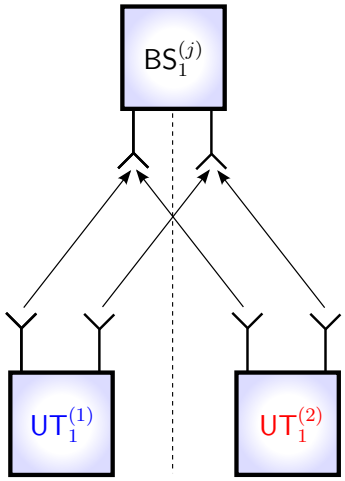

Figure 1.2: Topology B: Infrastructure sharing.

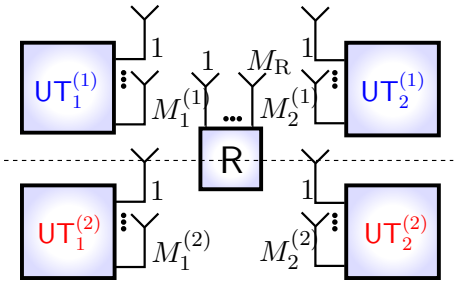

Figure 1.3: Topology C: Spectrum and infrastructure (relay) sharing.

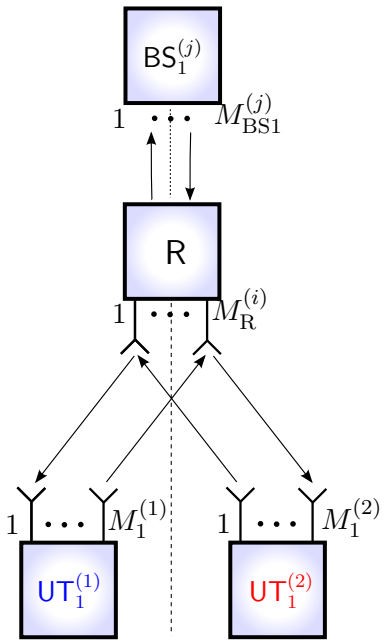

Figure 1.4: Topology D: Infrastructure sharing.

1.2 Structure of This Report

This report can be categorized into three parts. In the first part, the information exchange requirements for the algorithms developed in this work package are described. In the second part, physical layer techniques in interference channel (Topology A) are demonstrated. In the third part, transmission techniques for relay-assisted communications (Topology C) are presented.

First Part (Chapter 2)

Chapter 2 introduces the information exchange requirements for the algorithms that are described in this deliverable. Furthermore, as an example of an inter-operator exchange medium, it analyzes the performance of an inter-operator shared backhaul link.

Second Part (Chapter 3, 4)

Section 3.2 develops the achievable rate region for the K-User multiple-input single-output (MISO) interference channel (IC) where each BS has multiple antennas and each user has a single receive antenna.

Section 3.3 reviews parallels with existing work on the multiple-input multiple-output (MIMO) IC, including rate-optimizing and interference-alignment precoding techniques, showing how such techniques may be improved or re-interpreted through a common prism based on balancing egoistic and altruistic beamforming.

Chapter 4 proposes a distributed beamforming algorithm for the two-user MISO IC. It enables cooperation among the transmitters in order to increase both users' rates by lowering the overall interference. The outcome of the proposed algorithm is approximately Pareto-optimal.

Third Part (Chapter 5)

Section 5.2.1 studies the single-stream transmission in the interference relay channel. Two independent transceiver pairs with multiple antennas communicate with the assistance of one relay, which operates in half-duplex mode and employs an amplify-and-forward strategy. First, the interference relay channel is converted to the conventional interference channel via a preliminarily determined relay amplification matrix. Then, the flexible coordinated beamforming for the interference relay channel (IRC FlexCoBF) is proposed for the transceivers. Simulation results show that by sharing a relay between two transceiver pairs a significant gain in sum rate can be achieved compared to the relay channel.

Section 5.2.2 investigates the issue of resource allocation for MSE minimization in a DS/CDMA relay-assisted interference channel. The resource allocation process is assumed to take place in a hierarchical way. First, the relay announces his amplify-and-forward matrix, and then the multiple access users non-cooperatively react to the relay's choice. From a game-theoretic point of view, this process is well-modeled as a two-level Stackelberg game, with the relay as the leader, and the multiple access users as followers. First, the best response dynamics and the Nash Equilibria for the non-cooperative game played by the followers are derived for a given relay matrix. Then, the problem of optimum relay matrix design is dealt with. Finally, numerical results corroborating the theoretical results are provided, showing the merits of the proposed resource allocation techniques.

Section 5.3.1 presents a relay-assisted resource sharing scenario in which multiple communication partners (belonging to different operators) use one relay (possibly owned by another operator / virtual operator) to bidirectionally exchange information using the same spectrum. The relay has multiple antennas and operates in half-duplex mode. Sub-optimal algorithms for computing the relay amplification matrix at the relay as well as transmit and receive beamforming matrices at the UTs are proposed.

Section 5.3.2 studies the AF relaying strategy for MIMO two-way channels with multiple relays. The section presents one approach to compare recently proposed AF strategies with optimal node precoding under a fair average relay power constraint. When a single relay is used, the fixed AF strategy using a discrete Fourier transform (DFT) matrix performs reasonable well. However, with multiple relays the channel aware dual channel matching (DCM) outperforms DFT significantly. Multiple relays improve the sum rate performance and reduce the impact of the transmit strategies at the nodes.

2 Information Exchange Mechanisms Between Operators

2.1 Introduction

As a basis for this work, information exchange mechanisms between operators will be defined and taken into account in the novel signal processing algorithms. In particular, the amount and the format of this information exchange have to be specified. Moreover, the trade-off between the required overhead and the potential performance benefits will also be investigated for each scheme. These information exchange mechanisms might be assisted by suitable real-time spectrum analysis schemes at the base stations as well as the mobile terminals.

For the defined resource sharing topologies, each operator should be aware of

- the existence of other operators,
- their resources (spectrum, infrastructure) together with their conditions on sharing them (willingness, cost, and return), their features (number of antennas, elevation, coverage, power), their current status (traffic load), and
- their currently active users and demands (offered traffic, required QoS).

We need to classify

- how to formally define this type of information
- how to detect and distribute it in the final network
- how to agree on what should be shared (centralized/distributed).

In the following, the information exchange requirements of the algorithms that are developed in this deliverable will be presented.

2.2 Information Exchange Requirements

In Section 3.2, for the K-user MISO interference channel, and in Section 3.3 dealing with the MIMO interference channel, the transmitter antenna arrays are assumed to have perfect local channel state information. Transmitter i is assumed to know the channel from itself to all receivers (intended as well as unintended) perfectly. Furthermore, for this characterization, the operating point is determined cooperatively by all participating operators. Both assumptions are unrealistic in reality. However,

the results serve as an upper bound on the achievable SAPHYRE gain. More realistic CSI models and distributed bargaining algorithms are currently under investigation and will be reported in upcoming deliverables. Note that in order to achieve specific points on the rate region (practical algorithm design) additional feedback is typically required at each iteration between the receivers and the transmitters. This can be done implicitely through the use of pilot signals transmittedover the uplink channel.

In Chapter 4 an algorithm is proposed to distributively, but cooperatively, design the beamforming vectors of two multi-antenna base stations belonging to different operators and transmitting towards separate receivers. The main assumptions are that:

- the transmitted signals are received in synchronization

- there are feedback channels from both receivers to both transmitters.

Each transmitter has local channel state information (CSI), i.e. channel knowledge only of the direct link to its intended receiver and the crosstalk link to the other receiver. The feedback channels are initially used to provide CSI and in the sequel information about the algorithm evolution. The proposed algorithm can be equally used when the transmitters have either instantaneous CSI (i.e., perfect knowledge of the channel vectors) or statistical CSI (i.e., knowledge of the channel distributions). For synchronization and channel estimation to be possible, it is implicit that the pilot sequences of each operator are known to the other. No other information is exchanged between the operators; in particular there is no need to share the data streams. In every iteration of the proposed beamforming algorithm, the receivers measure the SINR and feed back one bit to inform both transmitters whether the strategies they used yield higher SINR, hence rate, as compared to the previous iteration. The feedback information is limited to a few bits (equal to the number of iterations) per coherent interval, but it is assumed to be received error-free and essentially without delay.

In Section 5.2.2, it is assumed for the relay-assisted interference channel that the transmitters know their own channel to the relay perfectly. In addition, the relay strategy (the amplify and forward relay matrix) is known perfectly, too. The transmitters do not cooperate but decide selfishly maximizing their own utility.

For the proposed transmit strategies for the multi-operator two-way relay channel in Section 5.3.1 and the relay-assisted interference channel in Section 5.2.1, the AF relays are highly preferable because they significantly reduce the delay and the complexity. Moreover, since each operator does not need to know the modulation and coding schemes of the other operators, they do not need to share their data which leads to more independences to the operators. Furthermore, since the relay can even belong to a third-party, this kind of relay sharing will not harm the competitiveness of operators.

2.3 Analytical Model of a Shared Backhaul Link

One of the possibilities to exchange information between the operators in the Reference Topology A and possibly also Reference Topology B (however not effectively) is to use backhaul links. LTE system architecture specifies backhaul link as a concatenation of two logical connections (X2 and S1), were X2 is used to inter-connect base stations and S1 to provide connectivity between Access Network and Core Network (as presented in Figure 2.1). In particular, X2 interface has been designed as a mechanism to support the exchange of side information between the base stations (e.g. ICIC is realized via X2), however if required also S1 interface can provide additional signaling related to resource sharing operation[1]. From the perspective of SAPHYRE, the most interesting case occurs when the backhaul link is shared between the multiple operators. Accordingly the following section provides an analytical model that is used to evaluate the performance of a shared backhaul link. The performance is analyzed in terms of potential rates available to the operators sharing backhaul (with respect to guaranteed QoS) and fairness in the backhaul resource distribution. Eventually the analysis gives an idea on how to specify information exchange mechanisms so that they fit the transportation capabilities of backhaul links. The presented solution concentrates on the last step of QoS provisioning mechanism (described in [5]) and more meaningfully on inter-operator rate limitation and allocation.

2.3.1 State of the Art Rate Limiting Algorithms

The most common state of the art solutions for rate limitation include a superposition of two mechanisms marker and dropper [6]. The marker is typically realized as either dual token bucket (dual token bucket provides a lower and upper limitation for the incoming traffic) or rate estimator algorithm. Whereas packet dropping is realized as AQM (Active Queue Management). There are a number of dual token bucket algorithms used for rate limitation, where the most acknowledged (standardized by IETF) are: srTCM (single rate Three Color Marking) [7] and trTCM (three Rate Color Marking) [8]. The color marking dual token bucket algorithm comprises of two buffers which collect tokens (an abstract beings used to represent bytes of transmitted data). Each of the buckets is filled with a constant rate of arriving tokens, whenever an incoming packet enters the marker and there are tokens in the bucket the packet is color-marked, and number of tokens in the bucket is decreased by a relative packet size. The first bucket constitutes for the traffic that is below or equal to the minimum guaranteed rate, whereas the second bucket provides excessive rate. Packets are marked with three colors: green (packet below or equal to minimum guaranteed rate), yellow (packet in the excessive rate) and red (packet above maximum excessive rate). The main difference between srTCM and trTCM

[1] More information on the LTE shared backhaul link architecture can be found in [5]

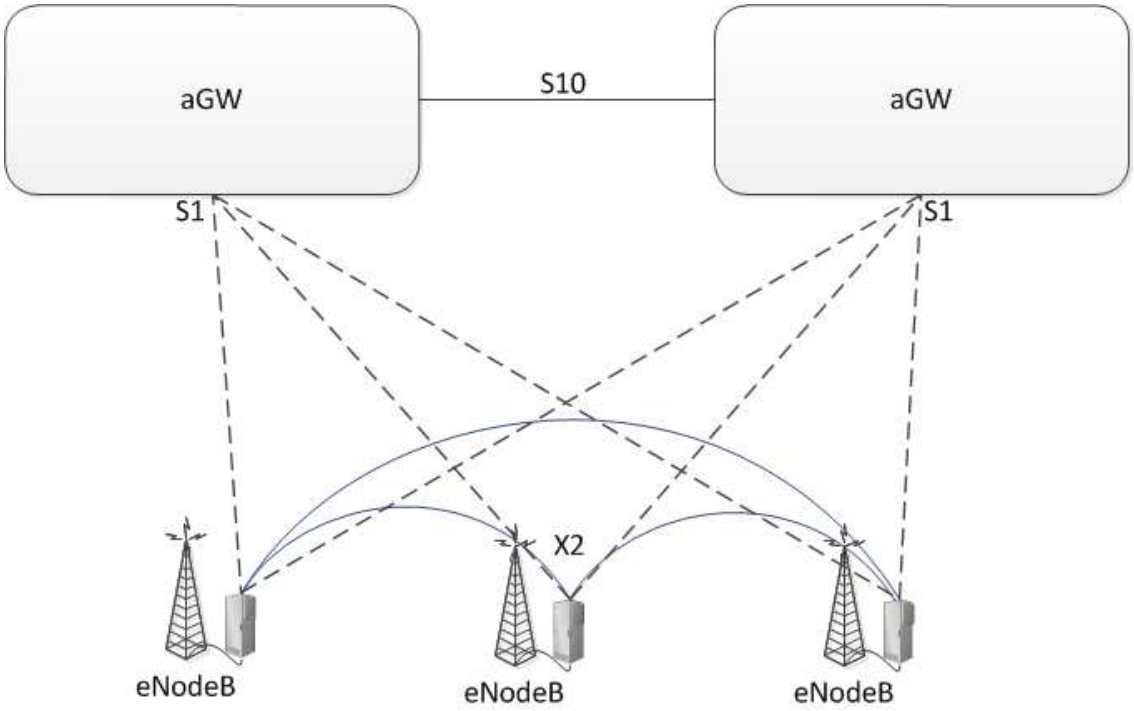

Figure 2.1: Flat architecture backhaul connectivity with inter-eNodeB communication.

is that, in the first solution buckets are filled sequentially (when the first bucket is full, the second is filled) and in trTCM both buckets are filled at the same time but they maintain different rates to support guaranteed and excessive rates. Other token bucket possibilities for rate limitation are Dynamic Token Bucket [9] and Adaptive Token Bucket [10], which however do not guarantee minimum throughput. Alternative to dual token bucket algorithms are rate estimation algorithms (TSW2CM and TSW3CM [11]). The rate estimation is based on the size of the received packet, the inter-arrival times between consecutive packets and the history of rate estimation over time window. When the average rate is equal or below the minimum threshold the packets are admitted as green, yellow if the rate is between minimum and excessive thresholds and red when the incoming packets rate is above excessive threshold. The typical problems of sliding window rate estimators are the window size and fairness in resource distribution. The marked packets are subject to AQM schemes, where the most typical solutions are based on RED (Random Early Detection) [12, 13, 14, 15]. In general RED scheme adds a dropping probability to each of the arriving packets, where the probability is dependent on the traffic class, operator or the current link congestion. In the rate limitation mechanism, different dropping probabilities are assigned to different traffic colors. Immanent advantage of rate limitation with color marking and active queue management is that it is easy to adapt differentiated charging rates based on the coloring of the traffic. Contradictive approach that combines marker and dropper mechanisms is

token bank algorithm, which directly uses bucket filling rates to schedule packets to the link, without color provisioning. This type of token bucket algorithms provide good fairness control capabilities as well as minimum rate guarantees. Different modifications of the token bank algorithm have been presented in [16, 17, 18]. The principle of token bank algorithm is to create common pool of resources that can be shared between different flows. This is realized via token bank that is filled with ratio corresponding to either whole link capacity or the part of the capacity which is shared. The tokens from the bank are borrowed by dedicated token buckets (per each flow) in the case that the dedicated are empty or the level of tokens has fallen below specific threshold (the dedicated token bucket is filled with minimum guaranteed rate). The token bank can pose a limitation on the number of tokens that can be borrowed by each flow, if the token bank is filled whenever the dedicated token buckets are overflowing with tokens (overflowing tokens are not discarded but returned to common pool of resources) [19]. Eventually with token bank algorithm the incoming traffic is assigned the required rate whenever it is equal or below guaranteed rate or there are still tokens in the shared pool of resources and the flow has not yet reached its minimum available number of borrowed tokens.

In the state of the art research, analytical models have been presented for dual token bucket algorithms with queue management [6] and dynamic token bucket approach [20]. The analytical descriptions for token bank algorithm presented in [16, 17, 18] are lacking the genericity and achievable throughput analysis in traffic conditions different than high load situation. The analysis of the token bucket class of algorithms is performed in terms of queuing system representation. The queues are described as deterministic or Poisson arrival process with finite number of users in the system. The analysis presented in this document will use similar notation to describe Saphyre shared backhaul token bank algorithm in terms of blocking probability and achievable rates in the presence of multiple operators sharing backhaul link of limited capacity.

2.3.2 SAPHYRE Shared Backhaul Analytical Model

The analyzed model is derived from Modified Token Bank Fair Queuing mechanism [17], which on contrary to classical Token Bank Fair Queuing [16] algorithm assumes that there is no threshold on possible number of borrowed tokens as well as the tokens are not returned to the token bank (token bank has its own filling rate). The method grants link capacity to the operators through the tokens generated in both dedicated buckets and token bank (D and TB). Where the D bucket is used to limit operator's flow traffic to the minimum guaranteed rate (and therefore it is filled with rate $R_{min,k}$) and the TB is used to provide maximum excessive rate whenever tokens are available. TB is filled with the rate corresponding to the available link capacity $C - \sum_k R_{min,k}$. Tokens that are overflowing both buckets are treated as unnecessary and are being discarded. The resource extension occurs whenever D if filled below certain threshold level, then D is additionally re-filled

with the tokens coming from the token bank. The excessive filling rate is equal to the difference between maximum excessive rate (EIR) and minimum guaranteed rate (CIR), $R_{max,k} - R_{min,k}$. Whenever new packet arrives and the dedicated bucket and the token bank are empty, the incoming packet is either blocked or dropped. Once D fills up to the threshold level, the tokens are no longer borrowed from the token bank. Using token bank class of rate limitation algorithms, both minimum and maximum rate can be supported, with respect to high utilization of the available link capacity.

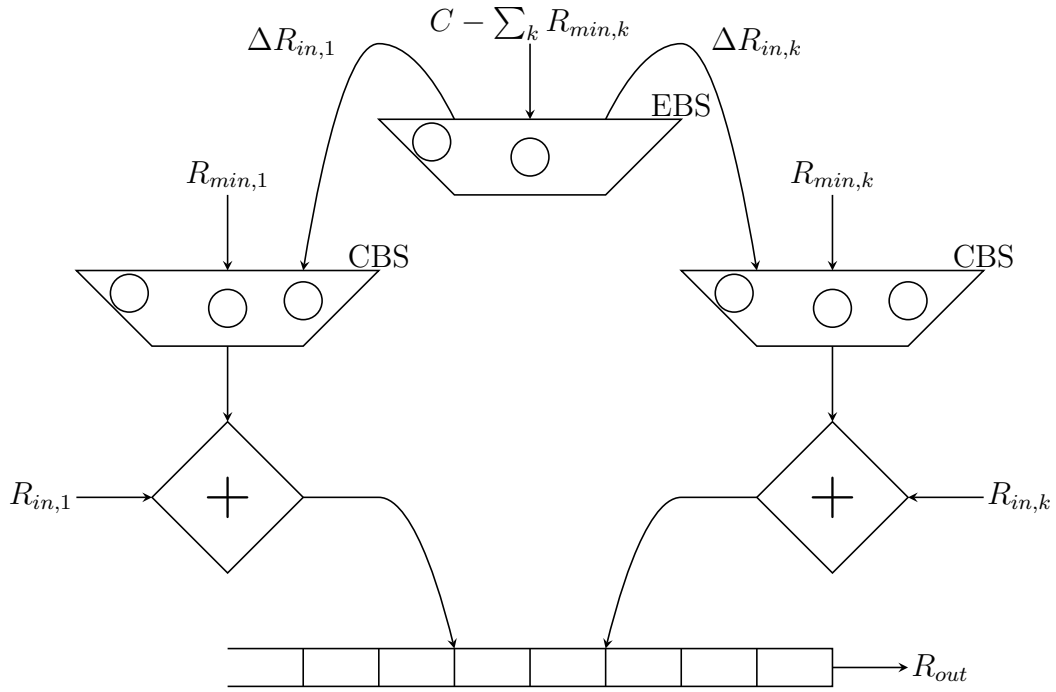

Figure 2.2: Abstraction of Token Bank Fair Queuing algorithm.

Let us consider now the relation between the proposed method and achievable rates by the operators. New packet from one of the operators arrives to the SAPHYRE backhaul scheduler with the rate $R_{in,k}$. The backhaul link capacity is C, the minimum guaranteed rate at the backhaul for this operator is $R_{min,k}$ and the maximum excessive rate is $R_{max,k}$[2]. Depending on the incoming rate from the operator, below dependencies shall hold true:

[2]The presented values shall comply with Ethernet Class of Service description, where $R_{min,k}$ = CIR, $R_{max,k}$ = EIR, T_D = EBS.

$$R_{out,k} = \begin{cases} R_{in,k}, \text{ if } \quad R_{in,k} \in < 0; R_{min,k}) \\ R_{min,k}, \text{ if } \quad R_{in,k} = R_{min,k} \\ R_{min,k}, \text{ if } \quad \{R_{in,k} \in (R_{min,k}, \infty) : (C - R_{min,k} - \sum_{i=1, i\neq k}^{n-1} R_{in,i} \leq 0)\} \\ R_{in,k}, \text{ if } \quad \{R_{in} \in (R_{min}; R_{max}) : (C - R_{min,k} - \sum_{i=1, i\neq k}^{n-1} R_{in,i} > 0)\} \\ R_{max}, \text{ if } \quad \{R_{in} \geq R_{max} : \cap (C - R_{max,k} - \sum_{i=1, i\neq k}^{n-1} R_{in,i} > 0)\} \end{cases} \tag{2.1}$$

From the above relations we can conclude that in order to provide guaranteed rates, SLA agreements shall be designed subject to the following constraints:

$$\begin{aligned} \text{1) For each } k \quad & R_{min,k} \leq R_{max,k} \\ \text{2) For each } k \quad & R_{max,k} \leq C \\ \text{3) } & \sum_k R_{min,k} \leq C \end{aligned} \tag{2.2}$$

The last constraint is strictly related to QoS provisioning at the backhaul and management of SLA classes of services. In case of violation of the constraint (e.g. due to physical failures of the link) the minimum guaranteed rate for the operators may be reachable only during low traffic periods, or it may not be reachable at all. The exact effect depends on the type of rate limitation algorithm.

Taking into consideration all the above mentioned constraints and relations, the token bank algorithms works as follows (where ΔT_D and ΔT_{TB} are bucket depths):

1. Whenever new packet arrives from operator A, it is checked with the dedicated token bucket (D) for operator A, whether it can be admitted to the backhaul. If $packet\_length \leq \Delta T_D$ traffic is scheduled to the link. Additionally number of tokens in D is decreased. In case D is empty the incoming packet is either discarded or blocked.
2. If after the first step there are not enough tokens in D for operator A (number of tokens is below threshold), the filling ratio of the bucket is increased by $\Delta R_k = R_{max,k} - R_{min,k}$. The rate is excessed, only if there are tokens available in the token bank T_{TB}.
3. The filling rate of D is returned to minimum level ($R_{min,k}$), when the number of tokens in D is above the threshold level or TB is empty.

In general token bucket class of algorithms can be described as a queuing system with finite buffer state [6]. Where the queue size is represented with bucket depth (T_D and T_{TB}). Mean arrival rate is equal to the bucket filling rate ($R_{min,k}$ and $C - \sum_k R_{min,k}$) and mean service rate is the rate of input ($R_{in,k}$) traffic subject to marking. According to the results achieved in [6] there are two possible queue models to represent the token bucket class algorithms: M/M/1/K with Poisson process

of arrivals and D/M/1/K with deterministic process of arrivals. For the trTCM algorithm which resembles the proposed algorithm with the rate duality, both models has been proven to be similarly accurate when modelling TCP traffic. This is in fact surprising as by definition the representation of a token bucket with deterministic filling rates shall follow D/M/1/K system behavior. However assumption on M/M/1/K queue type highly simplifies the analysis of the model, due to that the algorithm for SAPHYRE backhaul sharing has been analyzed as M/M/1/K system with queues that are initially fully occupied. Two important assumptions need to be carried in order to simplify the calculations, 1) the incoming traffic has always the same packet size and tokens represent incoming packets rather number of bytes, 2) the minimum occupation (threshold) of the dedicated token bucket is equal to zero, which means that whenever dedicated token bucket is empty it is filled with rate of $R_{max,k}$.

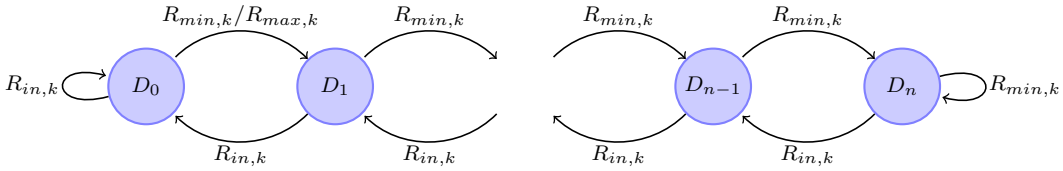

Figure 2.3: Dedicated token bucket as Markov process of finite states space (n =CBS).

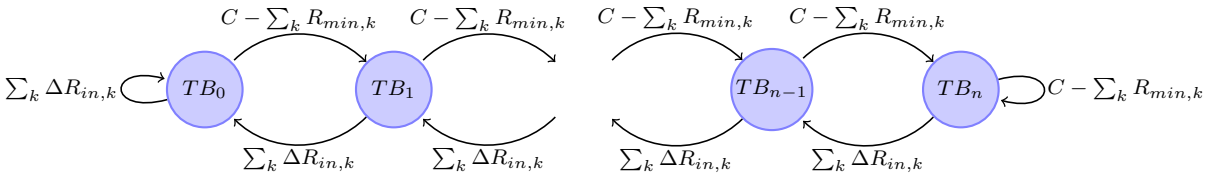

Figure 2.4: Common token bank as Markov process of finite states space (n =EBS).

Each of the token buckets can be represented as a discrete Markov chain with finite number of states [21], see figures 2.3 and 2.4. Where specific states correspond to the occupation level of the bucket (X_0 bucket is empty and X_{TB} full bucket). Arrivals rate (λ) is equal to the bucket filling rate and service rate (μ) to the incoming traffic rate. In fact the algorithm and the behavior of each of the buckets can be described as a birth-death process using a generic generator matrix as shown in [21]:

$$\mathbf{Q} = \begin{bmatrix} -\lambda_0 & -\lambda_0 & 0 & \dots & 0 \\ -\mu_1 & -(\lambda_1+\mu_1) & \lambda_1 & \dots & 0 \\ \vdots & \vdots & \vdots & \vdots & \vdots \\ \vdots & \vdots & -\mu_{T-1} & -(\lambda_{T-1}+\mu_{T-1}) & \lambda_{T-1} \\ 0 & 0 & \dots & -\mu_T & -(\lambda_T+\mu_T) \end{bmatrix} \tag{2.3}$$

In order to calculate the steady-state probabilities we need to take the assumption on ergodicity[3] of the Markov chain, which in facts holds true for both token bucket and token bank, as they are irreducible[4] and finite processes [5]. At the first stage we find steady-state probabilities for dedicated buckets and token bank being empty and based on the obtained formulas we try to derive blocking probability and achievable rate regions for token bank SAPHYRE backhaul sharing. The the steady-state probability of bucket being in state j, can be obtained via calculation of eigenvector from generator matrix[6] [21], as the formula is already well known for this type of generator matrix, we have used the result presented in [21]:

$$p_j = p_0 \prod_{i=0}^{j-1} \frac{\lambda_i}{\mu_{i+1}} \tag{2.4}$$

where p_0 is the probability of bucket being in state 0, obtained from the relation that $\sum_i p_i = 1$ [21]:

$$p_0 = \frac{1}{\sum_{j=0}^{\infty} \prod_{i=0}^{j-1} \frac{\lambda_i}{\mu_{i+1}}} \tag{2.5}$$

Based on the general equations 2.5 and 2.4, steady-state probabilities of finding empty the dedicated token bucket (p_j^D) and token bank (p_j^{TB}), can be written as follows:

$$p_0^D = \begin{cases} 0, \text{ if } \quad R_{min} > R_{in} \\ \frac{(1-\frac{R_{min}}{R_{in}})}{1-(\frac{R_{min}}{R_{in}})^{D+1}}, \text{ if } \quad TB = 0 \cap R_{min} \leq R_{in} \\ \frac{1}{\sum_{i=0}^{D-1} \frac{R_{max}^i}{R_{in}^{i+1}} + \frac{R_{max}^D}{R_{in}^{D+1}}}, \text{ if } \quad TB \neq 0 \cap R_{min} \leq R_{in} \end{cases} \tag{2.6}$$

$$p_0^{TB} = \begin{cases} 0, \text{ if } \quad C - \sum_k R_{min,k} > \sum_k \Delta R_{in,k} \\ \frac{(1-\frac{C-\sum_k R_{min,k}}{\sum_k \Delta R_{in,k}})}{1-(\frac{C-\sum_k R_{min,k}}{\sum_k \Delta R_{in,k}})^{TB+1}}, \text{ if } \quad C - \sum_k R_{min,k} \leq \sum_k \Delta R_{in,k} \end{cases} \tag{2.7}$$

[3]Markov chain is said to be ergodic if any of the states can be reached in finite number of steps.
[4]Markov chain is said to be irreducible, if it is possible to transit from any state j to any other state i in the chain.
[5]Since the number of tokens (and therfore number of states) is limited, the system is stable regardless from arrivals and departures.
[6]Where eigenvalue is equal to 1.

Blocking probability. Let us know derive the probability of incoming packet being dropped/blocked when arriving at the shared backhaul link. Specifically packet is being dropped/blocked when upon arrival the dedicated token bucket is empty, $D = 0$. What can be noticed, is the fact that the blocking probability is a superposition of two joint probabilities, of dedicated token bucket being empty, while token bank is either non-empty or empty. The above conclusions can be written as follows:

$$p(blocking) = \begin{cases} 0, \text{ if } \quad R_{min} > R_{in} \\ p(D = 0 \cap TB > 0) + p(D = 0 \cap TB = 0), \text{ otherwise} \end{cases} \tag{2.8}$$

Both joint probabilities occur independently, as in case the dedicated token bucket is empty, the token bank may either be empty or non-empty. The final equation for blocking probability can be rewritten as follows:

$$p(blocking) = \begin{cases} 0, \text{ if } \quad R_{min} > R_{in} \cup C - \sum_k R_{min,k} > \sum_k R_{in,k} \\ (1 - p_0^{TB})p_0^{D''} + p_0^{TB}p_0^{D'}, \text{ otherwise} \end{cases} \tag{2.9}$$

Expected output rate. Another important aspect for modeling of the shared backhaul is the expected achievable output rate that can be obtained by each of the operators. Let us know describe the expected rates that can be achieved by each of the operator depending on the other operators traffic [17]:

$$R_{out,k} = \begin{cases} R_{in,k}, \quad C \geq \sum_i R_{in,i} \\ R_{min,k} + w_k(C - \sum_k R_{in,k}, \text{ otherwise} \end{cases} \tag{2.10}$$

Thus it is obvious that in the situation where the traffic flow from different operators does not fully utilize the available capacity ($C \geq \sum_i R_{in,i}$) the expected output rate is:

$$R_{out,k} = \Big\{ R_{max,k}, \text{ if } \quad R_{in,k} \geq R_{max,k} \tag{2.11}$$

However the most interesting case is when the sum of operators traffic exceeds the available capacity. Due to the fact that token bank either assigns maximum exceeding rate or no rate at all, there are two possibilities at each time moment for dedicated bucket filling rate, 1) R_min, k (if no tokens in the bank are available) or 2) R_max, k (if there are tokens in the token bank). Authors of [17] have correctly concluded that in such a situation the expected rate is a sum of minimum guaranteed

rate and weighted filling rate from the token bank, where the weight is in fact probability that the token bank is not empty:

$$R_{out,k} = R_{min,k} + (1 - p_0^{TB})\Delta R_k, \text{ if } \quad C < \sum_i R_{in,i} \tag{2.12}$$

2.3.3 Simulation results

The performance of the derived analytical model was verified against different traffic situations that may occur on the backhaul link. The traffic parameters used in the simulations were taken for LTE Release 8 with 4x4 MIMO and 16QAM [22]:

- Peak data traffic rate per cell - DL:326 Mbps, UL:84 Mbps
- Average data traffic rate per cell - DL:61 Mbps, UL:24 Mbps

In order to calculate the required backhaul capacity let us assume also the overhead introduced by the underlying transport technology. According to [23], Carrier Ethernet header and VLAN tagging (only operator separation) would require additional 1.55% of rate for each 1,500 bytes of Ethernet payload. The signaling overhead is not included into the calculations as there are currently no practical numbers available for the transport link (available numbers describe overhead only in the radio link).

Based on the provided numbers we can assume for the simulations that:

- C = 1 Gbps typical capacity of a Carrier Ethernet backhaul link [24],
- CIR $= 3 * 87 = 261$ Mbps per 3 sector cell site of LTE operator,
- PIR $= 3 * 417 = 1251$ Mbps per 3 sector cell site of LTE operator (Peak Information Rate),
- EIR = 1000 Mbps per 3 sector cell site of LTE operator,
- CBS = 5 kB and EBS = 20 kB, and constant packet size of 1 kB (based on the assumptions from [6]).

In order to check the type of fairness that is provided by the token bank algorithm, we have analysed blocking probability and achievable rate in different scenarios for two operator case. The simulations were performed for three different cases resembling possible traffic situations at the backhaul link:

- Case 1 - Where both operators have the same incoming rate.
- Case 2 - Where Operator A has a maximum achievable rate of $R_{max}/2$.
- Case 3 - With the presence of high rate (reaching PIR) Operator B.

From the achieved results we can see that with the analyzed algorithm the link resources are allocated proportionally to the traffic agreements of the operator. The

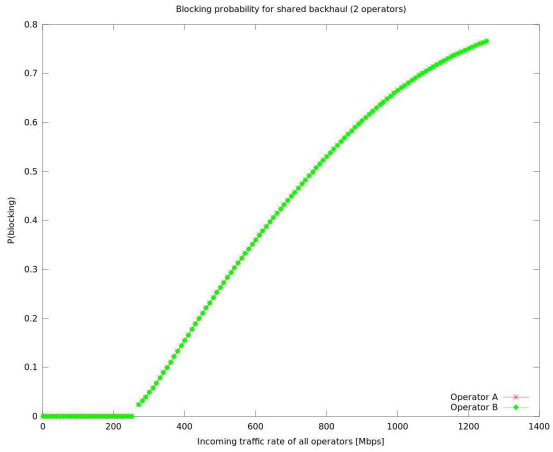

Figure 2.5: Blocking probabilities in case 1.

achievable rate is higher when: 1) the minimum guaranteed is higher and/or 2) the difference between excessive rate and guaranteed minimum rate is higher. This is a very important characteristic, as taking this into account we can state that in general algorithm provides proportional fairness in the resource access (2.9 and 2.8). This result is in accordance to [16, 17], which have suggested proportional fairness of the token bank model. The algorithm does not only provide proportional fair allocation of the avaialble resources but also reserves minimum required capacity for the operators even if the traffic of one operator does not exceed guaranteed level (figure 2.10 and 2.10). The reserved capacity is corresponding to the minimum guaranteed rate. Such a behavior promotes QoS maintenance but decreases link utilization. The algorithm does not provide maximum link utilization in the situation where both operator transmit but the traffic between them is highly unbalanced 2.10). Due to the properties of the algorithm the obtained results can also be generalized to multiple-operator situation.

2.3.4 Impact on the inter-operator information exchange

Based on the obtained results and design analysis from [5], we can conclude that the shared backhaul links can be effectively used as a mean to exchange information between the operators. However, an important observation is that in order to realize a real-time information exchange and aid the signal processing, a dedicated EVCs (Ethernet Virtual Circuits) need to be defined. The dedicated EVCs should be described via specific QoS requirements, which would be derived from the demands of novel signal processing solutions developed within the SAPHYRE. The requirements should specify the minimum required amount of inter-operator information, exchanged over the backhaul, as well as time constraints (delay) on the backhaul transmission. The two parameters should be used to specify the minimum

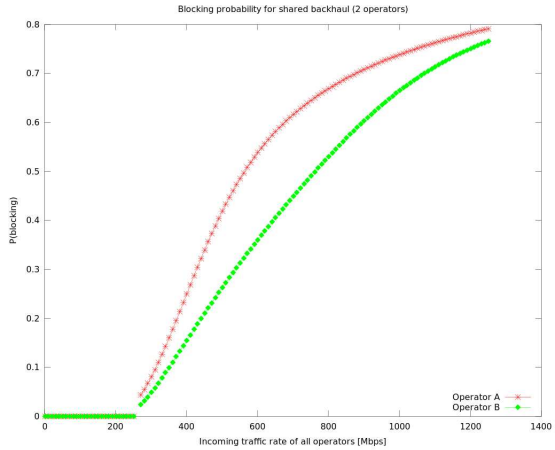

Figure 2.6: Blocking probabilities in case 2.

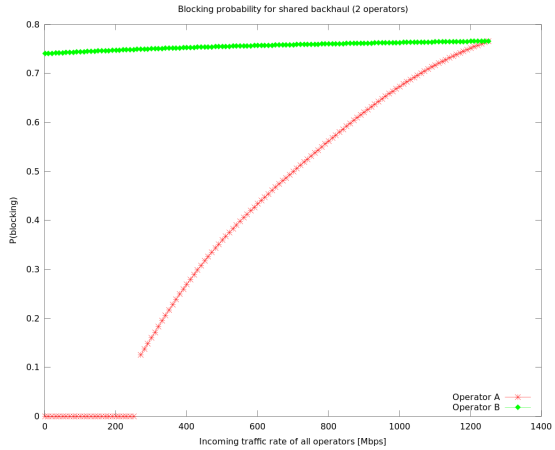

Figure 2.7: Blocking probabilities in case 3.

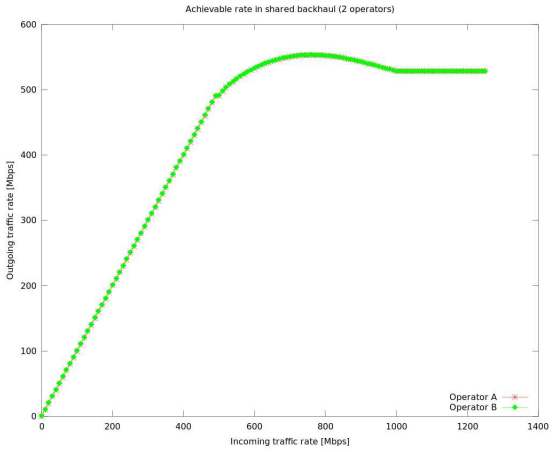

Figure 2.8: Achievable rate in case 1.

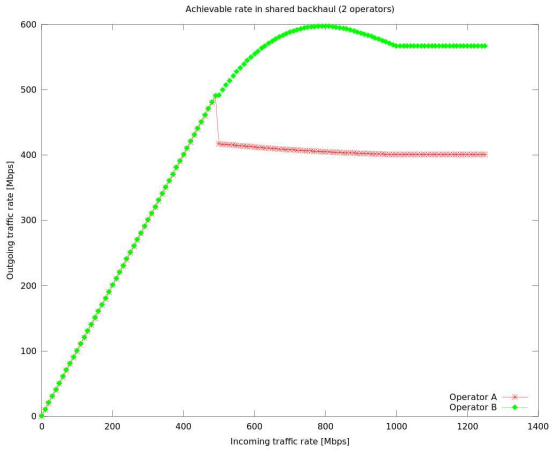

Figure 2.9: Achievable rate in case 2.

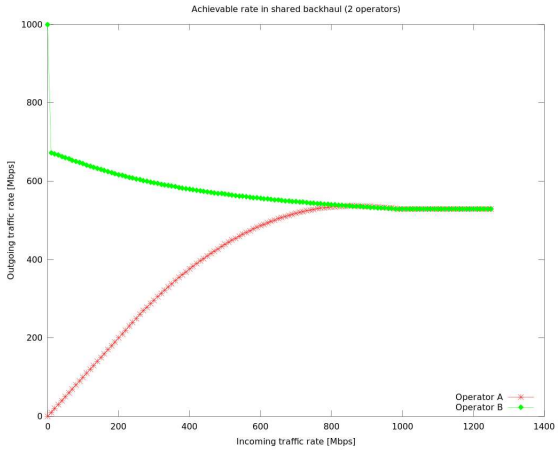

Figure 2.10: Achievable rate in case 3

rate that needs to be guaranteed in the backhaul, for a proper implementation of the SAPHYRE signal processing algorithms. Eventually the performance of information exchange over the backhaul link will follow the measured characterisitics of QoS provisioning mechanism, accordingly to the current load situation.

3 Transmit Interference Mitigation in Interference Networks

3.1 Introduction

In this chapter we will quantify the fundamental limits for coexistence of wireless systems in mobile environments and in particular in the context of competition between operators and selfish users. Spectrum and infrastructure sharing leads to interference at the air interface. On the physical layer, this problem is best analysed within the framework of interference channels (IFC). The classical two user interference channel consists of two transmitter/receiver pairs. Each pair wants to convey independent information on the same frequency at the same time causing interference at the other pair's receiver. Information-theoretic studies of the IFC have a long history [25, 26, 27, 28]. These references have provided various achievable rate regions, which are generally larger in the more recent papers than in the earlier ones. For certain operating points the capacity is known [29]. However, the capacity region of the general IFC remains an open problem. A deterministic approach to approximate the capacity region of the IFC [30] provides the capacity region within one bit. Recently, the characterisations of the capacity region or achievable rate regions have been used to compute efficient operating points of multi-antenna interference channels [31]. The achievable rate region depends on the information available at the transmitters, the co-operation at the transmitter and the receiver side.44 Furthermore, the fading statistics influence the average and outage rate region.

The chapter consists of two parts. In the first section, the characterization of the achievable rate region for the K-user MISO interference channel from Deliverable D2.1a is used to discuss the SAPHYRE gain by numerical simulations. In the second part, the idea of interference alignement in MIMO interference networks is applied and the optimal beamforming vector is characterized completeley. Basend on this, a distributed algorithm (DBA) is developed and asymptotically analyzed. Simulation results show the benefit of the DBA in terms of the SAPHYRE gain.

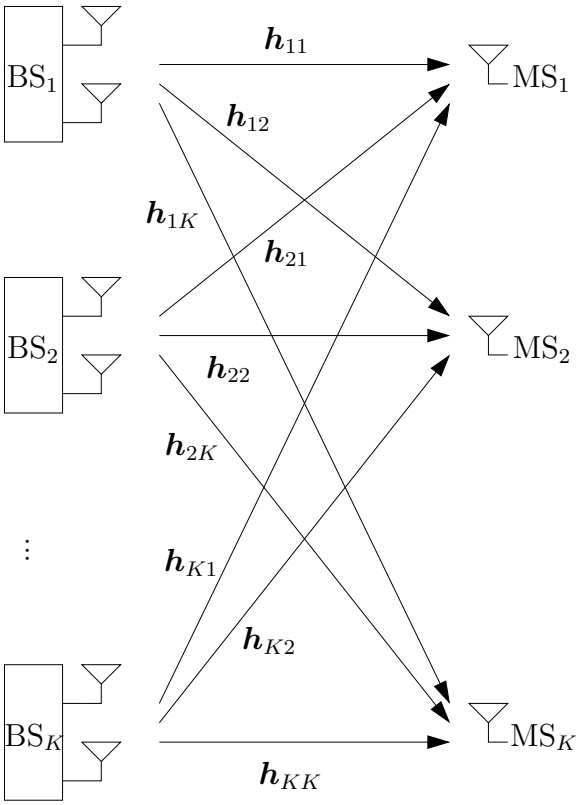

Figure 3.1: The K-user MISO interference channel under study (illustrated for $N = 2$ transmit antennas).

3.2 Achievable Rate Region for K-Users MISO Interference Channel

The MISO interference channel with K users is shown in Figure 3.1. All base stations BS_k have N transmit antennas each, that can be used with full phase coherency. The mobiles MS_k, however, have a single receive antenna each. We shall assume that transmission consists of scalar coding followed by beamforming, and that all propagation channels are frequency-flat. This leads to the following basic model for the matched-filtered, symbol-sampled complex baseband data received at MS_k:

$$y_k = \boldsymbol{h}_{kk}^T \boldsymbol{w}_k s_k + \sum_{l=1, l\neq k}^{K} \boldsymbol{h}_{lk}^T \boldsymbol{w}_l s_l + e_k, \tag{3.1}$$

where s_l, $1 \leq l \leq K$ is the symbol transmitted by BS_l, $\boldsymbol{h}_{ij}$ is the (complex-valued) $N \times 1$ channel-vector between BS_i and MS_j, and $\boldsymbol{w}_l$ is the beamforming vector used by BS_l. The variables e_k are noise terms which we model as i.i.d. complex Gaussian with zero mean and variance σ^2.

We assume that each base station can use the transmit power P, but that power cannot be traded between the base stations. Without loss of generality, we shall take $P = 1$. This gives the power constraints

$$||\boldsymbol{w}_k||^2 \leq 1, \quad 1 \leq k \leq K \tag{3.2}$$

Throughout, we define the SNR as $1/\sigma^2$. The precoding scheme that we will discuss requires that the transmitters (BS_k) have access to channel state information (CSI) for some of the links. However, at no point we will require phase coherency between the base stations. In [31], a characterization of the beamforming vectors that reach the Pareto boundary of the achievable rate region with interference treated as additive Gaussian noise is provided by a complex linear combination.

In what follows we will assume that all receivers treat co-channel interference as noise, i.e. they make no attempt to decode and subtract the interference. For a given set of beamforming vectors $\{\boldsymbol{w}_1, ..., \boldsymbol{w}_K\}$, the following rate is then achievable for the link $\mathrm{BS}_k \rightarrow \mathrm{MS}_k$, by using codebooks approaching Gaussian ones:

$$R_k(\boldsymbol{w}_1, ..., \boldsymbol{w}_K) = \log_2 \left(1 + \frac{|\boldsymbol{w}_k^T \boldsymbol{h}_{kk}|^2}{\sum_{l \neq k} |\boldsymbol{w}_l^T \boldsymbol{h}_{lk}|^2 + \sigma^2} \right). \tag{3.3}$$

We define the *achievable rate region* to be the set of all rates that can be achieved using beamforming vectors that satisfy the power constraint:

$$\mathcal{R} \triangleq \bigcup_{\{\boldsymbol{w}_k : ||\boldsymbol{w}_k||^2 \leq 1, 1 \leq k \leq K\}} \{R_1(\boldsymbol{w}_1, ..., \boldsymbol{w}_K), ..., R_K(\boldsymbol{w}_1, ..., \boldsymbol{w}_K)\} \subset \mathbb{R}_+^K. \tag{3.4}$$

The outer boundary of this region is called the *Pareto boundary*, because it consists of operating points $(R_1, ..., R_K)$ for which it is impossible to improve one of the rates, without simultaneously decreasing at least one of the other rates. More precisely we define the *Pareto optimality* of an operating point as follows.

3.1 Definition. A rate tuple $(R_1, ..., R_K)$ is Pareto optimal if there is no other tuple $(Q_1, ..., Q_K)$ with $(Q_1, ..., Q_K) \geq (R_1, ..., R_K)$ and $(Q_1, ..., Q_K) \neq (R_1, ..., R_K)$ (the inequality is component-wise).

In deliverable D2.1a, the following result is proposed and discussed:

3.2 Theorem. *All points of the Pareto boundary of the achievable rate region of the MISO interference channel can be reached by beamforming vectors*

$$\boldsymbol{w}_k(\boldsymbol{\lambda}_k) = \boldsymbol{v}_{max} \left(\sum_{\ell=1}^{K} \lambda_{k,\ell} e_\ell \boldsymbol{h}_{k,\ell} \boldsymbol{h}_{k,\ell}^H \right) \tag{3.5}$$

with $\boldsymbol{\lambda}_k \in \boldsymbol{\Lambda}$ *and*

$$e_\ell = \begin{cases} +1 & \ell = k \\ -1 & otherwise \end{cases}.$$

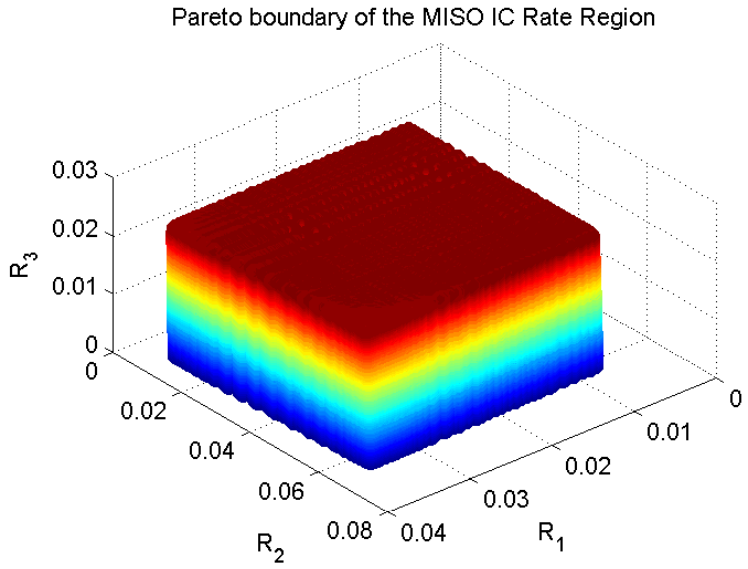

Figure 3.2: MISO IC achievable rate region for very low SNR (-20dB) with three links and two antennas at the transmitters.

The proof can be found in [32] where $\mathbf{\Lambda}$ is defined as

$$\mathbf{\Lambda} = \{\boldsymbol{\lambda} \in [0,1]^K : \sum_{\ell=1}^{K} \lambda_\ell = 1\}. \tag{3.6}$$

Based on the characterization, it is now possible to numerically illustrate the achievable rate regions. One of the most important questions is on the gain by sharing the same spectrum at the same time compared to the reference case in which the spectrum is exclusively used by the transmitters (operators).

The SAPHYRE gain Ξ_A is defined as the achievable rate of the sharing scenario compared to the time division between single-user transmission $R_1^{su}, R_2^{su}, R_3^{su}$. We choose the sum rate as the operating point and define the absolute gain as

$$\Xi_A = \max_{0 \le \boldsymbol{\lambda} \le 1} \sum_{k=1}^{K} R_k(\boldsymbol{\lambda}) - \frac{1}{K} \sum_{k=1}^{K} R_k^{su}. \tag{3.7}$$

The relative SAPHYRE gain Ξ_F is defined as

$$\Xi_F = \frac{\max_{0 \le \boldsymbol{\lambda} \le 1} \sum_{k=1}^{K} R_k(\boldsymbol{\lambda})}{\frac{1}{K} \sum_{k=1}^{K} R_k^{su}} \tag{3.8}$$

In Figure 3.2, the achievable rate region for very low SNR for a two antenna three user MISO IC is shown. It can be observed that the system is mainly noise limited and therefore the achievable rate region corresponds almost to a box. The

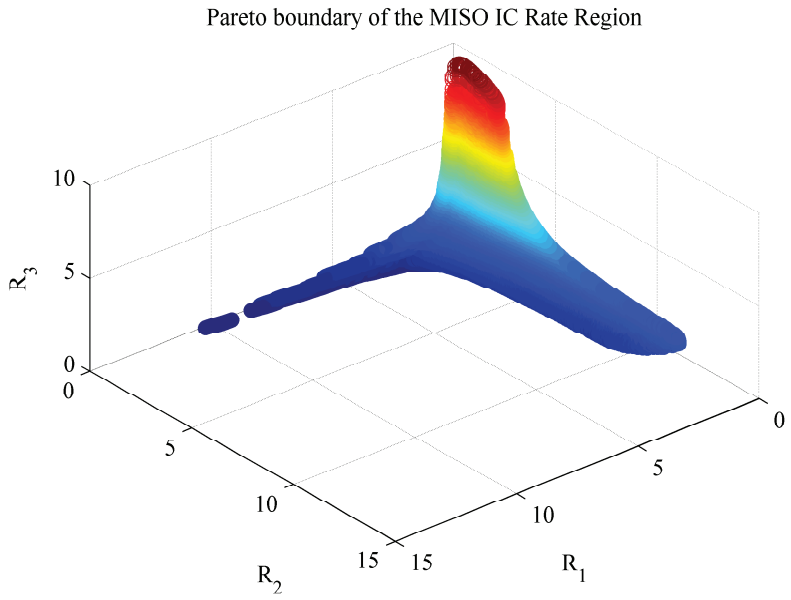

Figure 3.3: MISO IC achievable rate region for very high SNR (30dB) with three links and two antennas at the transmitters.

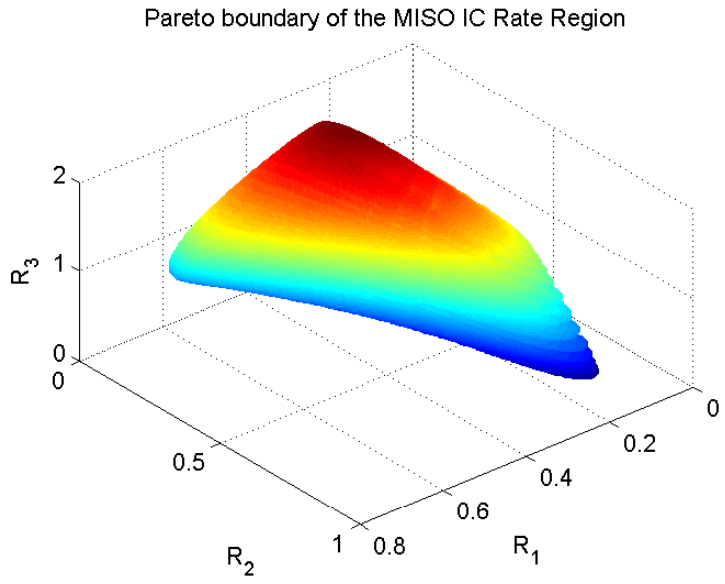

Figure 3.4: MISO IC achievable rate region for medium SNR (0dB) with three links and two antennas at the transmitters.

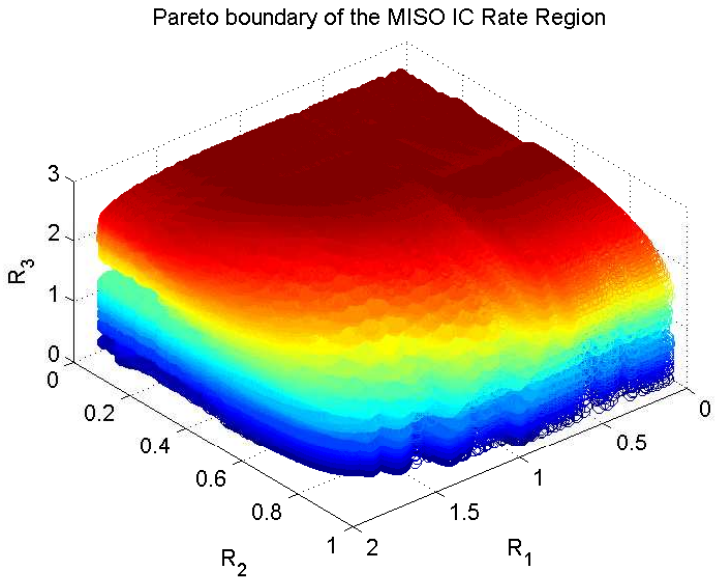

Figure 3.5: MISO IC achievable rate region for medium SNR (0dB) with three links and four antennas at the transmitters.

best strategies then are MRT at the three transmitters. In this case, the absolute SAPHYRE gain is easily computed as $\Xi_A = \sum_{k=1}^{K} R_k^{su} - \frac{1}{K}\sum_{k=1}^{K} R_k^{su} = \frac{K-1}{K}\sum_{k=1}^{K} R_k^{su}$. The relative gain is $\Xi_F = K$, i.e., the relative gain grows with the number of users K.

For very high SNR, the system becomes interference limited and the SAPHYRE gain shrinks down to $\Xi_A = 0$ and $\Xi_F = 1$. This can be clearly observed from the non-convex achievable rate region in Figure 3.3.

The impact of the number of transmit antennas is illustrated in the Figures 3.4 and 3.5 for medium SNR. For two antennas, the region in Figure 3.4 is non-convex and the gain is about $\Xi_A = 3.6 - 1/3*(1.8+0.5+1) = 2.5$ and $\Xi_F = \frac{3.6}{1.1} = 3.27$. Increasing the number of transmit antennas leads to new spatial degrees of freedom and the region looks more convex (see Figure 3.5. Thereby, the fairness of the resource allocation (for sum rate maximization) has increased. However, the SAPHYRE gain has not changed significantly. The absolute gain is about $\Xi_A = 4.4 - 1.8 = 2.6$ and $\Xi_F = \frac{4.4}{1.8} = 2.4$.

3.3 Interference Alignment in Asymmetric MIMO Interference Networks

We draw parallels with existing work on the MIMO-IC, including rate-optimizing and interference-alignment precoding techniques, showing how such techniques may

be improved or re-interpreted through a common prism based on balancing egoistic and altruistic beamforming. Our analysis and simulations currently limited to single stream transmission per user attest the improvements over known interference alignment based methods in terms of sum rate performance in the case of so-called asymmetric networks.

3.3.1 Introduction

The mitigation of interference in multi-point to multi-point radio systems is of utmost importance and has relevance in several practical contexts. Among the more popular cases, we may cite the optimization of multi cell multiple-input-multiple-output (MIMO) systems with full frequency reuse and cognitive radio scenarios featuring two or more service providers sharing an identical spectrum license on overlapping coverage areas. In all these cases, the system may be modeled as a network of N_c interfering radio links where each link consists of a sender trying to communicate messages to a unique receiver in spite of the interference arising from or created towards other links.

For system limitation or privacy reasons, when the backhaul network cannot support a complete sharing of data symbols across all transmitters (Txs), the channel remains an interference channel (IC). Coordination in terms of beamforming is required to be decentralized in the sense that global channel state information at transmitters (CSIT) may not be available everywhere. In the context of distributed beamforming, game theory appears as a sensible approach as a basis for algorithm design. Recently an interesting game theory framework for beamforming-based coordination was proposed for the multiple-input-single-output (MISO) case by which the transmitters (e.g. the base stations) seek to strike a compromise between selfishly serving their users while ignoring the interference effects on the one hand, and altruistically minimizing the harm they cause to other non-intended receivers on the other hand. An important result in this area was the characterization of all so-called Pareto rate optimal beamforming solutions for the two-cell case in the form of positive linear combinations of the purely selfish and purely altruistic beamforming solutions [33, 31] and [34] in the case of partial CSI. Unfortunately, how or whether at all this analysis can be extended to the context of MIMO interference channels (i.e. where receivers have themselves multiple antennas and interference cancelling capability) remains an open question.

In parallel, coordination on the MIMO interference channel has emerged as a very popular topic in its own right, with several important non-game related contributions shedding light on rate-scaling optimal precoding strategies based on so-called interference alignment, subspace optimization, alternated maximum signal to interference and noise ratio (SINR) optimization, [35, 36, 37] and rate-maximizing precoding strategies [38, 39], to cite just a few examples.

Interference alignment based strategies exhibit the designed feature of rendering

interference cancellable (when feasible, according to the available degrees of freedom) at both the transmitter and receiver side. Such a behaviour is optimal in the large signal to noise ratio (SNR) region when Rxs have single user decoder and interference is the key bottleneck. At finite SNR, various strategies exist which aim at maximizing a link quality metric individually over each link, while taking interference into account. This often takes the form of maximizing the link's SINR or minimizing minimum-mean-square-error (MMSE). This approach provides good rates in symmetric networks where all links are subject to impairments (noise, average interference) of similar level. In more general and practical situations however, we argue that a better sum rate may be obtained from a proper and different weighting of the egoistic and altruistic objective at each individual link. This situation is particularly important when more links are subject to statistically stronger interference than others, a case which has so far received little attention and which we shall refer here as asymmetric networks. For this purpose, we suggest to re-visit the problem of coordinated beamforming design by directly building on the game theoretic concept of egoistic and altruistic game equalibria. We exploit the obtained equilibria solution into heuristic design of a practical beamforming teachnique. The behaviour of our solution is then studied both theoretically (large SNR regime) and tested by simulations.

3.3.2 Channel Model

Let $\mathcal{N} = \{1, \ldots, N\}$ be a set containing a finite set $\mathcal{N}_c$, with cardinality $N_c \leq N$, of cooperating transmitters (Txs), also termed as players. From now on, we use players and Txs interchangably. We call the set $\mathcal{N}_c$ a coordination cluster and Txs outside the cluster will contribute to uncontrolled interference. The provided model has general applications in which the Txs can be base stations in cellular downlink where typically coordination is restricted to a subset of neighbouring cell sites while more distant sites cannot be coordinated over [40] ; nodes in ad-hoc network and cognitive radio.

Each Tx is equipped with N_t antennas and the Rx with N_r antennas. Each Tx communicates with a unique Rx at a time. Txs are not allowed or able to exchange users' packet (message) information, giving rise to an interference channel over which we seek some form of beamforming-based coordination. The channel from Tx i to Rx j $\mathbf{H}_{ji} \in \mathcal{C}^{N_r \times N_t}$ is given by:

$$\mathbf{H}_{ji} = \sqrt{\alpha_{ji}}\bar{\mathbf{H}}_{ji}, \quad i, j = 1, \ldots, N_c \tag{3.9}$$

Each element in channel matrix $\bar{\mathbf{H}}_{ji}$ is an independent identically distributed complex Gaussian random variable with zero

The received signal at Rx i is therefore

$$y_i = \mathbf{v}_i^H \mathbf{H}_{ii} \mathbf{w}_i + \sum_{j \neq i}^{N_c} \mathbf{v}_i^H \mathbf{H}_{ij} \mathbf{w}_j + n_i \tag{3.10}$$

where n_i is a gaussian noise with power σ_i^2. Note that the noise levels σ_i^2 depend on the link index which was not considered in previous work on transmitter coordination. The Rxs are assumed to employ maximum SINR (Max-SINR) beamforming throughout the paper so as to also maximize the link rates [41]. The receive beamformer $\mathbf{v}_i$ is classically given by:

$$\mathbf{v}_i = \frac{{\mathbf{C}_{Ri}}^{-1} \mathbf{H}_{ii} \mathbf{w}_i}{\| {\mathbf{C}_{Ri}}^{-1} \mathbf{H}_{ii} \mathbf{w}_i \|} \tag{3.11}$$

where $\mathbf{C}_{Ri}$ is the covariance matrix of received interference and noise

$$\mathbf{C}_{Ri} = \sum_{j \neq i} \mathbf{H}_{ij} \mathbf{w}_j \mathbf{w}_j^H \mathbf{H}_{ij}^H P + \sigma_i^2 \mathbf{I}. \tag{3.12}$$

P is the transmit power. Note that the receive beamformer $\mathbf{v}_i$ is a function of all transmit beamforming vectors $\mathbf{w}_i$. When the transmit beamforming vector $\mathbf{w}_i$ is optimized, the received beamforming vector is modified accordingly.

Importantly, the noise will in practice capture thermal noise effects but also any interference originating from the rest of the network, i.e. coming from transmitters located beyond the coordination cluster. Thus, depending on path loss and shadowing effects, the $\{\sigma_i^2\}$ may be quite different from each other [42]. Figure 3.6 illustrates a system of $N = 7$ cells where $N_c = 4$ form a coordination cluster. Note that we consider the sum of uncoordinated source of interference and thermal noise to be spatially white. The non-colored interference assumption is justified in the scenario where receivers cannot obtain specific knowledge of the interference covariance and can be interpreted as a worst case scenario, since the receivers cannot use their spatial degrees of freedom to further cancel uncontrolled interference.

3.3.3 Sum Rate Maximization with Receive Beamformer Feedback

Note that balancing altruism and egoism for player i can be done by trading-off between setting the beamformer close to the dominant eigenvectors of the egoistic $\mathbf{E}_i$ or that of the negative altruistic $\{-\mathbf{A}_{ji}\}$ $(j \neq i)$ matrices where

$$\begin{aligned} \mathbf{E}_i &= \mathbf{H}_{ii} \mathbf{w}_i \mathbf{w}_i^H \mathbf{H}_{ii} \\ \mathbf{A}_{ji} &= \mathbf{H}_{ji} \mathbf{w}_i \mathbf{w}_i^H \mathbf{H}_{ji}. \end{aligned} \tag{3.13}$$

Interestingly, it can be shown that sum rate maximizing precoding for the MIMO-IC does exactly that. Thus we hereby briefly re-visit rate-maximization approaches such as [39] with this perspective.

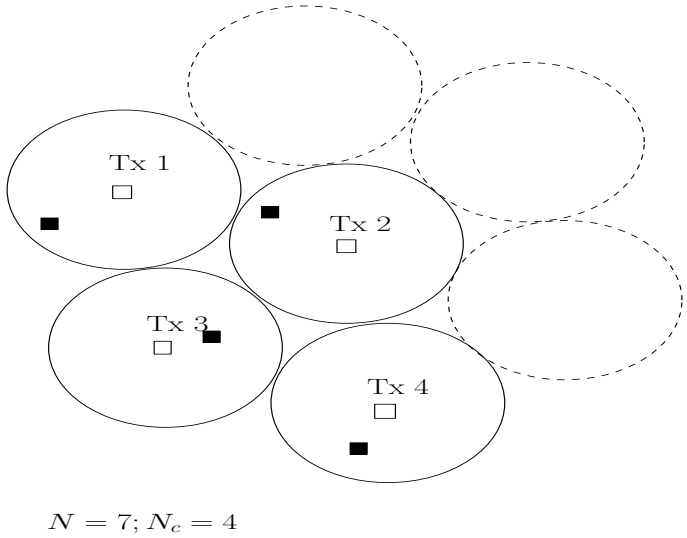

Figure 3.6: This figure illustrates a system of $N = 7$ cells where $N_c = 4$ form a coordination cluster. Empty squares represent transmitters whereas filled squares represent receivers. The noise power (which includes out of cluster interference) undergone in each cell varies from link to link.

Denote the sum rate by $\bar{R} = \sum_{i=1}^{N_c} R_i$ where $R_i = \log_2\left(1 + \frac{|\mathbf{v}_i^H \mathbf{H}_{ii}\mathbf{w}_i|^2 P}{\sum_{j\neq i}^{N_c} |\mathbf{v}_i^H \mathbf{H}_{ij}\mathbf{w}_j|^2 P + \sigma_i^2}\right)$.

3.3 Lemma. *The transmit beamforming vector which maximizes the sum rate $\bar{R}$ is the dominant eigenvector of a matrix, which is a linear combination of $\mathbf{E}_i$ and $\mathbf{A}_{ji}$:*

$$\left(\mathbf{E}_i + \sum_{j\neq i}^{N_c} \lambda_{ji}^{opt} \mathbf{A}_{ji}\right)\mathbf{w}_i = \mu_{max}\mathbf{w}_i \tag{3.14}$$

where

$$\lambda_{ji}^{opt} = -\frac{S_{jj}}{\sum_{k=1}^{N_c} S_{jk} + \sigma_j^2} \frac{\sum_{k=1}^{N_c} S_{ik} + \sigma_i^2}{\sum_{k\neq j}^{N_c} S_{jk} + \sigma_j^2} \tag{3.15}$$

where $S_{jk} = |\mathbf{v}_j^H \mathbf{H}_{jk}\mathbf{w}_k|^2 P$ and μ_{max} is defined in the proof.

Proof. see Appendix A. □

Note that the balancing between altruism and egoism in sum rate maximization is done using the dominant eigenvector of a simple *linear combination* of the altruistic and egoistic equilibrium matrices. The balancing parameters, $\{\lambda_{ji}^{opt}\}$, can be shown simply to coincide with the pricing parameters invoked in the iterative

algorithm proposed in [39]. Clearly, these parameters plays a key role, however their computation is a function of the *global* channel state information and requires additional message (price) exchange. Instead, we seek below a suboptimal egoism-altruism balancing technique which only requires statistical channel information, while exhibiting the right performance scaling when SNR grows large.

3.3.4 A Practical Distributed Beamforming Algorithm: *DBA*

We are proposing the following distributed beamforming algorithm (*DBA*) where one computes the transmit and receive beamformers iteratively as:

$$\mathbf{w}_i = V^{max}\left(\mathbf{E}_i + \sum_{j\neq i}^{N_c} \lambda_{ji}\mathbf{A}_{ji}\right) \tag{3.16}$$

$$\mathbf{v}_i = \frac{\mathbf{C}_{Ri}^{-1}\mathbf{H}_{ii}\mathbf{w}_i}{\|\mathbf{C}_{Ri}^{-1}\mathbf{H}_{ii}\mathbf{w}_i\|} \tag{3.17}$$

where λ_{ji} shall be made to depend on channel statistics only. At this stage, it is interesting to compare with previous schemes based on interference alignment such as the practical algorithms proposed in [37]. In such schemes, the transmit beamformer $\mathbf{w}_i$ is taken independent of $\mathbf{H}_{ii}$. Note that here however, $\mathbf{w}_i$ is correlated to the direct channel gain $\mathbf{H}_{ii}$ through the Egoistic matrix $\mathbf{E}_i$ in *DBA*. The correlation is useful in terms of sum rate as it allows proper weighting between the contributions of the egoistic and altruistic matrices in a link specific manner.

The Egoism-Altruism Balancing Parameters λ_{ji}

The egoism-altruism balancing parameters λ_{ji} are now found heuristically based on the statistical channel information. Recall from (3.15) that

$$\lambda_{ji}^{opt} = -\frac{S_j}{S_j + I_j + \sigma_j^2}\frac{S_i + I_i + \sigma_i^2}{I_j + \sigma_j^2} \tag{3.18}$$

where $S_j = |\mathbf{v}_j^H\mathbf{H}_{jj}\mathbf{w}_j|^2P$ and $I_j = \sum_{k\neq j}^{N_c}|\mathbf{v}_j^H\mathbf{H}_{jk}\mathbf{w}_k|^2P$.

Following the principle behind sum rate maximization, we conjecture that at convergence, residual coordinated interference shall be proportionate to the noise and out-of-cluster interference, i.e. $I_j = O(\sigma_j^2)$. Note that this should not be interpreted as an assumption in a proof but rather as a proposed design guideline. Based on this, we propose the following characterization:

$$\lambda_{ji}^{opt} = -\frac{S_j}{S_j + O(\sigma_j^2)}\frac{S_i + O(\sigma_i^2)}{O(\sigma_j^2)}. \tag{3.19}$$

Note that S_j and S_i are independent and we have

$$\lambda_{ji}^{opt} = -\frac{S_j}{S_j + O(\sigma_j^2)} \frac{S_i + O(\sigma_i^2)}{O(\sigma_j^2)} \tag{3.20}$$

$$\mathcal{E}\lambda_{ji}^{opt} \overset{(a)}{=} -\mathcal{E}\left(\frac{S_j}{S_j + O(\sigma_j^2)}\right) \frac{\mathcal{E}(S_i) + O(\sigma_i^2)}{O(\sigma_j^2)} \tag{3.21}$$

$$\overset{(b)}{\geq} -\frac{\mathcal{E}S_j}{\mathcal{E}S_j + O(\sigma_j^2)} + \frac{\mathcal{E}(S_i) + O(\sigma_i^2)}{O(\sigma_j^2)} \tag{3.22}$$

$$= -\frac{1}{1 + \frac{O(\sigma_j^2)}{\mathcal{E}S_j}} \frac{1 + \frac{O(\sigma_i^2)}{\mathcal{E}(S_i)}}{\frac{O(\sigma_j^2)}{\mathcal{E}(S_i)}} \tag{3.23}$$

where (a) is because S_i, S_j are independent and (b) is because the function $\frac{x}{x+c}$ is concave in x and therefore by Jensen's inequality, we have $\frac{\mathcal{E}x}{\mathcal{E}x+c} \geq \mathcal{E}\frac{x}{x+c}$.

Although $\mathcal{E}S_i$ is not known explicitly, it is strongly related to the strength of the direct channel $P\alpha_{ii}$. Let $\gamma_i = \frac{P\alpha_{ii}}{\sigma_i^2}$. In order to obtain an exploitable formulation for λ_{ji}, we replace $\mathcal{E}S_i$ by $P\alpha_{ii}$ and $O(\sigma_i^2)$ by σ_i^2, to derive:

$$\lambda_{ji} = -\frac{1}{1 + \gamma_j^{-1}} \frac{1 + \gamma_i^{-1}}{\frac{\sigma_j^2}{P\alpha_{ii}}}. \tag{3.24}$$

Interestingly, in the special case where direct channels have the same average strength, we obtain a simple expression

$$\lambda_{ji} = -\frac{1 + \gamma_i^{-1}}{1 + \gamma_j^{-1}} \gamma_j. \tag{3.25}$$

The above result suggests Tx i to behave more altruistically towards link j when the SNR of link j is high or when the SNR of link i is comparatively lower. This is in accordance with the intuition behind rate maximization over parallel gaussian channels.

DBA iterates between optimizing the transmit and receive beamformers, as summarized in Algorithm 1. Iterating between transmit and receive beamformers is reminiscent of recent interference-alignment based methods [36, 37]. However here, interference alignment is *not* a design criterion. In [36], an improved interference alignment technique based on alternately maximizing the SINR at both transmitter and receiver sides is proposed. In contrast, here the Max-SINR criterion is only used at the receiver side. Although the distinction is unimportant in the large SNR case (see below), it dramatically changes performance in certain situations at finite SNR (see Section 3.3.6).

Algorithm 1 Distributed Beamforming Algorithm (DBA)

1) Initialize beamforming vectors $\mathbf{w}_i, i = 1, \ldots, N_c$, to be predefined vectors.
2) For each Rx i, compute $\mathbf{v}_i = \frac{\mathbf{C}_{Ri}^{-1}\mathbf{H}_{ii}\mathbf{w}_i}{\|\mathbf{C}_{Ri}^{-1}\mathbf{H}_{ii}\mathbf{w}_i\|}$ where $\mathbf{C}_{Ri}$ is computed with $\mathbf{w}_i$ in previous step.
3) For each Tx i, compute $\mathbf{w}_i = V^{max}\left(\mathbf{E}_i + \sum_{j\neq i}^{N_c} \lambda_{ji}\mathbf{A}_{ji}\right)$ where λ_{ji} are computed from satistical parameters (3.24).
4) Repeat step 2 and 3 until convergence.

3.3.5 Asymtotic Interference Alignment

One important aspect of the algorithm above is whether it achieves the interference alignment in high SNR regime [36]. The following theorem answers this question positively.

3.4 Definition. Define the set of beamforming vectors solutions in downlink (respectively uplink) interference alignment to be [36]

$$\mathcal{IA}^{DL} = \{(\mathbf{w}_1, \ldots, \mathbf{w}_{N_c}) : \sum_{k\neq i}^{N_c} \mathbf{H}_{ik}\mathbf{w}_k\mathbf{w}_k^H\mathbf{H}_{ik}^H \text{ is low rank, } \forall i\} \tag{3.26}$$

$$\mathcal{IA}^{UL} = \{(\mathbf{v}_1, \ldots, \mathbf{v}_{N_c}) : \sum_{k\neq i}^{N_c} \mathbf{H}_{ki}^H\mathbf{v}_k\mathbf{v}_k^H\mathbf{H}_{ki} \text{ is low rank, } \forall i\}. \tag{3.27}$$

Thus, for all $(\mathbf{w}_i, \ldots, \mathbf{w}_{N_c}) \in \mathcal{IA}^{DL}$, there exist receive beamformers $\mathbf{v}_i, i = 1, \ldots, N_c$ such that the following is satisfied:

$$\mathbf{v}_i^H\mathbf{H}_{ij}\mathbf{w}_j = 0 \ \ \forall i, j \neq i. \tag{3.28}$$

Note that the uplink alignment solutions are defined for a virtual uplink having the same frequency and only appear here as a technical concept helping with the proof.

3.5 Theorem. *Assume the downlink interference alignment set is non-empty (interference alignment is feasible). Denote average SNR of link i by $\gamma_i = \frac{P\alpha_{ii}}{\sigma_i^2}$. Let $\lambda_{ji} = -\frac{1+\gamma_i^{-1}}{1+\gamma_j^{-1}}\gamma_j$, then in the large SNR regime, $P \to \infty$, any transmit beamforming vector in $\mathcal{IA}^{DL}$ is a convergence (stable) point of* DBA.

Proof. see Appendix A. □

Note that this does not prove global convergence, but local convergence, as is the case for other IA or rate maximization techniques [36, 37, 39]. Another way to characterize local convergence is as follows: assuming interference alignment is feasible

($\mathcal{IA}^{DL}$ is non-empty), the first algorithm in [36] was shown to converge to transmit beamformers belonging to $\mathcal{IA}^{DL}$ and the receivers are based on the minimum eigenvector of the dowlink interference covariance matrix, which tends to be low-rank. However, *DBA* selects its receive beamformer from the Max-SINR criterion which, in the large SNR situation, is also identical to selecting receive beamformers in the null space of the interference covariance matrix. Therefore when interference alignment is feasible, the algorithm in [36] and *DBA* coincide at large SNR. This aspect is confirmed by our simulations (see section 3.3.6).

3.3.6 Simulation Results

In this section, we investigate the sum rate performances of *DBA* in comparison with several related methods, namely the *Max-SINR* method [36], the alternated-minimization (*Alt-Min*) method for interference alignment [37] and the sum rate optimization method (*SR-Max*) [39]. The *SR-Max* method is by construction optimal but is more complex and requires extra sharing or feedback of pricing information among the transmitters. To ensure a fair comparison, all the algorithms in comparisons are initialized to the same solution and have the same stopping condition. The algorithms are considered to reach convergence if the sum rates achieved between successive iterations have difference less than 0.001. We perform sum rate comparisons in both symmetric channels and asymmetric channels where links undergo different levels of out-of-cluster noise. Define the Signal to Interference ratio of link i to be $\mathrm{SIR_i} = \frac{\alpha_{\mathrm{ii}}}{\sum_{\mathrm{j}\neq\mathrm{i}}^{\mathrm{N_c}} \alpha_{\mathrm{ij}}}$. The SIR is assumed to be 1 for all links, unless otherwise stated. Denote the difference in SNR between two links in asymmetric channels by ΔSNR. Note that the proposed algorithm is not limited to the following settings, but can be applied to network with arbitrary players and number of antennas.

Symmetric Channels

Figure 3.7 illustrates the sum rate comparison of *DBA* with *Max-SINR*, *Alt-Min* and *SR-Max* in a system of 3 links and each Tx and Rx have 2 antennas. Since interference alignment is feasible in this case, the sum rate performance of *SR-Max* and *Max-SINR* increases linearly with SNR. *DBA* achieves sum rate performance with the same scaling as *Max-SINR* and *SR-Max* (i.e. multiplexing gain of 3). Therefore these methods seem to perform similarly in symmetric channels.

Asymmetric Channels

In the asymmetric system, some links undergo uneven levels of noise and uncontrolled interference. Another aspect is that more links can experience greater path loss or shadowing than others. Here we consider a few typical scenarios for which could constitute asymmetric networks, as shown in Figure 3.8, 3.9 and 3.10.

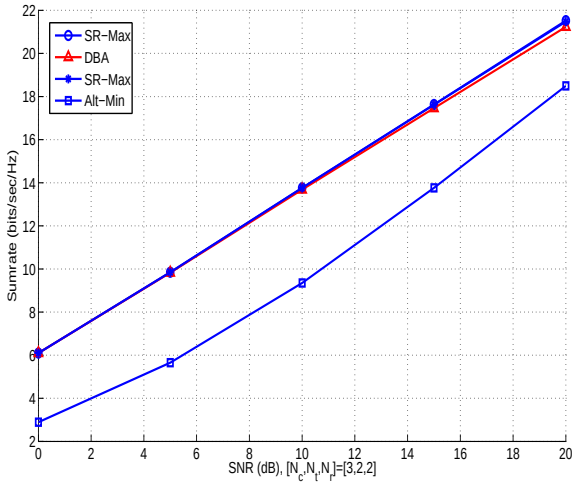

Figure 3.7: Sum rate comparison in multi links systems is illustrated with $[N_c, N_t, N_r] = [3, 2, 2]$ with increasing SNR. *DBA*, *SR-Max* and *Max-SINR* achieve very close performance in symmetric networks.

Asymmetric Uncontrolled Interference Power, Illustrated in Figure 3.8

In Figure 3.11, there are 3 links in the system in which the noise and unstructural interference in one of the links are 20 dB stronger than the other two links. This set up captures the scenario that one link is at the boundary of the coordination cluster and suffer from strong out-of-cluster noise. The SIR of every link is assumed to be 10 dB. in this scenario, *DBA* outperforms interference alignment based methods because they are unable to properly weigh the importance of each link in the overall sum rate. *SR-Max* is by construction sum rate optimal. However, in the asymmetric network, we observe by simulation that the convergence may require more iterations than other algorithms and the increment in sum rate per iteration can be small in some channel realizations.

Asymmetric Uncontrolled Interference Power and Interference within Cluster, Illustrated in Figure 3.9

In Figure 3.12, we compare the sum rate performance in the same set up as in Figure 3.11, except that the SIR's of the links are $[10, 10, 0.1]$ respectively. Thus, link 3 not only suffers from strong out of cluster noise, but also suffers from strong interference within the cluster. The asymmetry penalizes the *Max-SINR* and interference alignment methods because they are unable to properly weigh the contributions of the weaker link in the sum rate. The *Max-SINR* strategy turns out to make link 3 very egoistic in this example, while its proper behavior should be altruistic. In

contrast, *DBA* exploits useful statistical information, allowing weaker link to allocate their spatial degrees of freedom wisely towards helping stronger links and vice versa, yielding a better sum rate for the same feedback budget. The performance is very close to *SR-Max*, with less information exchange.

Asymmetric Desired Channel Power, Illustrated in Figure 3.10

In Figure 3.13, there are 3 links cooperating in the system. Each Tx and Rx has 2 antennas and has 1 stream transmission. The noise at each Rx is the same. The system is asymmetric in a sense that the direct channel gain H_{11} of link 1 is 30 dB weaker than other links in the network. This set up models a realistic environment where the user suffers strong shadowing. *DBA* achieves sum rate closed to *SR-Max* and much better than other interference alignment based schemes *Max-SINR* and *Alt-Min*.

The SAPHYRE Gain

We define here the SAPHYRE gain to be the sum rate performance differences between our proposed algorithm and a time-sharing scheme without further cooperation among transmitters. For illustration purposes, we show in the following the SAPHYRE gain in asymmetric channels in Figure 3.14 with three Tx-Rx pairs with two antennas everywhere.

3.3.7 Conclusions

We proposed a beamforming technique based on balancing the egoistic and the altruistic behavior with the aim of maximizing the sum rate is proposed. Such beamforming algorithm exhibits the same optimal rate scaling (when SNR grows) shown by recent iterative interference-alignment based methods. The proposed beamforming algorithm acheives close to optimal sum rate maximization method [39] without additional pricing feedbacks from users and outperform interference alignment based methods in terms of sum rate in asymmetric networks.

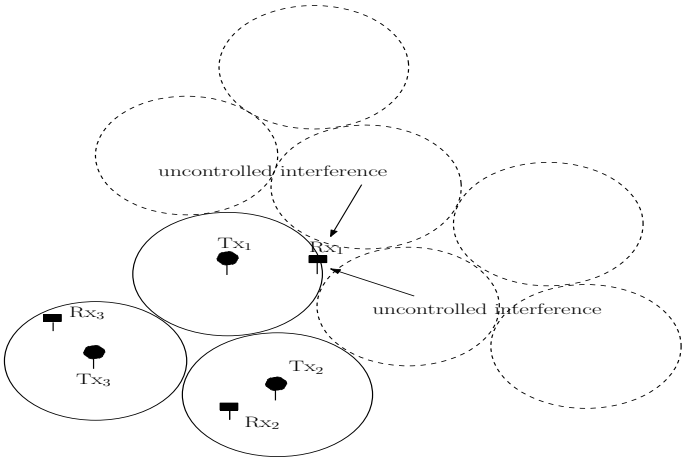

Figure 3.8: Asymmetric uncontrolled interference

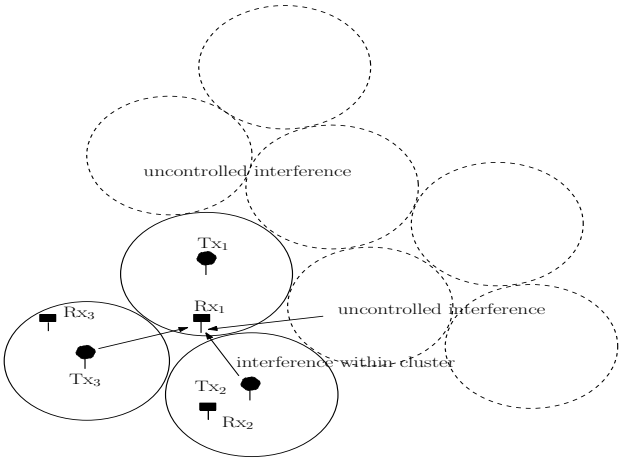

Figure 3.9: Asymmetric uncontrolled interference and interference within cluster

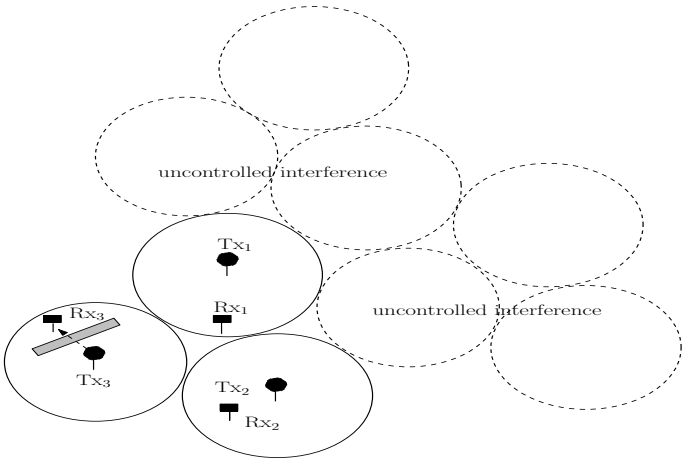

Figure 3.10: Asymmetric desired channel power

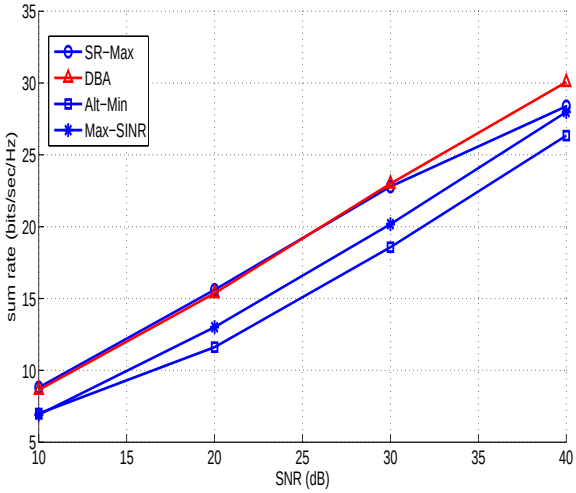

Figure 3.11: Sum rate performance for asymmetric channel, with one link under strong noise, is illustrated. The strong noise, from out of cluster interference, is 20 dB stronger than other links. *DBA* outperforms standard *IA* methods thanks to a proper balance between egoistic and altruistic beamforming algorithm.

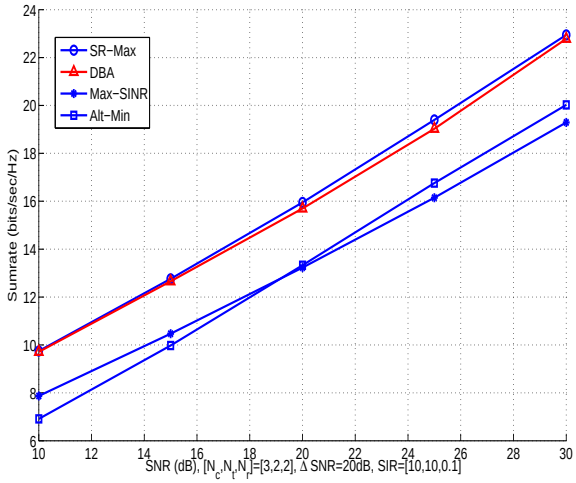

Figure 3.12: Sum rate performance for asymmetric channel, with one link under strong interference within the cooperating cluster, is illustrated.

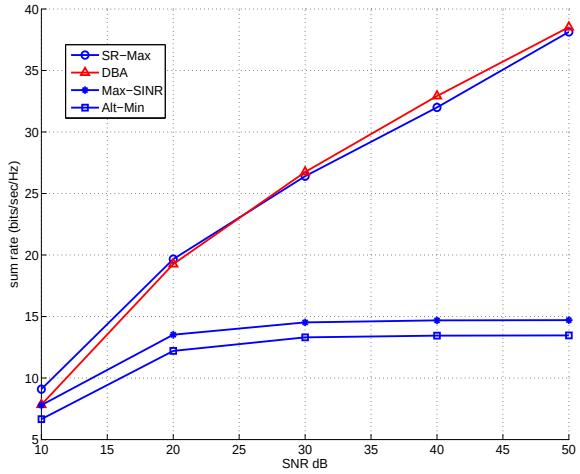

Figure 3.13: Sum rate performance for asymmetric channel is illustrated. The direct channel gain of link 1 is 30 dB weaker than other links.

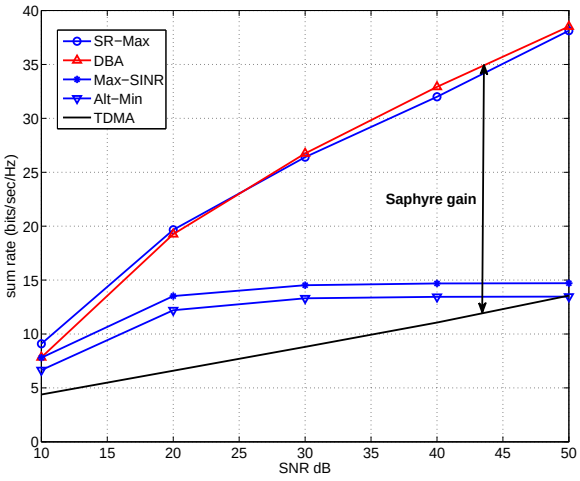

Figure 3.14: The SAPHYRE gain in sum rate performance for asymmetric channel is illustrated. The direct channel gain of link 1 is 30 dB weaker than other links.

4 Distributed MIMO Signal Processing

In this chapter, a distributed beamforming algorithm is proposed for the two-user multiple-input single-output (MISO) interference channel (IC). The algorithm is iterative and uses as bargaining value the interference that each transmitter generates towards the receiver of the other user. It enables cooperation among the transmitters in order to increase both users' rates by lowering the overall interference. In every iteration, as long as both rates keep on increasing, the transmitters mutually decrease the generated interference. They choose their beamforming vectors distributively, solving the constrained optimization problem of maximizing the useful signal power for a given level of generated interference. The algorithm is equally applicable when the transmitters have either instantaneous or statistical channel state information (CSI). The difference is that the core optimization problem is solved in closed-form for instantaneous CSI, whereas for statistical CSI an efficient solution is found numerically via semidefinite programming. The outcome of the proposed algorithm is approximately Pareto-optimal. Extensive numerical illustrations are provided, comparing the proposed solution to the Nash equilibrium, zero-forcing, Nash bargaining, and maximum sum-rate operating points.

4.1 Introduction

The situation when two wireless links operate in the same spectrum, and create mutual interference to one another, is well modeled by the interference channel (IC). Associated with any IC there is an achievable rate region, consisting of all pairs of transmission rates R_1 (for link 1) and R_2 (for link 2) that can be achieved, subject to constraints on the power used by the transmitters. The Pareto boundary of the rate region is the part of the outer boundary consisting of rate points, where increasing R_1 necessarily requires decreasing R_2 and vice versa. It is generally desirable to operate at rate points that lie on the Pareto boundary, such as the maximum-sum-rate (SR) point and the Nash bargaining solution (NBS) [43].

In this paper, we consider the two-user multiple-input single-output (MISO) IC, where the transmitters (TX_1 and TX_2) have multiple antennas and the receivers (RX_1 and RX_2) have a single antenna each. By using beamforming the transmitters are able to steer power in arbitrary directions. On one extreme, when the transmitters do not cooperate, it is natural to act "selfishly" and use the maximum-ratio (MR) beamforming vector, which maximizes the useful signal power without taking into account the interference generated towards the other receiver. Then, the outcome is the so-called in game-theoretic studies Nash equilibrium (NE), at

which none of the users can increase its rate by unilaterally changing its transmit strategy [43]. On the other extreme, the transmitters can be enforced by regulation to act "altruistically" and use the zero-forcing (ZF) beamforming vector, which maximizes the useful signal power without generating any interference towards the other receiver. When both transmitters use the altruistic strategy, we will refer to the corresponding rate pair as the ZF point. In general, both the NE and the ZF points lie far inside the Pareto boundary. Pareto-optimal (PO) operating points can only be achieved by combinations of the two aforementioned extreme strategies [31, 44, 45]. This is because the maximization of the useful signal power and the minimization of the generated interference are conflicting objectives.

It is evident that the transmitters need to cooperate and agree to mutually decrease the generated interference, in order to achieve larger rates than the NE. Herein, we propose a simple and self-enforcing algorithm for the distributed design of the beamforming vectors, with minimum required channel knowledge. We assume that the transmitters are synchronized and that there are feedback channels from all the receivers to all the transmitters. Each transmitter has CSI only of the direct link to its intended receiver and the crosstalk link to the other receiver. The feedback channels are initially used to provide channel state information (CSI) and in the sequel information about the algorithm evolution.

The proposed algorithm is iterative and uses as bargaining value the level of generated interference. It is natural to initialize the algorithm with the MR transmit strategy. Then, in every iteration, each transmitter will decrease the upper bound on the generated interference and distributively compute a new beamforming vector solving the optimization problem of maximizing the useful power, given the interference bound and the power constraint. Inevitably, in every iteration the optimal value (max useful signal) of each system decreases, since the feasibility set of the optimization is constricted. But, in return, the experienced interference decreases too. The iterations continue as long as the signal-to-interference-plus-noise ratio (SINR), hence the rate, of both users benefits from them. The algorithm can be interpreted as a walk from selfish towards altruistic choices of beamforming vectors. The bargaining outcome is approximately PO.

When the signal-to-noise ratio (SNR) is high and the spatial correlation among the direct and crosstalk channels is strong, the ZF point corresponds to larger rates, than the NE, i.e. it is closer to the Pareto boundary. In such a case, the algorithm will converge to a solution faster if it is initialized with the ZF transmit strategy. Then, the interference levels need to be increased in every iteration, to expand the feasibility set, and the walk is from altruistic towards selfish transmit strategies.

The proposed algorithm can be equally used when the transmitters have either instantaneous CSI (i.e., perfect knowledge of the channel vectors) or statistical CSI (i.e., knowledge of the channel distributions). In the former case, the achievable region is comprised by instantaneous rates, whereas in the latter by ergodic rates. We propose a generic formulation of the beamforming problem as constrained op-

timization, which is common for both CSI cases. For instantaneous CSI, we solve the optimization in closed-form, using the parameterization in [31]. For statistical CSI, we find an efficient numerical solution via semidefinite programming (SDP), as described in [45].

In this paragraph, we summarize some known bargaining algorithms and cooperative beamforming solutions. In [46], the authors presented a bargaining algorithm, similar in spirit to the one we propose herein. Their algorithm requires instantaneous CSI, starts with the MR strategy, and exploits the parametrization in [31]. In every iteration, a portion of the ZF strategy is added to the previously computed strategy until a stopping criterion is met. This algorithm converges to an operating point which is better than the NE. Compared to [46], the main contributions of our paper are the use of the generated interference level as bargaining value and the fact that the proposed algorithm works for both instantaneous and statistical CSI. In [47], the authors presented a solution to the cooperative beamforming problem in the case of instantaneous CSI, using the notion of virtual SINR. The aforementioned algorithms were also extended in the context of multicell MIMO channels in [48].

We compare the outcome of our algorithm to the NE, ZF, NBS, and SR points, for different cases of CSI, SNR values and spatial correlation levels. Also, we provide exemplary illustrations of the bargaining trajectory and discuss the complexity of the algorithm.

4.2 Preliminaries

4.2.1 System Model

We assume that transmission consists of scalar coding followed by beamforming[1] and that all propagation channels are frequency-flat. The matched-filtered symbol-sampled complex baseband data received by RX_i is modeled as[2]

$$y_i = \boldsymbol{h}_{ii}^H \boldsymbol{w}_i s_i + \boldsymbol{h}_{ji}^H \boldsymbol{w}_j s_j + e_i, \;\; j \neq i, \;\; i,j \in \{1,2\}, \tag{4.1}$$

where $s_i \sim \mathcal{CN}(0,1)$ and $\boldsymbol{w}_i \in \mathbb{C}^n$ are the transmitted symbol and the beamforming vector, respectively, employed by TX_i. Also, $e_i \sim \mathcal{CN}(0,\sigma_i^2)$ models the receiver noise. The (conjugated) channel vector between TX_i and RX_j is modeled as $\boldsymbol{h}_{ij} \sim \mathcal{CN}(\boldsymbol{0}, \mathbf{Q}_{ij})$. We denote $r_{ij} \triangleq \mathrm{rank}\{\mathbf{Q}_{ij}\}$. In the case of instantaneous CSI, TX_i accurately knows the channel realizations $\boldsymbol{h}_{ii}$ and $\boldsymbol{h}_{ij}$, whereas for statistical CSI it only knows the channel covariance matrices $\mathbf{Q}_{ii}$ and $\mathbf{Q}_{ij}$.

[1] This is optimal in the case of instantaneous CSI, but not necessarily for statistical CSI, see [34].

[2] Whenever an expression is valid for both systems, it is denoted once with respect to system i and the index $j \neq i$ refers to the other system.

The transmission power is bounded due to regulatory and hardware constraints, such as battery and amplifiers. Without loss of generality, we set this bound to 1. Hence, the set of feasible beamforming vectors is

$$\mathcal{W} \triangleq \{\boldsymbol{w} \in \mathbb{C}^n \mid \|\boldsymbol{w}\|^2 \leq 1\}. \tag{4.2}$$

Note that the set $\mathcal{W}$ is convex. In what follows, a specific choice of $\boldsymbol{w}_i \in \mathcal{W}$ is denoted as a *transmit strategy* of TX_i.

4.2.2 Instantaneous CSI

When the transmitters perfectly know the channel vectors and the receivers treat interference as noise, the achievable *instantaneous* rate (in bits/channel use) for link i is [31]

$$R_i(\boldsymbol{w}_i, \boldsymbol{w}_j) = \log_2\left(1 + \frac{|\boldsymbol{h}_{ii}^H \boldsymbol{w}_i|^2}{|\boldsymbol{h}_{ji}^H \boldsymbol{w}_j|^2 + \sigma_i^2}\right). \tag{4.3}$$

It is evident that the rate on each link depends on the choice of both beamforming vectors. We define the power that RX_i receives from TX_j as

$$p_{ji}(\boldsymbol{w}_j) \triangleq |\boldsymbol{h}_{ji}^H \boldsymbol{w}_j|^2 = \boldsymbol{w}_j^H \boldsymbol{h}_{ji} \boldsymbol{h}_{ji}^H \boldsymbol{w}_j. \tag{4.4}$$

Then, we can write (4.3) as

$$R_i(\boldsymbol{w}_i, \boldsymbol{w}_j) = \log_2\left(1 + \frac{p_{ii}(\boldsymbol{w}_i)}{p_{ji}(\boldsymbol{w}_j) + \sigma_i^2}\right), \tag{4.5}$$

which is monotonously increasing with the useful signal power $p_{ii}(\boldsymbol{w}_i)$ for fixed received interference power $p_{ji}(\boldsymbol{w}_j)$ and monotonously decreasing with $p_{ji}(\boldsymbol{w}_j)$ for fixed $p_{ii}(\boldsymbol{w}_i)$.

The main goal of the bargaining algorithm we introduce in Section 4.3 is to agree on a PO solution. Hence, we restrict our attention to the beamforming vectors which are candidates to achieve PO points. From [31], we know that the PO beamforming vectors use full power and that they are linear combinations of the MR and ZF strategies

$$\boldsymbol{w}_i^{\mathrm{PO}}(\lambda_i) = \frac{\lambda_i \boldsymbol{w}_i^{\mathrm{MR}} + (1-\lambda_i)\boldsymbol{w}_i^{\mathrm{ZF}}}{\|\lambda_i \boldsymbol{w}_i^{\mathrm{MR}} + (1-\lambda_i)\boldsymbol{w}_i^{\mathrm{ZF}}\|} \tag{4.6}$$

for $\lambda_i \in [0, 1]$, where

$$\boldsymbol{w}_i^{\mathrm{MR}} = \frac{\boldsymbol{h}_{ii}}{\|\boldsymbol{h}_{ii}\|} \quad \text{and} \quad \boldsymbol{w}_i^{\mathrm{ZF}} = \frac{\boldsymbol{\Pi}_{\boldsymbol{h}_{ij}}^{\perp} \boldsymbol{h}_{ii}}{\left\|\boldsymbol{\Pi}_{\boldsymbol{h}_{ij}}^{\perp} \boldsymbol{h}_{ii}\right\|}. \tag{4.7}$$

The outcome when both transmitters use their MR strategies is the NE. When both use their ZF we refer to the ZF point.

4.2.3 Statistical CSI

When the transmitters only have statistical knowledge of the channels, it is natural to design the achievable the beamforming vectors with respect to the *ergodic* rates, which are obtained by averaging over the channel realizations. From [44], we have[3]

$$\begin{aligned} R_i(\boldsymbol{w}_i, \boldsymbol{w}_j) &\triangleq \mathbb{E}\left\{ \log_2 \left(1 + \frac{|\boldsymbol{h}_{ii}^H \boldsymbol{w}_i|^2}{|\boldsymbol{h}_{ji}^H \boldsymbol{w}_j|^2 + \sigma_i^2} \right) \right\} \\ &= \frac{p_{ii}(\boldsymbol{w}_i)}{\ln 2} \frac{f_i(p_{ii}(\boldsymbol{w}_i)) - f_i(p_{ji}(\boldsymbol{w}_j))}{p_{ii}(\boldsymbol{w}_i) - p_{ji}(\boldsymbol{w}_j)}, \end{aligned} \tag{4.8}$$

where

$$f_i(x) \triangleq e^{\sigma_i^2/x} \int_{\sigma_i^2/x}^{\infty} \frac{e^{-t}}{t} dt. \tag{4.9}$$

In (4.8), $p_{ji}(\boldsymbol{w}_j)$ denotes the *average* power that RX_i receives from TX_j

$$p_{ji}(\boldsymbol{w}_j) = \mathbb{E}\{ \boldsymbol{w}_j^H \boldsymbol{h}_{ji} \boldsymbol{h}_{ji}^H \boldsymbol{w}_j \} = \boldsymbol{w}_j^H \mathbf{Q}_{ji} \boldsymbol{w}_j. \tag{4.10}$$

Note that the final terms in both (4.4) and (4.10) are convex homogeneous quadratics. The difference is that the parameter (channel) matrix in (4.4) is rank-1 by definition, whereas in (4.10) it can have any rank.

The ergodic rate (4.8) has the same behavior as the instantaneous rate (4.3), i.e., it is monotonously increasing (decreasing) with $p_{ii}(\boldsymbol{w}_i)$ ($p_{ji}(\boldsymbol{w}_j)$) for fixed $p_{ii}(\boldsymbol{w}_i)$ ($p_{ji}(\boldsymbol{w}_j)$) [44]. Also, for points on the Pareto boundary we know that $\boldsymbol{w}_i \in \mathcal{R}\{\mathbf{Q}_{ii}, \mathbf{Q}_{ij}\}$ [34]. The MR strategy $\boldsymbol{w}_i^{\mathrm{MR}}$ is the dominant eigenvector of $\mathbf{Q}_{ii}$ [44]. When $\mathcal{R}\{\mathbf{Q}_{ii}\} \nsubseteq \mathcal{R}\{\mathbf{Q}_{ij}\}$, the ZF strategy $\boldsymbol{w}_i^{\mathrm{ZF}}$ is the dominant eigenvector of $\boldsymbol{\Pi}_{\mathcal{N}\{\mathbf{Q}_{ij}\}} \mathbf{Q}_{ii} \boldsymbol{\Pi}_{\mathcal{N}\{\mathbf{Q}_{ij}\}}$ and when $\mathcal{R}\{\mathbf{Q}_{ii}\} \subseteq \mathcal{R}\{\mathbf{Q}_{ij}\}$, e.g., when $\mathbf{Q}_{ij}$ is full-rank, then $\boldsymbol{w}_i^{\mathrm{ZF}} = \mathbf{0}$ [44].

4.2.4 Important Operating Points

In the following, we introduce some operating points, which are important in the sense that they lie on the outer boundary of the rate region; see, e.g., [43] and references therein.

Single-user (SU): The points achieved when one transmitter employs its MR strategy while the other refrains from transmission.

Maximum sum-rate (SR): The point where the sum of the rates is maximum. Graphically, it is the point where a line of slope -1 touches the Pareto boundary of the rate region.

[3] We deliberately use the same symbols, as in the case of instantaneous CSI, to denote the rate and the power (R and p, respectively) in order to facilitate in the sequel a uniform treatment of both CSI scenarios.

Nash bargaining solution (NBS): The outcome of a Nash bargaining is a point $(\bar{R}_1, \bar{R}_2)$ such that $(\bar{R}_1 - R_1^*)(\bar{R}_2 - R_2^*)$ is maximized for some threat point (R_1^*, R_2^*) and $\bar{R}_i \geq R_i^*$. It is natural to use the NE as the threat point, since it is the only reasonable outcome if the systems are not able to agree on a solution. The NBS is only defined on convex utility regions, but we will call the solution to the corresponding optimization problem the NBS.

4.3 Cooperative Beamforming Algorithm

In this section, we elaborate the proposed bargaining algorithm that enables the transmitters to distributively design their beamforming vectors. We assume that there exists a feedback link from every receiver to every transmitter. The receivers use these links to feedback CSI. Each transmitter has CSI only on the links it is affecting. The transmitters are assumed synchronized, but no information (CSI or user data) is exchanged between them.

In the algorithm, we use as bargaining value an upper bound on the interference generated by system i to system j. This bound, denoted c_{ij}, is adjusted in every iteration. During the bargaining, the receivers feed back a one-bit message that tells the transmitters whether the iteration was successful or not, i.e. whether the rates increased or not. We denote l the iteration counter, which also acts as a quantitative measure of the overhead (total number of bits per RX-TX feedback link) and the computational complexity (total number of optimization problems that need to be solved).

A flowchart of the algorithm is illustrated in Figure 4.1. The first step of the algorithm is the decision whether the initialization point will be the NE or the ZF point. For this reason, the transmitters send two pilots using their MR and ZF beamforming vectors. The receivers measure the SINR for each transmission and feed back one-bit of information telling the transmitters which strategy yields higher SINR, hence rate. If $R_i(\boldsymbol{w}_i^{\mathrm{ZF}}, \boldsymbol{w}_j^{\mathrm{ZF}}) \geq R_i(\boldsymbol{w}_i^{\mathrm{MR}}, \boldsymbol{w}_j^{\mathrm{MR}})$ for both systems, the algorithm is initialized with the ZF point, since it is closer than the NE to the Pareto boundary. Hence, the algorithm will require fewer iterations to converge to a solution. If only one system achieves higher rate with the ZF strategies, there is no incentive for the other to accept the ZF point as initial point. The algorithm is then initialized with the NE point.

Then, the algorithm sets the stepsize for updating c_{ij}. As with any iterative algorithm, the best output is obtained for an infinitesimal stepsize. However, this is not practical, so we consider instead a fixed stepsize[4]. We assume that TX_i samples the interval $[0, p_{ij}(\boldsymbol{w}_i^{\mathrm{MR}})]$ uniformly in $N+1$ points, to allow up to N iterations. This gives the step $\delta_{ij} = \pm p_{ij}(\boldsymbol{w}_i^{\mathrm{MR}})/N$. The sign of δ_{ij} depends on the initial point. If the algorithm is initialized with the NE, δ_{ij} will be negative (decreasing

[4]Also, an adaptive stepsize can easily be incorporated to the algorithm.

interference). Otherwise, δ_{ij} will be positive (increasing interference). At iteration l, TX_i updates the interference level as $c_{ij}^l = c_{ij}^{l-1} + \delta_{ij}$ and solves the problem

$$\max_{\boldsymbol{w}_i \in \mathcal{W}} \; p_{ii}(\boldsymbol{w}_i) \tag{4.11}$$

$$\text{s.t.} \quad p_{ij}(\boldsymbol{w}_i) \leq c_{ij}^l. \tag{4.12}$$

The optimal solution of problem (4.11)–(4.12) is the beamforming vector which maximizes the useful power given that the generated interference is c_{ij}^l. As long as c_{ij}^l is chosen in the range $[0, p_{ij}(\boldsymbol{w}_i^{\mathrm{MR}})]$, there always exists a feasible solution to (4.11)–(4.12) [45]. The lower and upper end on the interference level correspond to the ZF and MR strategies, respectively. Furthermore, the bound will be tight at the optimum; hence, the inequality in (4.12) can be equivalently replaced with equality. We propose a solution to the optimization problem (4.11)–(4.12) in Sections 4.3.1 and 4.3.2 for the case of instantaneous and statistical CSI, respectively. TX_i uses $\boldsymbol{w}_i^l$ to transmit a pilot. RX_i measures $R_i(\boldsymbol{w}_i^l, \boldsymbol{w}_j^l)$ and if it is no smaller than $R_i(\boldsymbol{w}_i^{l-1}, \boldsymbol{w}_j^{l-1})$, it feeds back a one-bit message telling the transmitters to continue updating the interference level. As soon as the rate decreases for at least one of the receivers, the algorithm terminates and the transmitters will use the beamforming vectors from the previous iteration.

We claim that the algorithm is self-enforced. Suppose that, in one of the steps, TX_i chooses to cheat by not decreasing the interference level. Then, the rate of system j will decrease and RX_j will feedback a negative bit. According to the last step of the algorithm, the transmitters are expected to choose the beamforming vectors from the previous iteration. If TX_i does not, RX_j will notice and report it to TX_j. Then, TX_j will leave the bargaining and employ its MR beamforming vector instead. That is, if one system tries to cheat, then the cooperation is canceled and the operation falls back to the NE (the so-called threat point, in the context of Nash bargaining).

4.3.1 Instantaneous CSI

By inserting the expression (4.4) in (4.11)–(4.12), with inequality changed to equality, we get the problem

$$\max_{\boldsymbol{w}_i \in \mathcal{W}} \; |\boldsymbol{h}_{ii}^H \boldsymbol{w}_i|^2 \tag{4.13}$$

$$\text{s.t.} \quad |\boldsymbol{h}_{ij}^H \boldsymbol{w}_i|^2 = c_{ij}. \tag{4.14}$$

Since the objective of the algorithm is to find a PO point, the transmitters are only willing to use beamforming vectors that are candidates for achieving PO points. Any other beamforming vector will be a waste of power. Using (4.6) we get

$$\max_{\lambda_i \in [0,1]} \; |\boldsymbol{h}_{ii}^H \boldsymbol{w}_i^{\mathrm{PO}}(\lambda_i)|^2 \tag{4.15}$$

$$\text{s.t.} \quad |\boldsymbol{h}_{ij}^H \boldsymbol{w}_i^{\mathrm{PO}}(\lambda_i)|^2 = c_{ij}. \tag{4.16}$$

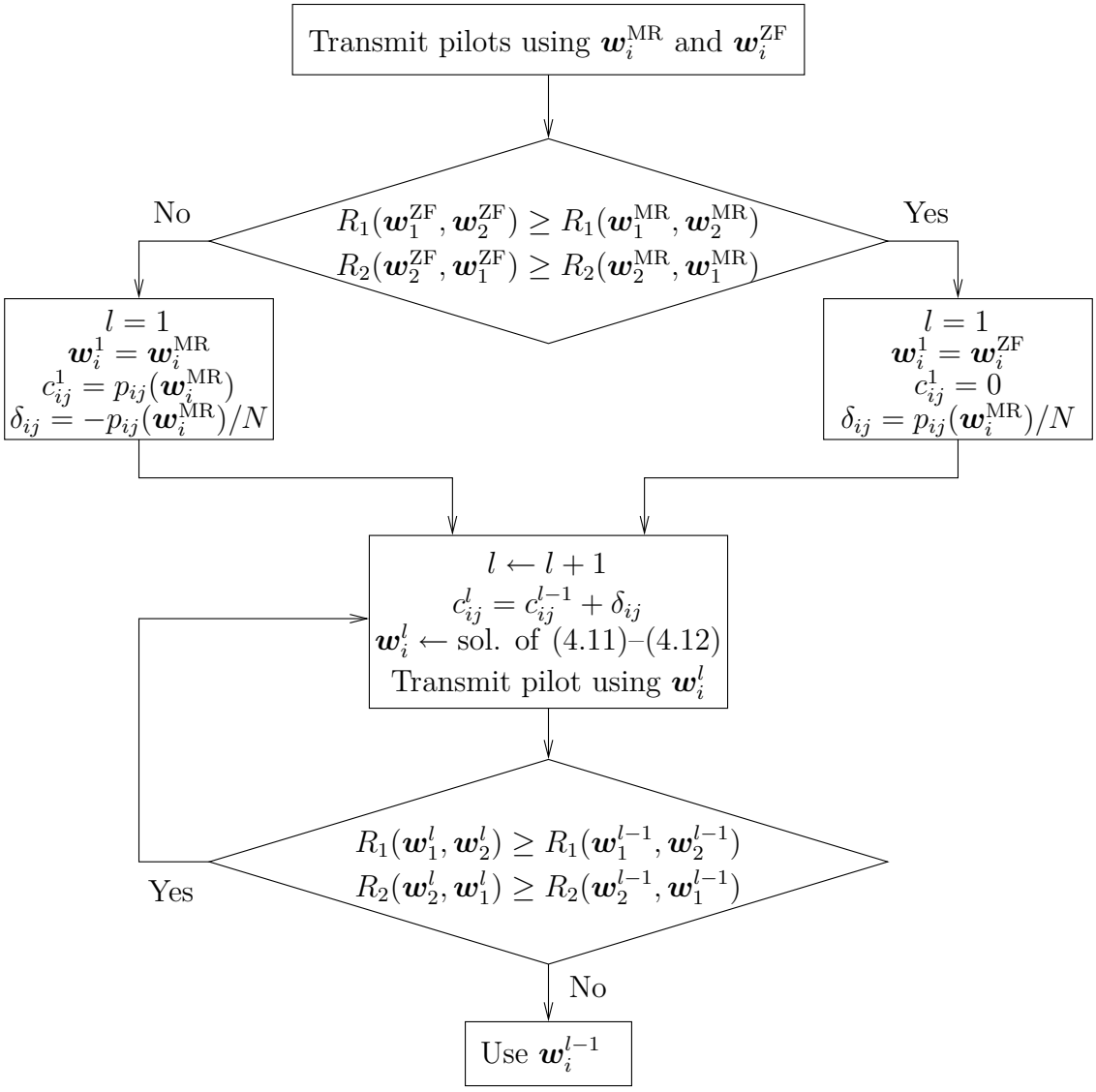

Figure 4.1: Flowchart describing the proposed cooperative beamforming algorithm

Note that the optimization (4.15)–(4.16) is now only with respect to the real scalar λ_i. Furthermore, the power constraint is obsolete, since the PO beamforming vectors use full power. That is, the inequality constraint in (4.2) is met with equality. Instead, we have a constraint on the range of the weighting factor λ_i. Finally, it is straightforward to see that the objective function (4.15) is monotonously increasing with λ_i. Thus, we can equivalently rewrite (4.15)–(4.16) as

$$\max_{\lambda_i \in [0,1]} \lambda_i \tag{4.17}$$

$$\text{s.t.} \quad |\boldsymbol{h}_{ij}^H \boldsymbol{w}_i^{\mathrm{PO}}(\lambda_i)|^2 = c_{ij}. \tag{4.18}$$

To simplify notation, we define

$$\alpha_i \triangleq (|\boldsymbol{h}_{ij}^H \boldsymbol{h}_{ii}| / \|\boldsymbol{h}_{ij}\|)^2 \text{ and } \beta_i \triangleq \left\| \boldsymbol{\Pi}_{\boldsymbol{h}_{ij}}^{\perp} \boldsymbol{h}_{ii} \right\| / \|\boldsymbol{h}_{ii}\| . \tag{4.19}$$

The values (4.19) are only calculated once per channel realization. For $c_{ij} > 0$ we write (4.18) as

$$\frac{\lambda_i^2 \alpha_i}{\lambda_i^2 + (1-\lambda_i)^2 + 2\lambda_i(1-\lambda_i)\beta_i} = c_{ij} \Leftrightarrow$$
$$\lambda_i^2(\alpha_i/c_{ij} + 2\beta_i - 2) + \lambda_i(2 - 2\beta_i) - 1 = 0.$$

When $c_{ij} = 0$, the ZF strategy is the optimal solution (i.e, $\lambda_i = 0$). Now, we write (4.17)–(4.18) as

$$\max \ \lambda_i \tag{4.20}$$
$$\text{s.t.} \quad \lambda_i^2(\alpha_i/c_{ij} + 2\beta_i - 2) + \lambda_i(2 - 2\beta_i) - 1 = 0, \tag{4.21}$$
$$0 \leq \lambda_i \leq 1. \tag{4.22}$$

The solution to (4.20)–(4.22) is the largest of the two solutions to (4.21) that satisfies (4.22).

4.3.2 Statistical CSI

By inserting (4.10) in (4.11)–(4.12) we get

$$\max_{\boldsymbol{w}_i \in \mathbb{C}^n} \ \boldsymbol{w}_i^H \mathbf{Q}_{ii} \boldsymbol{w}_i \tag{4.23}$$
$$\text{s.t.} \quad \boldsymbol{w}_i^H \mathbf{Q}_{ij} \boldsymbol{w}_i \leq c_{ij}, \tag{4.24}$$
$$\boldsymbol{w}_i^H \boldsymbol{w}_i \leq 1. \tag{4.25}$$

Problem (4.23)–(4.25) is a quadratically constrained quadratic program (QCQP). The feasibility set determined by (4.24)–(4.25) is convex. However, the optimization is non-convex owing to the form of the objective function. However, it can still be solved optimally and efficiently using semidefinite relaxation. This is because semidefinite relaxation is tight for QCQP problems of the form in (4.23)–(4.24), as shown in [49].

We briefly elaborate the procedure, similar to the way we did in [45]. We change the optimization variables to $\mathbf{W}_i \triangleq \boldsymbol{w}_i \boldsymbol{w}_i^H$. Note that

$$\mathbf{W}_i = \boldsymbol{w}_i \boldsymbol{w}_i^H \Leftrightarrow \mathbf{W}_i \succeq \mathbf{0} \text{ and } \operatorname{rank}\{\mathbf{W}_i\} = 1. \tag{4.26}$$

Using (4.26) and the property that $\operatorname{tr}\{\mathbf{YZ}\} = \operatorname{tr}\{\mathbf{ZY}\}$ for matrices $\mathbf{Y}$, $\mathbf{Z}$ of compatible dimensions, the average power term in (4.24) can be written as

$$\begin{aligned} \boldsymbol{w}_i^H \mathbf{Q}_{ij} \boldsymbol{w}_i &= \operatorname{tr}\left\{ \boldsymbol{w}_i^H \mathbf{Q}_{ij} \boldsymbol{w}_i \right\} = \operatorname{tr}\left\{ \mathbf{Q}_{ij} \boldsymbol{w}_i \boldsymbol{w}_i^H \right\} \\ &= \operatorname{tr}\left\{ \mathbf{Q}_{ij} \mathbf{W}_i \right\}. \end{aligned} \tag{4.27}$$

Due to (4.26) and (4.27), we equivalently recast (4.23)–(4.24) as

$$\max_{\mathbf{W}\in\mathbb{C}^{n\times n}} \quad \mathrm{tr}\left\{\mathbf{Q}_{ii}\mathbf{W}_i\right\} \tag{4.28}$$

$$\text{s.t.} \quad \mathrm{tr}\left\{\mathbf{Q}_{ij}\mathbf{W}_i\right\} \leq c_{ij}, \tag{4.29}$$

$$\mathrm{tr}\left\{\mathbf{W}_i\right\} \leq 1, \tag{4.30}$$

$$\mathbf{W}_i \succeq \mathbf{0}, \tag{4.31}$$

$$\mathrm{rank}\{\mathbf{W}_i\} = 1. \tag{4.32}$$

The objective function (4.28), the constraints (4.29) and (4.30) are linear. The cone of positive semidefinite matrices (4.31) is convex. But the rank constraint (4.32) is non-convex. Dropping it, the remaining problem (4.28)–(4.31) is a semidefinite programming (SDP) problem, which can be solved efficiently. Due to the absence of (4.32), the SDP problem will not necessarily return rank-1 optimal matrices. We experienced through extensive simulations that it actually *does* yield rank-1 matrices.

4.4 Numerical Illustrations

In this section, we present extensive simulation results to evaluate the performance of the algorithm we propose. We focus on the case of statistical CSI, but also provide some results for instantaneous CSI. In Section 4.4.1, we explain how we generate CSI (i.e., channel covariance matrices or channel vectors) for simulation purposes. In Sections 4.4.2 and 4.4.3, we compare the outcome of the algorithm to the NE, ZF, SR, and NBS. Furthermore, in Section 4.4.4, we show exemplary bargaining trajectories. Finally, in Section 4.4.5 we illustrate the SAPHYRE gain.

Throughout the simulations, we assume that the transmitters use $n = 5$ antennas. We allow our algorithm run up to $N = 20$ iterations. The results reported in Figure 4.2–4.7 are averages over 100 Monte-Carlo (MC) runs. Figure 4.2–4.7 illustrate the sum of the transmission rates, i.e., $R_1 + R_2$. Figure 4.8–4.11 show examples of achievable rate regions, i.e., for a single CSI realization.

4.4.1 Generating the Channels

We generate the direct and the crosstalk channels in two different ways, to model the scenarios of weak or strong spatial correlation. Specifically, in the case of instantaneous CSI and weak correlation, we generate the channel vectors $\boldsymbol{h}_{ii}$ and $\boldsymbol{h}_{ij}$ drawing independent samples from $\mathcal{CN}(\mathbf{0}, \boldsymbol{I})$. For the scenario of strong correlation, we use the formula

$$\boldsymbol{h}_{ij} = \mu_i \boldsymbol{h}_{ii} + \sqrt{1-\mu_i^2}\tilde{\boldsymbol{h}}_{ij}, \tag{4.33}$$

where $\boldsymbol{h}_{ii}$ and $\tilde{\boldsymbol{h}}_{ij}$ are drawn from $\mathcal{CN}(\mathbf{0}, \boldsymbol{I})$, and $\mu_i \in [0, 1]$. A value of μ_i close to 1 refers to the case of strong interference.

In the case of statistical CSI, we construct the covariance matrices, of rank r, randomly as

$$\mathbf{Q} = \sum_{k=1}^{r} \mathbf{q}_k \mathbf{q}_k^H, \tag{4.34}$$

where $\mathbf{q}_k \sim \mathcal{CN}(\mathbf{0}, \boldsymbol{I})$. For the scenario of weak correlation, we generate the covariance matrices $\mathbf{Q}_{ii}$ and $\mathbf{Q}_{ij}$ independently according to (4.34). For the scenario of strong correlation, we construct the matrices such that the angle between the eigenvectors of the direct matrix and the eigenvectors of the crosstalk matrix is small. Assuming that $r_{ii} \leq r_{ij}$, we first generate $\mathbf{Q}_{ii}$ as in (4.34). Then, we construct the vectors $\{\mathbf{q}_{ij,k}\}_k$ that define $\mathbf{Q}_{ij}$ as

$$\begin{cases} \mathbf{q}_{ij,k} = \mu_i \mathbf{q}_{ii,k} + \sqrt{1-\mu_i^2}\tilde{\mathbf{q}}_{ij,k}, & k \leq r_{ii} \\ \mathbf{q}_{ij,k} = \tilde{\mathbf{q}}_{ij,k}, & k > r_{ii} \end{cases} \tag{4.35}$$

where $\tilde{\mathbf{q}}_{ij,k} \sim \mathcal{CN}(\mathbf{0}, \boldsymbol{I})$ and $\mu_i \in [0,1]$. If $r_{ii} > r_{ij}$, the matrices are constructed the other way around.

4.4.2 Statistical CSI

In this section, we provide results for statistical CSI, both for weak and strong spatial correlation. Also, we distinguish among the cases of having full-rank and low-rank covariance matrices. In the low-rank scenario, the covariance matrices of the direct-channels have rank $r_{11} = r_{22} = 2$, and covariance matrices of the cross-talk channels have rank $r_{12} = r_{21} = 4$. For strong correlation, we use $\mu_i = 0.8$.

In Figure 4.2 and 4.3, we study the full-rank scenario. First, we note that the ZF sum rate is equal to 0 since full-rank crosstalk matrices correspond to $\boldsymbol{w}_i^{\mathrm{ZF}} = \mathbf{0}$. Second, we see that the sum rates for the proposed algorithm, the NBS, and the NE saturate for high SNR. The reason is that when the SNR is high, interference is the main limiting factor. Since the interference cannot become zero, except for the SU-points, there should be a limitation. Third, since there is no interference at the SU points, the corresponding rates will grow unbounded with SNR and the SR will be found at a SU point for high SNR.

In Figure 4.4 and 4.5, we illustrate the low-rank scenario. Here, all points but the NE converge to the same sum rate at high SNR. The difference is that, for strong correlation they converge at higher SNR value than for weak correlation. Also, we see that the rates grow almost linearly with the SNR. In general, there exists a non-trivial zero-forcing point for the case of low-rank matrices. Using this, the noise is the only limitation. When the noise decreases, the rates increase. At low SNR, the ZF starts growing later for strong correlation than for weak correlation.

Furthermore, we evidence that weak correlation (Figure 4.2 and 4.4) gives higher rates for the proposed algorithm, the NE, and the NBS, than strong correlation

(Figure 4.3 and 4.5). As a general remark, low SNR means operation in the noise-limited regime and all the rates but the ZF are almost the same.

Concluding, we see that the performance of the proposed algorithm is slightly below the NBS and close to the SR, except for full-rank matrices and high SNR. Most important, the algorithm performs consistently much better than the NE, which would be the outcome if there was no cooperation.

4.4.3 Instantaneous CSI

In Figure 4.6 and 4.7 we report the results for weak and strong correlation ($\mu_i = 0.9$), respectively. We note that the curves behave similarly to the ones in Figure 4.4 and 4.5. The reason for this is that the case of instantaneous CSI can be regarded as a specific instance of the low-rank statistical CSI when all covariance matrices are rank-1.

4.4.4 Bargaining Trajectory

In this section, we give examples of the bargaining trajectory, i.e., the rate points (marked with stars) reached at every iteration of the proposed algorithm. Here, the maximum number of iterations used is $N = 10$. Figure 4.8 and 4.9 illustrate the trajectories for statistical CSI with full-rank covariance matrices and SNR equal to 0 and 10 dB, respectively. The Pareto boundary is calculated using the technique proposed in [45]. Figure 4.10 and 4.11 illustrate the trajectories for instantaneous CSI and SNR equal to 0 and 10 dB, respectively. The Pareto boundary is calculated using the technique proposed in [31].

For statistical CSI and full-rank matrices, the algorithm is always initialized with the NE, since a non-trivial ZF point does not exist. For instantaneous CSI and low SNR it is initialized with the NE point, while for high SNR with the ZF point. We note that the final outcome of the bargaining algorithm is close to the Pareto boundary, but does not necessarily lie on it. On one hand, the final outcome depends on the stepsize of the algorithm. On the other hand, the algorithm terminates when either of the rates stops increasing, i.e., when the tangent of the trajectory stops being positive. More on, the outcome is close to NBS, but generally far from SR. We note that the SR does not imply that both systems have increased their rates compared to NE, while the proposed algorithm and NBS guarantee that both systems get at least their NE rates. Finally, in all figures we show what the bargaining trajectory would look like if the algorithm went the entire way from one extreme point (NE or ZF) to the other with small steps. Note that for statistical CSI and full-rank matrices the ZF point corresponds to the origin of the rate region.

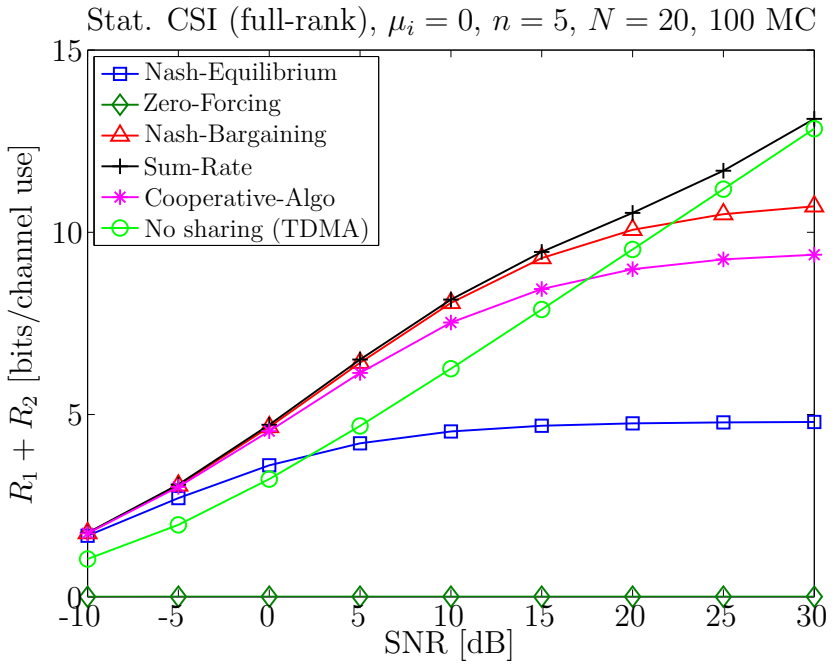

Figure 4.2: Sum rate; stat. CSI (full-rank), $\mu_i = 0$

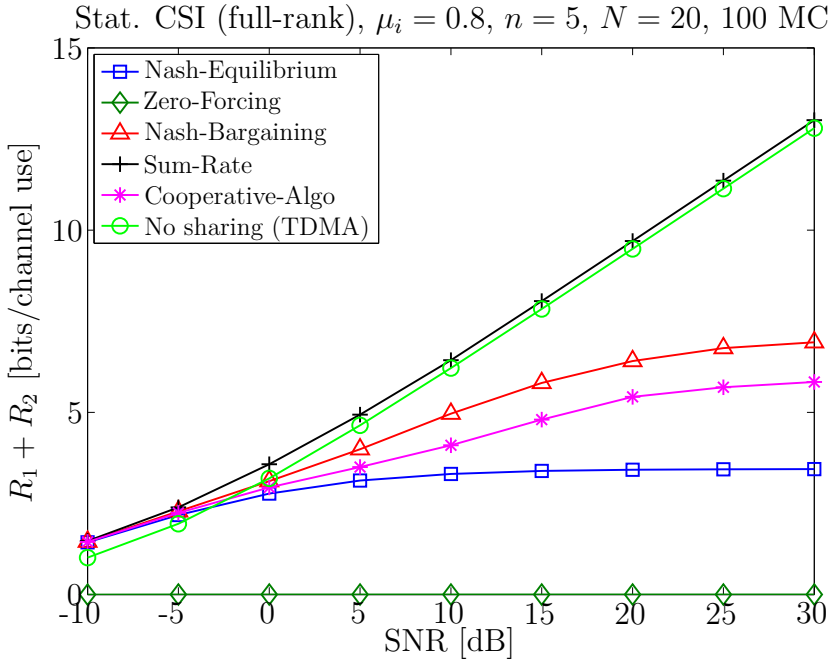

Figure 4.3: Sum rate; stat. CSI (full-rank), $\mu_i = 0.8$

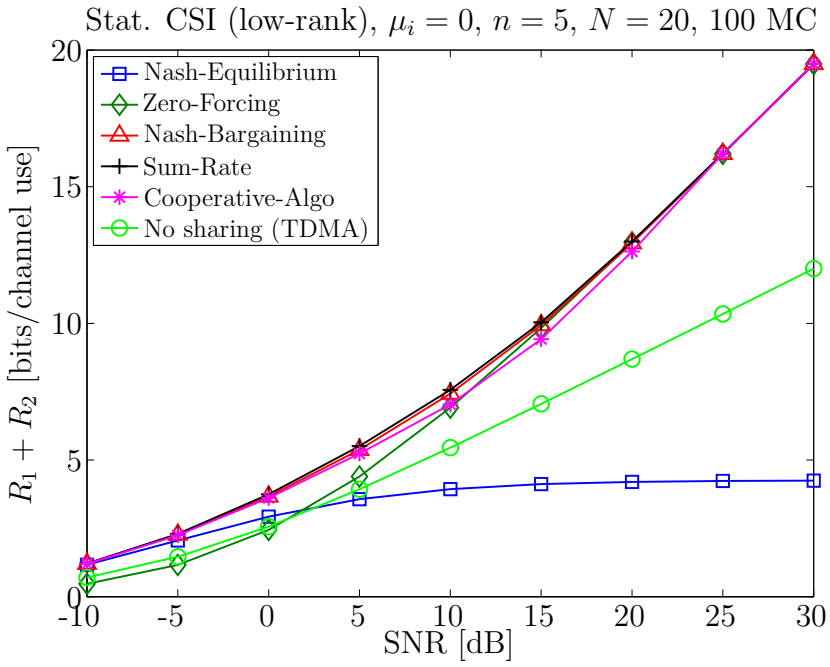

Figure 4.4: Sum rate; stat. CSI (low-rank), $\mu_i = 0$

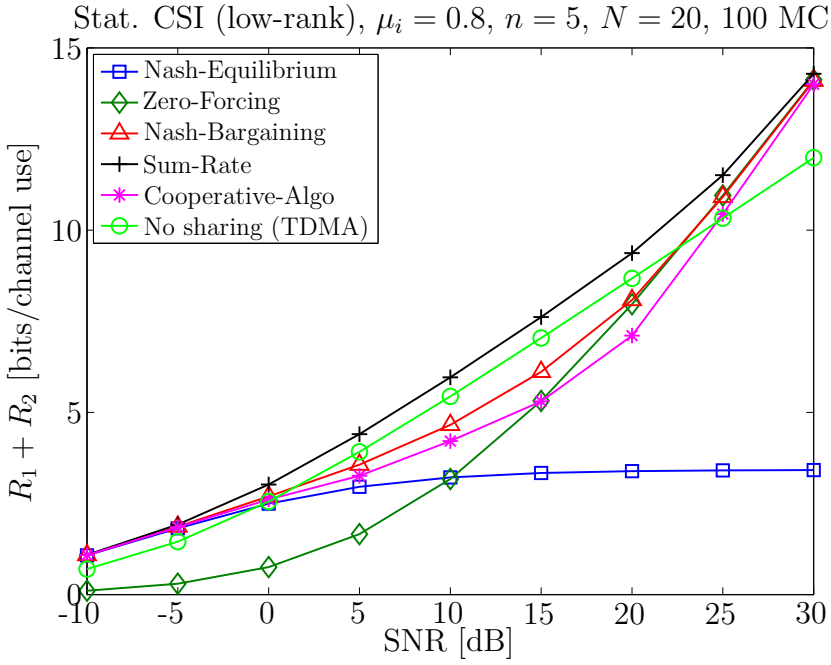

Figure 4.5: Sum rate; stat. CSI (low-rank), $\mu_i = 0.8$

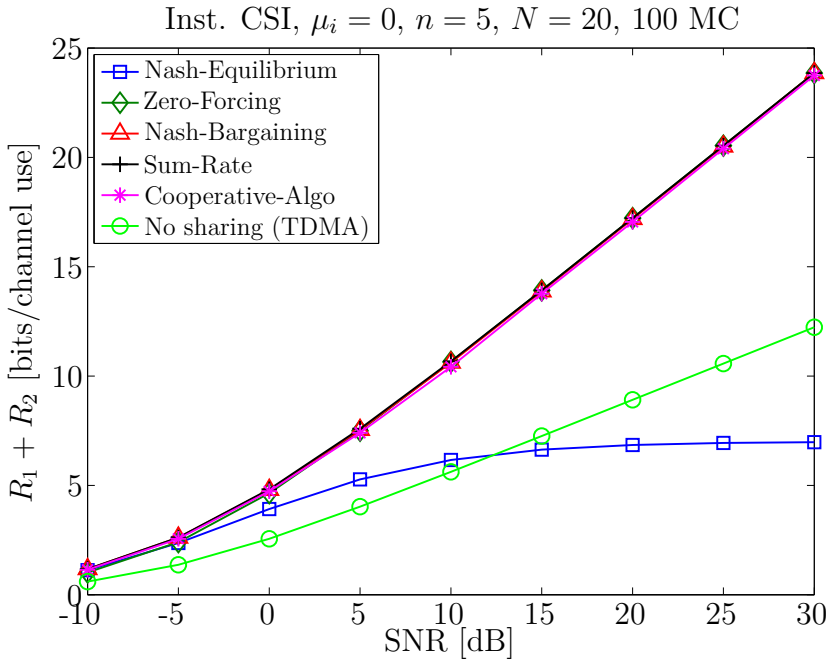

Figure 4.6: Sum rate; inst. CSI, $\mu_i = 0$

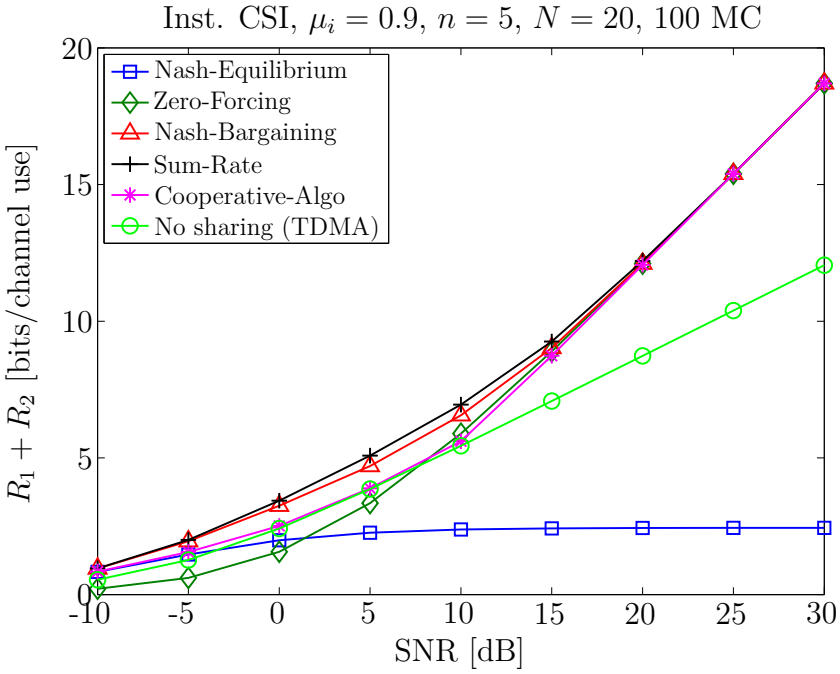

Figure 4.7: Sum rate; inst. CSI, $\mu_i = 0.9$

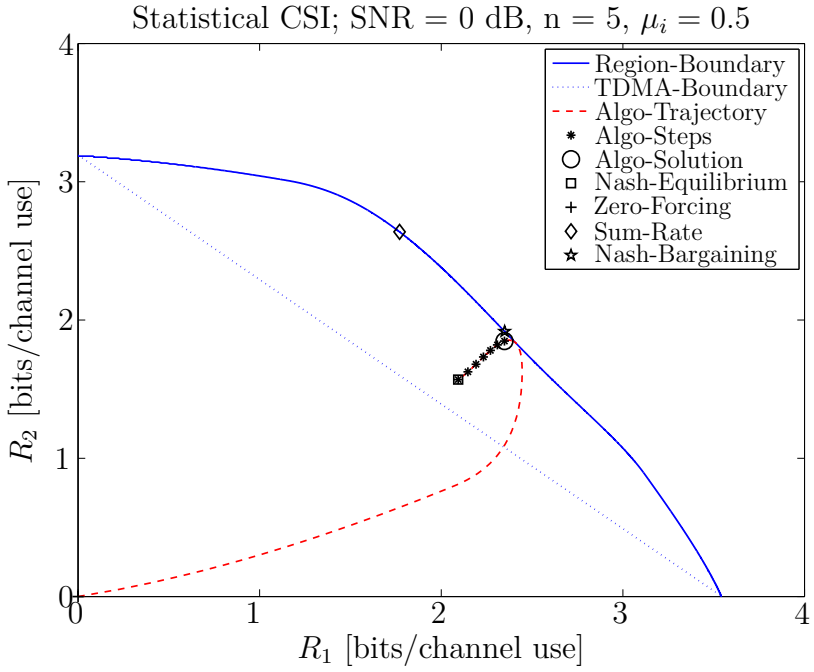

Figure 4.8: Bargaining trajectory; stat. CSI, SNR = 0 dB

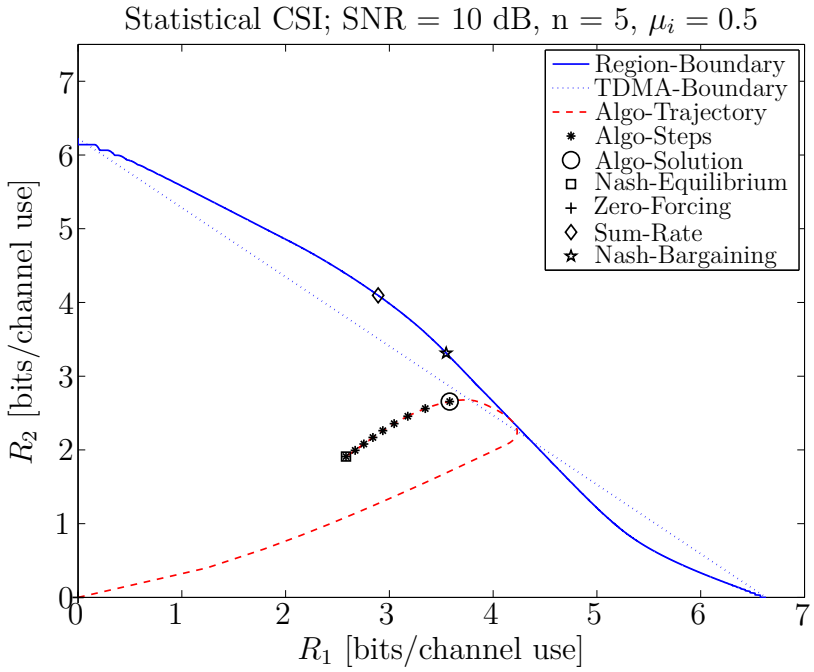

Figure 4.9: Bargaining trajectory; stat. CSI, SNR = 10 dB

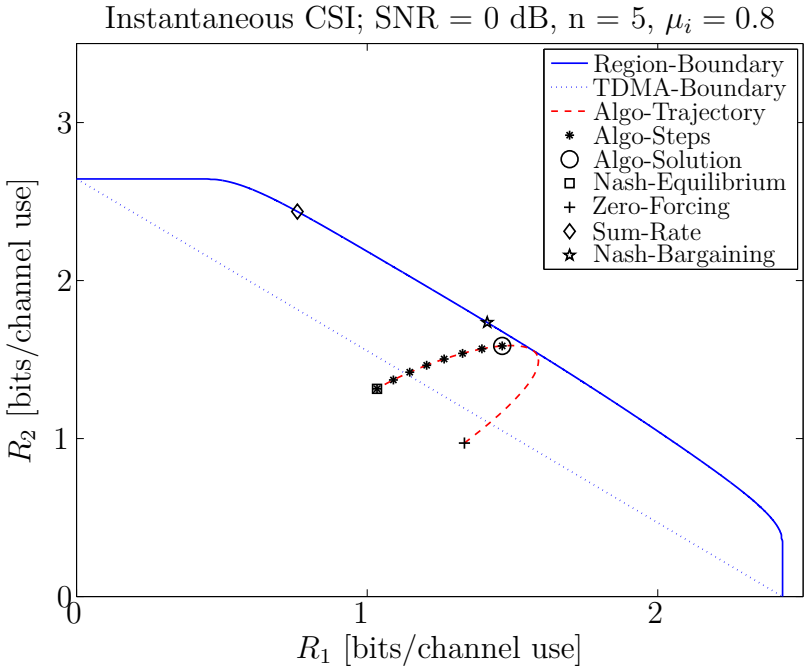

Figure 4.10: Bargaining trajectory; inst. CSI, SNR = 0 dB

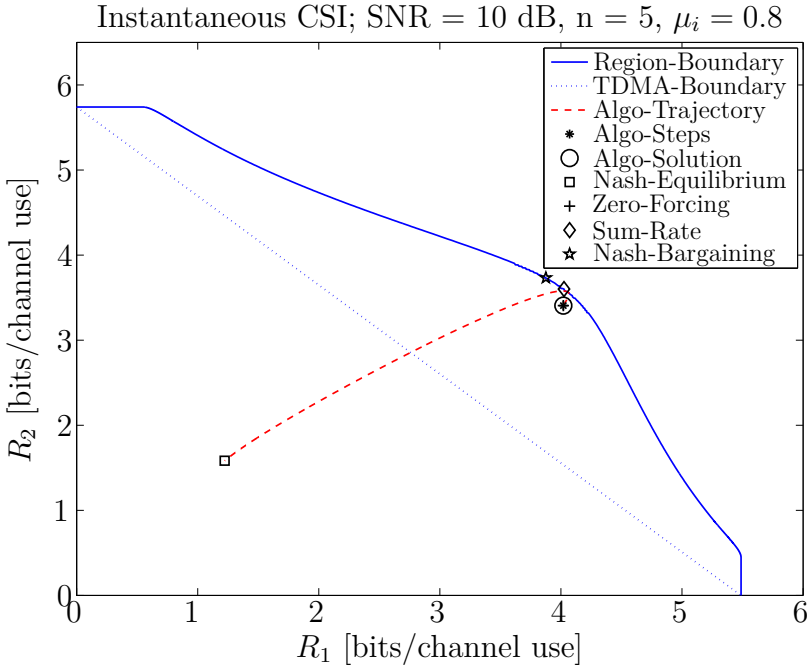

Figure 4.11: Bargaining trajectory; inst. CSI, SNR = 10 dB

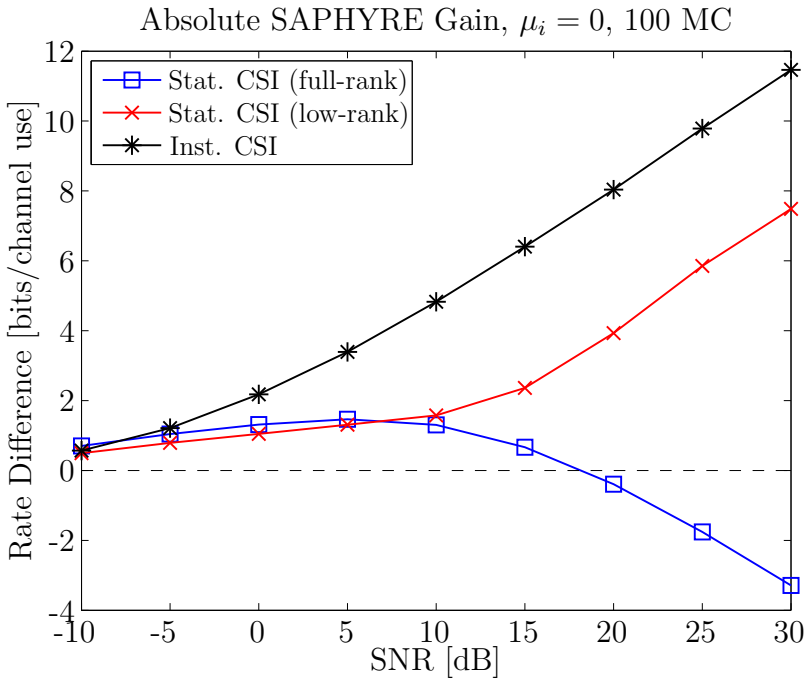

Figure 4.12: Absolute SAPHYRE Gain

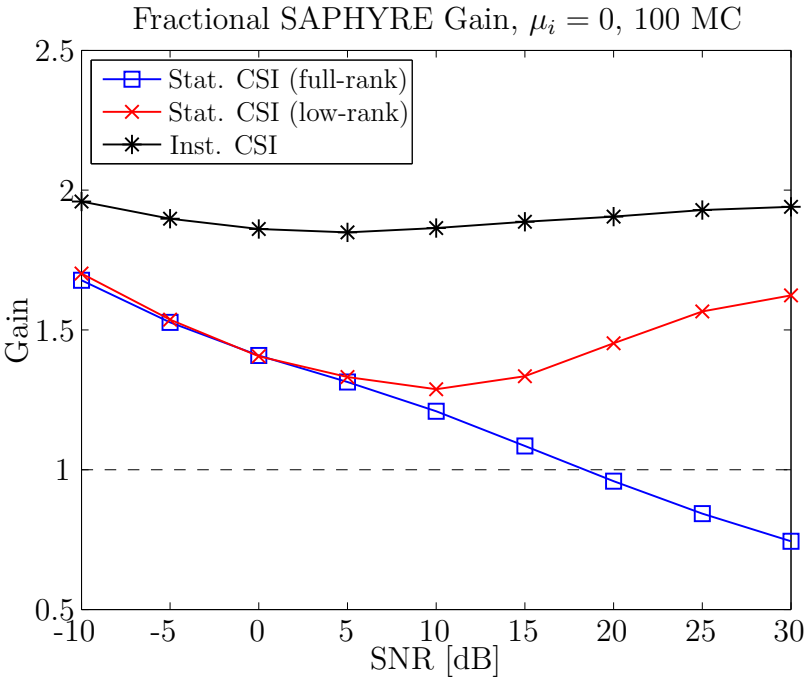

Figure 4.13: Fractional SAPHYRE Gain

4.4.5 The SAPHYRE Gain

Here, we illustrate the SAPHYRE gain of the proposed algorithm over the non-sharing situation as a function of the SNR. In Figure 4.2–4.7 we illustrate the sum-rate of the orthogonal (TDMA) sharing. We see, Figure 4.2 and 4.3, that TDMA sharing performs better than the proposed algorithm for the case of statistical CSI and full-rank covariance matrices and high SNR. Also, for statistical CSI with low-rank covariance matrices and medium SNR, Figure 4.5, the TDMA scheme gives higher rates than our algorithm. In Figure 4.12 and 4.13 we illustrate the absolute and fractional SAPHYRE gains, respectively. The illustrations are made for the weak spatial correlation scenario. For each SNR value we have made 100 Monte-Carlo simulations. The absolute SAPHYRE gain is defined as in (1.1), but for $K = 2$ users. We see that the absolute gain increases with increasing SNR for the scenarios of instantaneous CSI and statistical CSI with low-rank matrices. For statistical CSI the gain starts to decrease at SNR $\approx$ 5dB and becomes negative at SNR $\approx$ 18dB. The reason is that the non-sharing line will be outside the rate region, which follows from the discussion in section 4.4.2 and partly can be seen in Figure 4.9. We define the fractional SAPHYRE gain as in (1.2). In Figure 4.13, we see that the more we know about the channels, the higher is the fractional SAPHYRE gain. For the scenario of instantaneous CSI, we have a fractional gain close to 2.0, i.e., the rate is doubled. Again, we see that scenario of high SNR and statistical CSI with full-rank covariance matrices yield a fractional SAPHYRE gain $\Xi_{\mathrm{F}} < 1$.

From the rate regions in Figure 4.8, 4.10, and 4.11 we see that the orthogonal (TDMA) sharing region lies inside the non-orthogonal sharing region. Also, we notice that the outcome of the proposed algorithm lies outside the TDMA region. Studying Figure 4.9 (statistical CSI and high SNR), we see that the TDMA region does not entirly contained in the nonorthogonal sharing region. The outcome of the algorithm lies south-west of the TDMA boundary. This illustrates why we get $\Xi_{\mathrm{F}} < 1$.

4.5 Conclusions and Future Perspectives

We considered the distributed design of beamforming vectors for the MISO IC. We proposed a cooperative algorithm that achieves an operating point which is almost Pareto optimal. The final solution is in all cases better than the NE, which would be the outcome if there was no cooperation. The novel element of the proposed algorithm is the use of the generated interference level as bargaining value. The algorithm is equally applicable to the case of instantaneous and statistical CSI. We validated the merit of our algorithm via extensive numerical illustrations.

5 Advanced Signal Processing for Relay Assisted Communications

5.1 Introduction

Coverage in wireless cellular networks is an important user-centric performance factor. In order to support cell-edge users with high-data rate services under agile frequency reuse there are several options for service providers and operators. One possibility is to install new small base stations and reduce cell sizes. This leads to femtocells which offer significant advantages for next-generation broadband wireless communication systems [50]. Another approach is to install additional relay stations at certain points in the existing cellular infrastructure [51] to improve coverage by assisting cell edge users in their multiple access attempt to the base station.

Cooperative communications is proposed to improve the reliability in wireless communications [52]. There, multiple wireless devices (possibly user terminals) help each other by relaying messages for each other [53]. In a cellular context, the relay stations are dedicated to assist communications, they do not move and they do not need an artificial incentive for helping the mobile terminals.

5.2 Transmission Techniques for Relay Assisted Interference Channel

5.2.1 Linear Precoding Design for Single Relay Sharing

Abstract. In this work, single-stream transmission in the interference relay channel is studied. Two independent transceiver pairs with multiple antennas communicate with the assistance of one relay, which operates in half-duplex mode and employs an amplify-and-forward strategy. First, the interference relay channel is converted to the conventional interference channel via a preliminarily determined relay amplification matrix. Various relay amplification matrices are investigated for this conversion. Then, the flexible coordinated beamforming for the interference relay channel (IRC FlexCoBF) is proposed for the transceivers. The IRC FlexCoBF algorithm is compared to the alternative schemes proposed in literature. Simulations show that IRC FlexCoBF achieves a better sum rate performance. Furthermore, a higher robustness to the interferences is demonstrated for IRC FlexCoBF compared to the state of the art. At last, simulation results show that by sharing a relay be-

tween two transceiver pairs a significant gain in sum rate can be achieved compared to the relay channel.

Background. The interference channel (IC) models two concurrent point-to-point transmissions interfering each other, which is one of the fundamental building blocks in communication networks. It has been intensely studied over last few decades starting from [26]. Furthermore, it is known since the pioneering work in [54] that relays assisting the communications can significantly improve the end-to-end throughput, outage performance, etc. This has sparkled the interest for finding efficient relaying schemes. In this work, we investigate an IC assisted by a relay which we refer to as the interference relay channel (IRC) as depicted in Figure 5.1, where the relay is accessed by both transmitters jointly. We show the possible advantages of this scheme compared to an exclusive access via TDMA. We can view this issue as a special case of voluntary infrastructure and spectrum sharing.

In this work, a single stream transmission of the IRC is studied. It is shown that the IRC can be simplified to the IC as long as the relay amplification matrix is fixed. First, we summarize several relaying algorithms which are adapted to the IRC. After that precoders designed for the IC can be applied at the transceivers. Inspired by the idea from [55], we propose a linear precoding method. The recent work [56] is taken as a benchmark, where a linear coordinated beamformer was designed under zero interference constraints. Simulations demonstrate that the IRC FlexCoBF achieves a better sum rate performance. Furthermore, the robustness to the interferences is investigated for the IRC FlexCoBF as well as previous methods. Finally, it is observed that there is a sum rate gain of the IRC over the traditional relay channel (RC) that consists of a relay in addition to a point-to-point transmission, which strongly shows the advantage of the relay sharing instead of accessing the relay in a TDMA mode.

System Model. The system model is shown in Figure 5.1, where two base stations (BSs) transmit data to their target user terminals (UTs) with the assistance of a shared relay. In this work, a half-duplex relaying protocol using the amplify-and-forward (AF) strategy is utilized. The BSs and UTs are equipped with $M_{\mathrm{T},i}$ and $M_{\mathrm{U},i}$ antennas respectively, where $i = 1, 2$ denotes the index of each transceiver pair. The relay has M_{R} antennas. We assume that a single data stream per UT is transmitted.

The transmission process is divided into two phases. During the first phase, both BSs transmit to their desired UTs and the relay. The received signal at each UT and the relay is

$$\begin{aligned}
\boldsymbol{y}_1^{(1)} &= \boldsymbol{H}_{11}\boldsymbol{w}_1 s_1 + \boldsymbol{H}_{21}\boldsymbol{w}_2 s_2 + \boldsymbol{n}_1^{(1)}, \\
\boldsymbol{y}_2^{(1)} &= \boldsymbol{H}_{22}\boldsymbol{w}_2 s_2 + \boldsymbol{H}_{12}\boldsymbol{w}_1 s_1 + \boldsymbol{n}_2^{(1)}, \\
\boldsymbol{y}_{\mathrm{R}} &= \boldsymbol{H}_{1\mathrm{R}}\boldsymbol{w}_1 s_1 + \boldsymbol{H}_{2\mathrm{R}}\boldsymbol{w}_2 s_2 + \boldsymbol{n}_{\mathrm{R}},
\end{aligned}$$

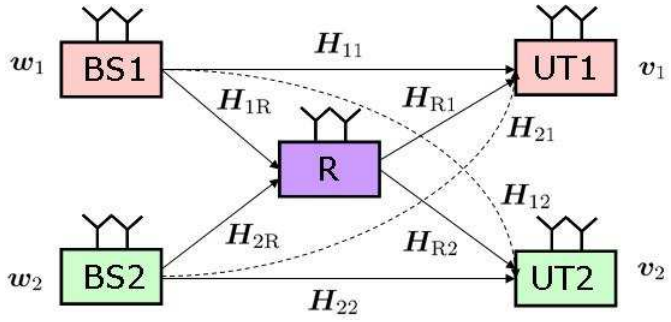

Figure 5.1: Block Diagram of the Interference Relay Channel

where $\boldsymbol{H}_{ij} \in \mathbb{C}^{M_{\mathrm{U},j} \times M_{\mathrm{T},i}}$, $i, j \in \{1, 2, \mathrm{R}\}$ denotes the channel matrices between BSs, UTs, and relay, which are assumed to undergo frequency flat quasi static block fading. The precoder at each BS is $\boldsymbol{w}_i \in \mathbb{C}^{M_{\mathrm{T},i} \times 1}$ and the transmitted data signal is s_i. In the second phase, the relay amplifies the received signal from phase 1 and forwards it to the UTs. The signal vectors received at UTs during phase 2 are given by

$$\begin{aligned}\boldsymbol{y}_1^{(2)} =& \boldsymbol{H}_{\mathrm{R}1}\boldsymbol{A}\boldsymbol{y}_{\mathrm{R}} + \boldsymbol{n}_1^{(2)},\\ \boldsymbol{y}_2^{(2)} =& \boldsymbol{H}_{\mathrm{R}2}\boldsymbol{A}\boldsymbol{y}_{\mathrm{R}} + \boldsymbol{n}_2^{(2)},\end{aligned}$$

where $\boldsymbol{A} \in \mathbb{C}^{M_{\mathrm{R}} \times M_{\mathrm{R}}}$ is the relay amplification matrix. Applying the linear receive filters $\boldsymbol{v}_1^{\mathrm{H}}$ and $\boldsymbol{v}_2^{\mathrm{H}}$ at each UT, we finally get the received signals

$$y_1 = \boldsymbol{v}_1^{\mathrm{H}} \underbrace{\begin{bmatrix}\boldsymbol{H}_{11}\\ \boldsymbol{H}_{\mathrm{R}1}\boldsymbol{A}\boldsymbol{H}_{1\mathrm{R}}\end{bmatrix}}_{\boldsymbol{H}_1} \boldsymbol{w}_1 s_1 + \boldsymbol{v}_1^{\mathrm{H}} \underbrace{\begin{bmatrix}\boldsymbol{H}_{21}\\ \boldsymbol{H}_{\mathrm{R}1}\boldsymbol{A}\boldsymbol{H}_{2\mathrm{R}}\end{bmatrix}}_{\boldsymbol{G}_1} \boldsymbol{w}_2 s_2 + \boldsymbol{v}_1^{\mathrm{H}} \underbrace{\begin{bmatrix}\boldsymbol{n}_1^{(1)}\\ \boldsymbol{H}_{\mathrm{R}1}\boldsymbol{A}\boldsymbol{n}_{\mathrm{R}} + \boldsymbol{n}_2^{(1)}\end{bmatrix}}_{\boldsymbol{e}_1},$$

$$y_2 = \boldsymbol{v}_2^{\mathrm{H}} \underbrace{\begin{bmatrix}\boldsymbol{H}_{22}\\ \boldsymbol{H}_{\mathrm{R}2}\boldsymbol{A}\boldsymbol{H}_{2\mathrm{R}}\end{bmatrix}}_{\boldsymbol{H}_2} \boldsymbol{w}_2 s_2 + \boldsymbol{v}_2^{\mathrm{H}} \underbrace{\begin{bmatrix}\boldsymbol{H}_{12}\\ \boldsymbol{H}_{\mathrm{R}2}\boldsymbol{A}\boldsymbol{H}_{1\mathrm{R}}\end{bmatrix}}_{\boldsymbol{G}_2} \boldsymbol{w}_1 s_1 + \boldsymbol{v}_2^{\mathrm{H}} \underbrace{\begin{bmatrix}\boldsymbol{n}_1^{(2)}\\ \boldsymbol{H}_{\mathrm{R}2}\boldsymbol{A}\boldsymbol{n}_{\mathrm{R}} + \boldsymbol{n}_1^{(2)}\end{bmatrix}}_{\boldsymbol{e}_2},$$

where $\boldsymbol{n}_1^{(i)}$, $\boldsymbol{n}_2^{(i)}$ and $\boldsymbol{n}_{\mathrm{R}}$ contain independent, identically distributed additive white Gaussian noise samples with the variance σ_n^2. It can be seen that the system model can be simplified to a classical two-user IC based on the equivalent channels $\boldsymbol{H}_1, \boldsymbol{H}_2, \boldsymbol{G}_1$, and $\boldsymbol{G}_2$, which requires the relay precoder $\boldsymbol{A}$ to be designed first.

Relay Amplification Matrix Design. In the section, we propose a relay amplification matrix design so that the IRC is converted to an IC. To start, we derive a relay amplification matrix which is inspired by the algebraic norm maximization method (ANOMAX) [57]. Since $\boldsymbol{H}_1$ and $\boldsymbol{H}_2$ are the equivalent channels for the desired signals, maximizing the norm $\beta^2 \|\boldsymbol{H}_1\|_F^2 + (1-\beta)^2 \|\boldsymbol{H}_2\|_F^2$ enhances the desired signal's energy and therefore improves the SNR, where β is the weighting factor

ranging between 0 and 1. The solution of the one-way ANOMAX (OW-ANOMAX) is given by

$$\begin{aligned}
&\arg\max_{\boldsymbol{A},\|\boldsymbol{A}\|_{\mathrm{F}}=1} \beta^2 \|\boldsymbol{H}_1\|_F^2 + (1-\beta)^2 \|\boldsymbol{H}_2\|_F^2 \\
=&\arg\max_{\boldsymbol{A},\|\boldsymbol{A}\|_{\mathrm{F}}=1} \Big\| \underbrace{\big[\beta(\boldsymbol{H}_{1\mathrm{R}} \otimes \boldsymbol{H}_{\mathrm{R}1}^{\mathrm{T}}), (1-\beta)(\boldsymbol{H}_{2\mathrm{R}} \otimes \boldsymbol{H}_{\mathrm{R}2}^{\mathrm{T}})\big]^{\mathrm{T}}}_{\boldsymbol{K}_\beta} \underbrace{\mathrm{vec}\{\boldsymbol{A}\}}_{\boldsymbol{a}} \Big\|_2^2 \\
=&\arg\max_{\boldsymbol{a},\|\boldsymbol{a}\|_2=1} \frac{\boldsymbol{a}^{\mathrm{H}} \boldsymbol{K}_\beta^* \boldsymbol{K}_\beta^{\mathrm{T}} \boldsymbol{a}}{\boldsymbol{a}^{\mathrm{H}} \boldsymbol{a}} \\
=&\lambda_{\max}(\boldsymbol{K}_\beta^* \boldsymbol{K}_\beta^{\mathrm{T}})
\end{aligned}$$

Here, the Kronecker product between two matrices $\boldsymbol{A}$ and $\boldsymbol{B}$ is symbolized by $\boldsymbol{A} \otimes \boldsymbol{B}$. By performing a singular value decomposition (SVD) $\boldsymbol{K}_\beta = \boldsymbol{U}_\beta \cdot \boldsymbol{\Sigma}_\beta \cdot \boldsymbol{V}_\beta^{\mathrm{H}}$, the relay amplification matrix is designed as $\boldsymbol{a} = \boldsymbol{u}_1^*$, where $\boldsymbol{u}_1$ is the first column of $\boldsymbol{U}_\beta$, i.e., the dominant left singular vector of $\boldsymbol{K}_\beta$. There are also other alternatives which are inspired by well-known two-way relaying strategies as follows.

- Dual Channel Matching (DCM) [58]
  $\boldsymbol{A} = \boldsymbol{H}_{\mathrm{R}1}^{\mathrm{H}} \boldsymbol{H}_{1\mathrm{R}}^{\mathrm{H}} + \boldsymbol{H}_{\mathrm{R}2}^{\mathrm{H}} \boldsymbol{H}_{2\mathrm{R}}^{\mathrm{H}}$
- Discrete Fourier Transform (DFT) matrix
  $\boldsymbol{A} = \mathrm{DFT}(\boldsymbol{I}_{M_{\mathrm{R}}})$
- MMSE [59]
  $\boldsymbol{A} = \boldsymbol{A}_{\mathrm{Tx}} \boldsymbol{A}_{\mathrm{Rx}}$
  $\boldsymbol{A}_{\mathrm{Rx}} = \boldsymbol{H}_{\mathrm{Rx}}^{\mathrm{H}} (\boldsymbol{H}_{\mathrm{Rx}} \boldsymbol{H}_{\mathrm{Rx}}^{\mathrm{H}} + \frac{\sigma_n^2}{P_{\mathrm{T}1}+P_{\mathrm{T}2}} \boldsymbol{I}_{M_{\mathrm{R}}})^{-1}$
  $\boldsymbol{A}_{\mathrm{Tx}} = (\boldsymbol{H}_{\mathrm{Tx}}^{\mathrm{H}} \boldsymbol{H}_{\mathrm{Tx}} + \frac{\sigma_n^2}{P_{\mathrm{T}1}+P_{\mathrm{T}2}} \boldsymbol{I}_{M_{\mathrm{R}}})^{-1} \boldsymbol{H}_{\mathrm{Tx}}^{\mathrm{H}}$
  where $\boldsymbol{H}_{\mathrm{Tx}} = \begin{bmatrix} \boldsymbol{H}_{\mathrm{R}1} \\ \boldsymbol{H}_{\mathrm{R}2} \end{bmatrix}$ and $\boldsymbol{H}_{\mathrm{Rx}} = [\boldsymbol{H}_{1\mathrm{R}}, \boldsymbol{H}_{2\mathrm{R}}]$.
- ZF [59]
  $\boldsymbol{A} = \boldsymbol{H}_{\mathrm{Rx}}^{+} \boldsymbol{H}_{\mathrm{Tx}}^{+}$
  The superscript + represent the pseudo inverse. Same $\boldsymbol{H}_{\mathrm{Rx}}$ and $\boldsymbol{H}_{\mathrm{Tx}}$ are used as for MMSE.

We compute $\boldsymbol{A}$ as $\boldsymbol{A} = \gamma \boldsymbol{A}_n$, where $\boldsymbol{A}_n$ is the normalized relay amplification matrix obtained by one of the aforementioned methods such that $||\boldsymbol{A}_n|| = 1$. The scalar γ adjusts the transmit power level, such that the relay transmit power constraint is satisfied. Let $P_{\mathrm{T,R}}$ be the available transmit power at the relay. Then we can find γ via the approximation $\|\gamma \boldsymbol{A}_n \boldsymbol{y}_{\mathrm{R}}\|_2^2 \leq \gamma^2 (M_{\mathrm{T}1} M_{\mathrm{R}} P_{\mathrm{T}1} + M_{\mathrm{T}2} M_{\mathrm{R}} P_{\mathrm{T}2} + M_{\mathrm{R}} \sigma_n^2) = P_{\mathrm{T,R}}$, where $P_{\mathrm{T}1}$ and $P_{\mathrm{T}2}$ are the transmit power of BS1 and BS2 respectively. For simplicity, we choose γ as

$$\gamma = \sqrt{\frac{P_{\mathrm{T,R}}}{M_{\mathrm{T}1} M_{\mathrm{R}} P_{\mathrm{T}1} + M_{\mathrm{T}2} M_{\mathrm{R}} P_{\mathrm{T}2} + M_{\mathrm{R}} \sigma_n^2}}$$

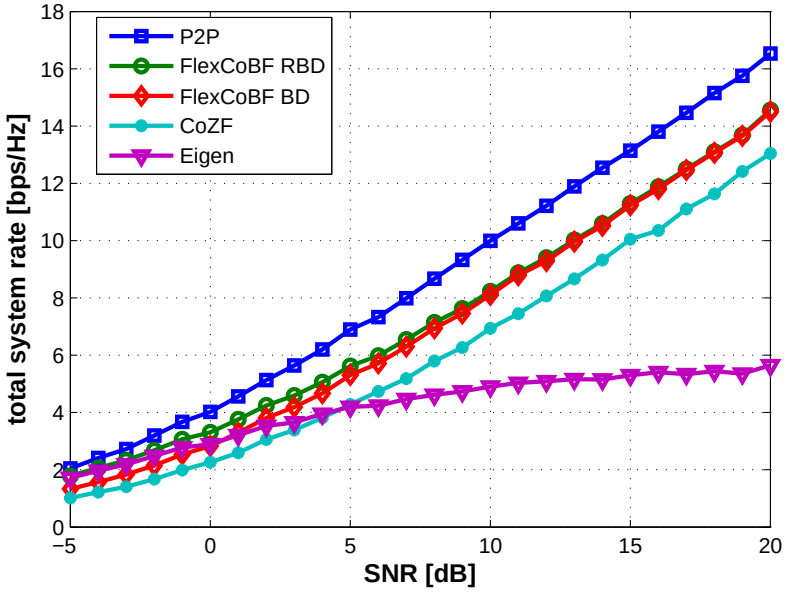

Figure 5.2: Sum rate vs SNR for the interference channel

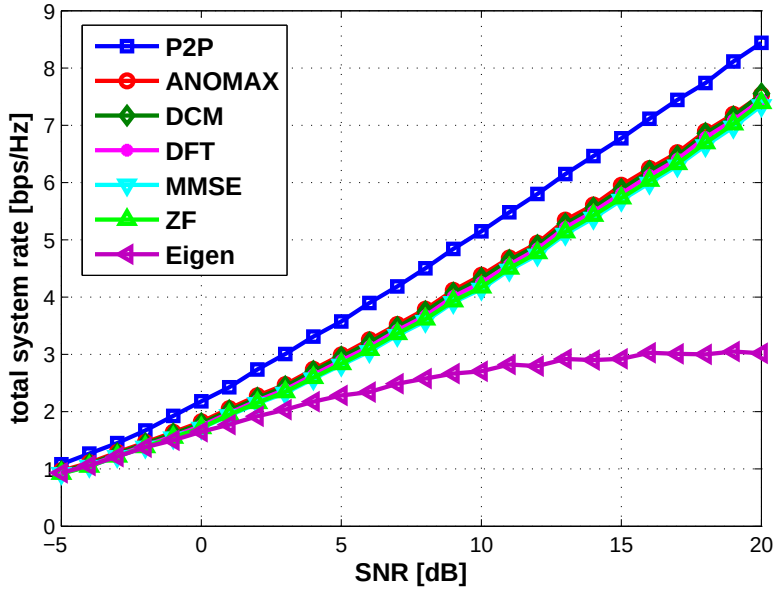

Figure 5.3: Sum rate of the interference relay channel for different relaying strategies

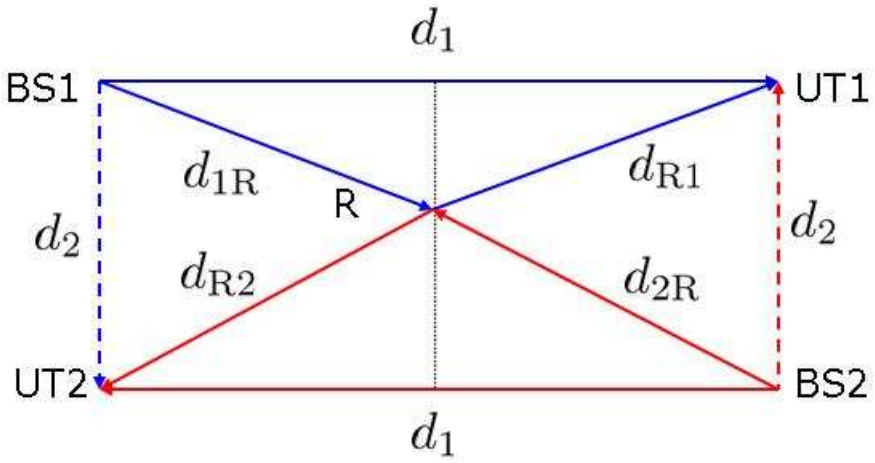

Figure 5.4: Path loss model of the interference relay channel

Precoder Design at the BSs. After the design of $\boldsymbol{A}$, all the equivalent channel matrices $\boldsymbol{H}_i$ and the interference matrices $\boldsymbol{G}_i$ can be estimated from the downlink dedicated pilot transmission. Then the IRC corresponds to a conventional IC model. We assume that $\boldsymbol{H}_i$ and $\boldsymbol{G}_i$ are available at the BSs. At this point, no path loss is considered.

A recent technique dealing with linear precoding design at the BSs for the IC is named zero-forcing coordinated beamforming (CoZF) [56], which forces all the interferences to be zero assuming maximum ratio combining (MRC) at the receiver $\boldsymbol{v}_i = \boldsymbol{H}_i\boldsymbol{w}_i$ for $i = 1, 2$. The precoders are chosen as a generalized eigenvector of $\boldsymbol{G}_i^{\mathrm{H}}\boldsymbol{H}_i$ and $\boldsymbol{H}_j^{\mathrm{H}}\boldsymbol{G}_j$ for $i, j = 1, 2$ and $i \neq j$. Although simple, this method has the dimensionality constraint that $M_{\mathrm{T},i} \leq M_{\mathrm{U},j}$ due to the full rank requirement of these equivalent channel matrices.

Taking [56] as a benchmark, we propose a method called flexible coordinated beamforming for the interference relay channel (IRC FlexCoBF) to improve the system sum rate performance and relax the dimensionality constraint. The original FlexCoBF algorithm [55] has been designed to iteratively suppress the inter-user interferences on the downlink of the multi-user MIMO systems, which utilizes either block diagonalization (BD) [60] or regularized block diagonalization (RBD) [61] at the transmitter combined with MRC at the receiver. Inspired by this idea, we derive a method suitable for the IC.

To start, the receive beamformer $\boldsymbol{v}_1$, $\boldsymbol{v}_2$ are randomly initialized. In the following, we sketch the design of $\boldsymbol{w}_2$ ($\boldsymbol{w}_1$ is designed analogously) If BD is applied at the BS2, we take the SVD of the equivalent interference channel $\tilde{\boldsymbol{g}}_1^{\mathrm{T}} = \boldsymbol{v}_1^{\mathrm{H}}\boldsymbol{G}_1 = 1 \cdot \tilde{\boldsymbol{\sigma}}_1^{\mathrm{T}} \cdot [\tilde{\boldsymbol{v}}_1^{(1)}\ \tilde{\boldsymbol{V}}_1^{(0)}]^{\mathrm{H}}$, where the signal subspace and the null subspace of $\tilde{\boldsymbol{g}}_1^{\mathrm{T}}$ is spanned by the columns of $\tilde{\boldsymbol{v}}_1^{(1)} \in \mathbb{C}^{M_T}$ and $\tilde{\boldsymbol{V}}_1^{(0)} \in \mathbb{C}^{M_T \times (M_T - 1)}$, respectively. In order to maximize the throughput of the second transceiver pair under zero-interference constraint to user 1, we take the SVD on the equivalent channel $\boldsymbol{v}_2^{\mathrm{H}}\boldsymbol{H}_2\tilde{\boldsymbol{V}}_1^{(0)} = 1 \cdot \tilde{\boldsymbol{\sigma}}_2^{\mathrm{T}} \cdot \tilde{\boldsymbol{V}}_2^{\mathrm{H}}$ and the precoder $\boldsymbol{w}_2$ is obtained as $\boldsymbol{w}_2 = \tilde{\boldsymbol{V}}_1^{(0)}\tilde{\boldsymbol{v}}_2$, where $\tilde{\boldsymbol{v}}_2$ is the dominant singular vector

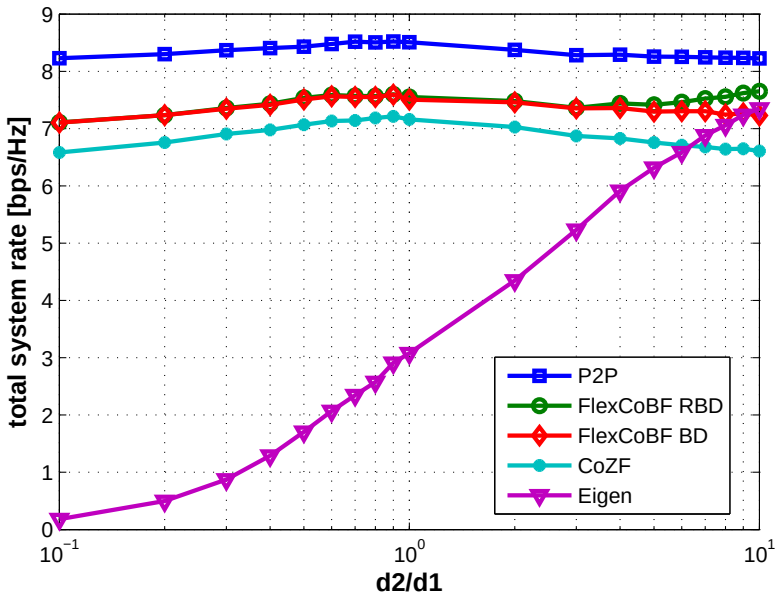

Figure 5.5: Sum rate for interference relay channel path loss model at SNR = 20 dB

of $\tilde{\boldsymbol{V}}_2$. On the other hand, when RBD is applied at the BS2, the precoder is designed in two steps. Let $\boldsymbol{w}_2 = \beta \boldsymbol{W}_{2a}\boldsymbol{w}_{2b}$, where $\boldsymbol{W}_{2a}$ is used to suppress the interference, $\boldsymbol{w}_{2b}$ facilitates the sum rate optimization of the second link, and β is a real factor that scales the transmit power. Assuming that $||\boldsymbol{w}_{2b}|| = 1$ and that the s_i are temporally uncorrelated with zero mean and unit variance $\mathbb{E}\{|s_i|^2\} = 1$, we have $\beta^2||\boldsymbol{W}_{2a}\boldsymbol{w}_{2b}s_i||^2 = \beta^2||\boldsymbol{W}_{2a}||^2 \leq P_{T2}$. Therefore, we choose $\beta = P_{\mathrm{T2}}/\mathrm{tr}\{\boldsymbol{W}_{2a}\boldsymbol{W}_{2a}^{\mathrm{H}}\}$ with P_{T2} denoting the transmit power of BS2. After computing the SVD of $\tilde{\boldsymbol{g}}_1^{\mathrm{T}} = \boldsymbol{v}_1^{\mathrm{H}}\boldsymbol{G}_1 = 1 \cdot \tilde{\boldsymbol{\sigma}}_1^{\mathrm{T}} \cdot \tilde{\boldsymbol{V}}_1^{\mathrm{H}}$, we get $\boldsymbol{W}_{2a} = \boldsymbol{M}_{2a}\boldsymbol{D}_{2a}$, where $\boldsymbol{M}_{2a} = \tilde{\boldsymbol{V}}_1$ and $\boldsymbol{D}_{2a} = (\tilde{\boldsymbol{\sigma}}_1\tilde{\boldsymbol{\sigma}}_1^{\mathrm{T}} + \frac{M_{\mathrm{R}}\sigma_n^2}{P_{\mathrm{T2}}}\boldsymbol{I}_{M_{\mathrm{T},1}})^{-1/2}$ is a diagonal power loading matrix. The vector $\boldsymbol{w}_{2b}$ is obtained from the SVD of the equivalent channel $\boldsymbol{v}_2^{\mathrm{H}}\boldsymbol{H}_2\boldsymbol{W}_{2a} = 1 \cdot \tilde{\boldsymbol{\sigma}}_2^{\mathrm{T}} \cdot \tilde{\boldsymbol{V}}_2^{\mathrm{H}}$ as $\boldsymbol{w}_{2b} = \tilde{\boldsymbol{v}}_2$, where $\tilde{\boldsymbol{v}}_2$ is the right dominant singular vector of $\boldsymbol{v}_2^{\mathrm{H}}\boldsymbol{H}_2\boldsymbol{W}_{2a}$. A similar procedure can be obtained for $\boldsymbol{w}_1$. With this transmit precoder obtained from either BD or RBD, the receive filter is updated as $\boldsymbol{v}_i = \boldsymbol{H}_i\boldsymbol{w}_i$ $(i = 1, 2)$ for the next iteration. The procedure continues until the stopping criterion is fulfilled, i.e., the interference is below a predefined threshold.

Simulation Results. We assume that perfect link adaptation and perfect synchronization can be achieved. Each element of the $\boldsymbol{H}_{ij}$ is a zero mean circularly symmetric complex Gaussian random variable with unit variance $\mathcal{CN}(0, 1)$. The transmit power of the BSs is $P_{\mathrm{T1}} = P_{\mathrm{T2}} = P_{\mathrm{T}}$ and the SNR is defined as $P_{\mathrm{T}}/\sigma_n^2$.

The sum rate performance of the IC is given in Figure 5.2 including IRC FlexCoBF as well as CoZF. Both transmitters and receivers are equipped with 2 antennas. As a reference, we also include an upper bound (P2P transmission) and a reference

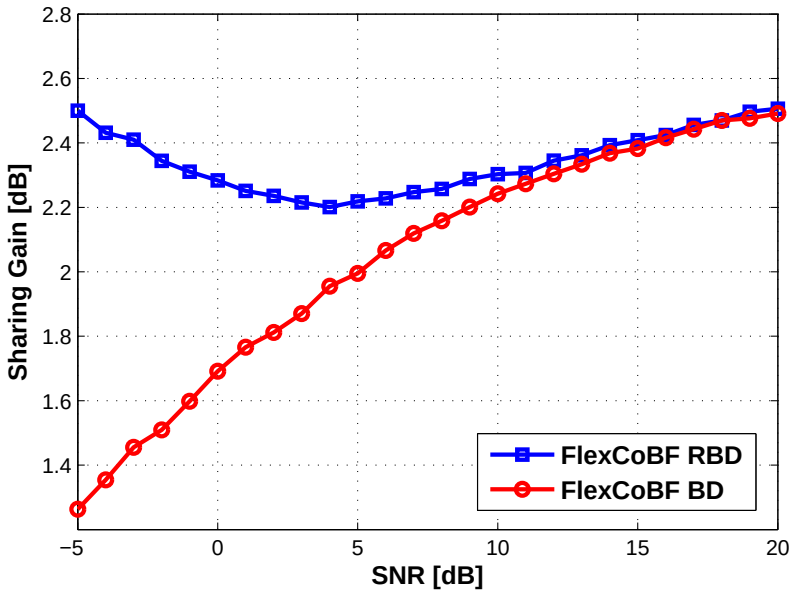

Figure 5.6: Sharing gain of the IRC over the RC

scheme (Eigen), by performing eigen-beamforming for both links without and with taking the interference into account, respectively. It is observed that IRC FlexCoBF with either RBD or BD performs much better than CoZF within all SNR ranges. Especially at low SNRs, CoZF performs even worse than Eigen. IRC FlexCoBF RBD improves the sum rate compared to BD because it allows some residual interferences to balance with the noise enhancement. After that by fixing the precoders at the BSs using IRC FlexCoBF RBD, different relaying strategies are compared, as shown in Figure 5.3. We observe that all the proposed AF relay precoders almost give the same sum rate, of which OW-ANOMAX with $\beta = 0.5$ performs slightly better than others. With respect to the complexity consideration, we propose to use the DFT as the relay amplification matrix and use it in the following simulations.

Furthermore, a path loss model is introduced to test the robustness to the interference of the proposed method compared to the CoZF in [56]. As shown in Figure 5.4, the distance between the BSs and the UTs is d_1 and that the distance between these two interfering links is d_2. The relay is assumed to be in the center of the two interfering links, which means $d_{1\mathrm{R}} = d_{\mathrm{R}1} = \frac{\sqrt{d_1^2+d_2^2}}{2}$ and $d_{2\mathrm{R}} = d_{\mathrm{R}2} = \frac{\sqrt{d_1^2+d_2^2}}{2}$. The channel is constructed by scaling the channel matrix with unit variance channel coefficients by $d^{-\frac{\alpha}{2}}$, where α is the path loss exponent.

By using the DFT as the relay amplification matrix with $M_{\mathrm{R}} = 2$, Figure 5.5 depicts the sum rate depending on the ratio of d_2/d_1 for the path loss model of the IRC for SNR $= 20\,\mathrm{dB}$. When d_2/d_1 is small, it means that strong interferences exist between the two transceiver pairs. On the other hand, a larger d_2/d_1 results in weaker interferences. It can be seen that all types of the precoders except Eigen are resistant to the interferences. Furthermore, as d_2/d_1 increases, the gap between

IRC FlexCoBF RBD and IRC FlexCoBF BD as well as CoZF is even larger due to a smaller loss caused by the interference mitigation. When the interference is quite small, IRC FlexCoBF converges to the P2P bound.

We refer to the ratio of throughput (TP) $\mathrm{TP}_{\mathrm{IRC}}$ / $\mathrm{TP}_{\mathrm{RC}}$ as the *sharing gain* due to the use of the shared relay instead of accessing the relay in a TDMA mode. This sharing gain of the IRC over the RC is shown in Figure 5.6, where IRC FlexCoBF and Eigen are applied at the BS for the IRC and the RC, respectively. It can be seen that the IRC utilizing either IRC FlexCoBF RBD or IRC FlexCoBF BD provides a sharing gain over RC which uses the relay exclusively. For IRC FlexCoBF BD, the sharing gain becomes larger as the SNR increases. When IRC FlexCoBF RBD is applied, there is even an improvement at low SNRs due to the regularization of RBD. This shows that relay sharing is more advantageous compared to the exclusive use of the infrastructure resources (i.e., the relay in the considered scenario).

Conclusions. In this work, the linear precoding design for the interference relay channel is studied. Various relaying strategies are investigated for this scenario. First we consider the conversion of the IRC to the IC, where we propose to use the DFT as the relay amplification matrix. After that we recommend the precoding method IRC FlexCoBF at the BSs, which achieves a better sum rate performance compared to CoZF as well as eigen-beamforming [56]. IRC FlexCoBF is also more robust to the interference. Last but not least, the sum rate performance of the IRC is compared to the RC and there exists a large sharing gain, which strongly supports the use of a shared relay instead of operating in the TDMA mode.

5.2.2 Game Theory Based Resource Allocation

Abstract. The issue of resource allocation for MSE minimization in a DS/CDMA relay-assisted interference channel is addressed in this paper. The resource allocation process is assumed to take place in a hierarchical way. First, the relay announces his amplify-and-forward matrix, and then the multiple access users non-cooperatively react to the relay's choice. From a game-theoretic point of view, this process is well-modeled as a two-level Stackelberg game, with the relay as the leader, and the multiple access users as followers. First, the best response dynamics and the Nash Equilibria for the non-cooperative game played by the followers are derived for a given relay matrix. Then, the problem of optimum relay matrix design is dealt with.
Finally, numerical results corroborating the theoretical results are provided, showing the merits of the proposed resource allocation techniques.

Introduction. Coverage in wireless cellular networks is an important user-centric performance factor. In order to support cell-edge users with high-data rate services

under agile frequency reuse there are several options for service providers and operators. One possibility is to install new small base stations and reduce cell sizes. This leads to femtocells which offer significant advantages for next-generation broadband wireless communication systems [50]. Another approach is to install additional relay stations at certain points in the existing cellular infrastructure [62, 51] to improve coverage by assisting cell edge users in their multiple access attempt to the base station.

Cooperative communications is proposed to improve reliability in wireless communications [63, 52]. There, multiple wireless devices (possibly user terminals) help each other by relaying messages for each other [53, 64]. In a cellular context, the relay stations are dedicated to assist communications, they do not move and they do not need an artificial incentive for helping the mobile terminals.

In this work, we consider a relay-assisted interference channel (IC), in which multiple terminals simultaneously use one relay to transmit their data to separate receiver nodes. In a cellular context, this models the case in which one relays assists mobiles from different service providers in communication with their separate base stations. This is an instance of *infrastructure sharing* since the relay is used by multiple operators.

The combination of code-division multiple-access (CDMA) communications systems with cooperative protocols is studied in [65]. There, a MMSE multiuser detector is used to suitably combine the signals from the direct and the relay path. An additional diversity gain is observed. In [66], decode-and-forward, and amplify-and-forward are applied as relay schemes and the SINR and bit error rate performance achieved by linear multiuser detection is analyzed. The uplink capacity of a multihop cellular system design is studied in [67]. The cell is divided into inner and outer region in which the mobiles communicate directly to the base station or to a relay node. The results indicate that the capacity can be improved significantly by the use of relay nodes. Random CDMA for amplify-and-forward relay channels is studied in [68]. The optimal and the linear MMSE receiver are compared in terms of mutual information.

Relaying is well studied for single- and multiple-antenna channels. Amplify-and-forward and decode-and-forward relaying with different multiple access protocols and space-time signal processing is discussed in [69] with respect to average and outage performance. The application of space-time codes is also studied. The cross-layer joint optimization of relay strategies and resource allocations in cooperative cellular networks is studied in [70]. In [71], resource allocation for MIMO half-duplex relay in cellular systems is addressed.

In this paper, we study the achievable MSE performance of a relay assisted IC in which the mobiles act selfishly to find their signature sequences, while the relay determines its amplify-and-forward matrix based on a system wide utility function. The conflict situation is modeled as a two-level Stackelberg game in normal form

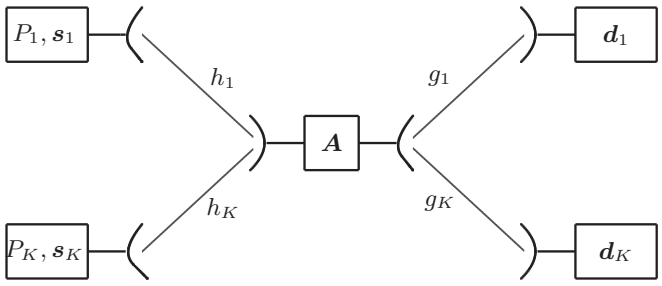

Figure 5.7: Relay-assisted IC system

[72], [73], with the relay as the leader, and the non-cooperating terminals as followers. First we present the system model and formally state the considered problem. Then, we solve the problems of individual MSE minimization, given the relay matrix, and of optimum relay matrix design, respectively. Finally illustrations about the theoretical results, and concluding remarks are provided.

Consider a relay-assisted, synchronous, K-user IC as in Figure 5.7. Direct sequence code division multiple access (DS/CDMA) with processing gain N, is considered as multiple access technique. Assuming flat fading, the discrete-time model of the signal received by the relay in each symbol interval, is the N-dimensional received vector

$$\boldsymbol{y}_r = \sum_{k=1}^{K} \sqrt{P_k}\boldsymbol{h}_k b_k \boldsymbol{s}_k + \boldsymbol{n}_r = \boldsymbol{S}\boldsymbol{P}^{1/2}\mathbf{H}\boldsymbol{b} + \boldsymbol{n}_r \ , \tag{5.1}$$

where P_k, b_k, and $\boldsymbol{s}_k$ are the transmit power, the unit-modulus information symbol, and the unit-norm spreading code of the k-th user, respectively; $h_k e^{j\phi_k}$ is the channel gain between the k-th user and the relay, modeled as a realization of a zero-mean complex Gaussian random process with covariance matrix $\boldsymbol{I}_N$; $\boldsymbol{n}_r$ is the thermal noise at the relay, assumed to be a zero-mean white Gaussian random process with covariance matrix $\sigma^2\boldsymbol{I}_N$, and where we have defined the matrices $\boldsymbol{S} = [\boldsymbol{s}_1 \dots \boldsymbol{s}_K]$, $\boldsymbol{P} = \mathrm{diag}\,(P_1 \dots P_K)$, $\mathbf{H} = \mathrm{diag}\left(h_1 e^{j\phi_1} \dots h_K e^{j\phi_K}\right)$, and the vector $\boldsymbol{b} = [b_1 \dots b_K]^T$.

At the relay, the received signal is first normalized by a factor $\sqrt{P_t}$ where, $P_t = E[\|\boldsymbol{y}_r\|^2] = \sum_{k=1}^{K} P_k h_k^2 + \sigma^2 N^2$, and we have assumed that the information symbols and the noise are all independent of one another. Then, the received vector is linearly processed by the matrix $\mathbf{A}$, yielding the vector $\mathbf{A}\boldsymbol{y}_r = \frac{1}{\sqrt{P_t}}\mathbf{A}(\boldsymbol{S}\boldsymbol{P}^{1/2}\mathbf{H}\boldsymbol{b} + \boldsymbol{n}_r)$, with the power constraint $\mathrm{Tr}\{(\mathbf{A}^H\mathbf{A})\} = N^2$.

Finally, the signal is forwarded to the K IC terminals. We assume that each transmitter is interested in communicating with just one of the IC terminals, and therefore we can denote each transmitter-receiver link by the same index k. Then, considering the case when a direct link between transmitters and receivers is not available, and assuming a flat fading channel between the relay and the receivers, the signal

received by the k-th receiver, is

$$\boldsymbol{y}_k = \boldsymbol{g}_k \left(\sum_{k=1}^{K} \sqrt{P_k} \boldsymbol{h}_k b_k \mathbf{A} \boldsymbol{s}_k + \mathbf{A} \boldsymbol{n}_r \right) + \boldsymbol{n}_k \tag{5.2}$$

where $\boldsymbol{g}_k$ accounts for the power normalization term P_t, and for the channel gain between the relay and the k-th receiver, modeled as a realization of a zero-mean complex Gaussian random process with covariance matrix $\boldsymbol{I}_N$, and $\boldsymbol{n}_k$ is the thermal noise at the receiver, assumed to be a zero-mean white Gaussian random process with covariance matrix $\sigma^2 \boldsymbol{I}_N$. Note that the relay processing colors the noise, unless the relay matrix is set to the identity matrix. Indeed, the overall noise covariance matrix is $\mathbf{W}_k = \sigma^2 \left(g_k^2 \mathbf{A}\mathbf{A}^H + \boldsymbol{I}_N \right)$, while the covariance matrix of the received data vector at the k-th receiver is $\boldsymbol{R}_k = \mathbf{A}\boldsymbol{S}\boldsymbol{D}_k\boldsymbol{S}^H\mathbf{A}^H + \mathbf{W}_k$, with $\boldsymbol{D}_k = g_k^2 \mathbf{H}\boldsymbol{P}\mathbf{H}^H$. We point out that this model can be specialized to the relevant case where only one receiver is present, which models the uplink of a relay-assisted multiple access channel (MAC), and all results that will be derived in the sequel, will also hold for relay-assisted MACs.

In the sequel the problem of non-cooperative spreading code and linear receiver choice for individual MSE minimization, and the problem of relay matrix design for global MSE minimization, will be addressed from a game-theoretic point of view. The resource allocation process is assumed to take place in a hierarchical way. First, the relay chooses his amplify-and forward matrix, and announces it to all users. Then, the multiple access users non-cooperatively react to the relay's choice by selfishly choosing their spreading codes and linear receive filters. This decision-making process is well-modeled by a two-level Stackelberg game. In their more general form, Stackelberg games have multiple levels of hierarchy, with players on higher hierarchical levels, termed as leaders, going first and publicly announcing their strategies, whereas players on lower hierarchical levels, termed as followers, non-cooperatively react to the leaders' strategies. For the case at hand there is one leader, the relay, and many followers, the multiple access users.

In the sequel, we will first focus on the non-cooperative game that is played by the multiple access users after the relay matrix $\mathbf{A}$ has been announced, and then we will turn to the problem of optimum relay matrix design.

Non-Cooperative MSE Minimization. In this part we address the problem of optimum spreading code and receive filter choice for non cooperative, individual MSE minimization in a relay-assisted IC, given the relay matrix $\mathbf{A}$. We will assume that each transmitter knows the matrices $\boldsymbol{P}$, and $\mathbf{H}$. Instead, we do not assume that the coefficients $\{g_k\}_{k=1}^K$ are known to the users. We remark that this is a typical situation in the considered amplify-and-forward relay-aided system, where no direct link between transmitters and receivers is present. Each player's goal is to minimize his own Mean Square Error (MSE), with respect to his transmit spreading

code $\boldsymbol{s}_k$, and to the corresponding linear filter at the receiver $\boldsymbol{c}_k$. Formally, the proposed non-cooperative game can be described in normal form as $\{\mathcal{K}, \mathcal{A}_k, u_k\}$, where $\mathcal{K} = 1, \ldots, K$ is the set of players, $\mathcal{A}_k = \mathbb{C}^N \times \mathbb{C}_1^N$ is the k-th player's strategy space, and $u_k = \mathrm{MSE}_k$ is the k-th player's utility function. Then, for all $k = 1, \ldots, K$, the best response of player k is

$$\arg \min_{\boldsymbol{s}_k, \boldsymbol{c}_k} u_k(\boldsymbol{s}_k, \boldsymbol{c}_k) \; . \tag{5.3}$$

Assuming a linear receive filter $\boldsymbol{c}_k$ is used, the mean square error for user k is

$$\mathrm{MSE}_k = 1 + \boldsymbol{c}_k^H \boldsymbol{R}_k \boldsymbol{c}_k - 2\mathrm{Re}\left(\boldsymbol{g}_k \sqrt{P_k} \boldsymbol{h}_k \boldsymbol{c}_k^H \mathbf{A} \boldsymbol{s}_k\right) . \tag{5.4}$$

Minimization of (5.4) with respect to $\boldsymbol{c}_k$ yields the MMSE receiver, which for the case at hand can be expressed as

$$\boldsymbol{c}_k = \boldsymbol{g}_k \sqrt{P_k} \boldsymbol{h}_k \boldsymbol{R}_k^{-1} \mathbf{A} \boldsymbol{s}_k \; . \tag{5.5}$$

Minimization with respect to $\boldsymbol{s}_k$ with the constraint $\|\boldsymbol{s}_k\|^2 = 1$ can be carried out with standard Lagrangian techniques. After some algebra we get

$$\boldsymbol{s}_k = \frac{\mathbf{A}^H \boldsymbol{c}_k}{\|\mathbf{A}^H \boldsymbol{c}_k\|} \; . \tag{5.6}$$

Then, defining the vector $\boldsymbol{d}_k = \mathbf{A}^H \boldsymbol{c}_k$, we obtain the following best response dynamics for all $k = 1, \ldots, K$.

$$\begin{cases} \boldsymbol{d}_k = \boldsymbol{g}_k \sqrt{P_k} \boldsymbol{h}_k \mathbf{A}^H \boldsymbol{R}_k^{-1} \mathbf{A} \boldsymbol{s}_k \\ \boldsymbol{s}_k = \dfrac{\boldsymbol{d}_k}{\|\boldsymbol{d}_k\|} \end{cases} \tag{5.7}$$

In the following, for brevity's sake we assume that the relay matrix is full-rank. However, all the results that will be derived, hold for singular relay matrices as well, but we omit details due to space limitations. Now, upon defining the effective received data, and noise covariance matrices

$$\begin{aligned} \mathbf{B}_k &= \mathbf{A}^{-1} \boldsymbol{R}_k \mathbf{A}^{-H} = \boldsymbol{S} \boldsymbol{D}_k \boldsymbol{S}^H + \boldsymbol{N}_k \\ \boldsymbol{N}_k &= \mathbf{A}^{-1} \mathbf{W}_k \mathbf{A}^{-H} = \sigma^2 ((\mathbf{A}^H \mathbf{A})^{-1} + g_k^2 \boldsymbol{I}) \end{aligned} \tag{5.8}$$

we can finally express the best response dynamics for all $k = 1, \ldots, K$ as

$$\begin{cases} \boldsymbol{d}_k = \boldsymbol{g}_k \sqrt{P_k} \boldsymbol{h}_k \left(\boldsymbol{S} \boldsymbol{D}_k \boldsymbol{S}^H + \boldsymbol{N}_k\right)^{-1} \boldsymbol{s}_k \\ \boldsymbol{s}_k = \dfrac{\boldsymbol{d}_k}{\|\boldsymbol{d}_k\|} \end{cases} \tag{5.9}$$

Iterations (5.9) resembles the well-known MMSE update algorithm for interference avoidance, [74], [75], [76]. However, the presence of different coefficients $\{g_k\}_{k=1}^K$ makes things more involved with respect to the original algorithm. In particular, the convergence proof that is to be found in [74] cannot be straightforwardly extended to this case. Luckily, the following result holds

Results. For any initial signature matrix, iterations (5.9) always converge.

As for the fixed points of (5.9), we have the following result: Let $\boldsymbol{D} = \mathbf{H}\boldsymbol{P}\mathbf{H}^H$. Then, at the fixed point of (5.9) the matrices $\boldsymbol{S}\boldsymbol{D}\boldsymbol{S}^H$ and $\mathbf{A}^H\mathbf{A}$ commute, and the set of fixed points of iterations (5.9) is the set of all matrices whose columns are unit-norm eigenvectors of $\boldsymbol{S}\boldsymbol{D}\boldsymbol{S}^H$ and $\mathbf{A}^H\mathbf{A}$.

In the following, we derive the Nash Equilibria for the proposed non-cooperative game, and we address the problem of optimum relay matrix design. Due to space limitations, the focus will be on underloaded systems ($K \leq N$). However, we point out that all results can be extended to the overloaded case, too.

Nash Equilibria in an Underloaded IC. Assume $K \leq N$, and denote by $\{g_k^2\lambda_k\}_{k=1}^K$ the eigenvalues of $\boldsymbol{S}\boldsymbol{D}_k\boldsymbol{S}^H$. Note that for any $k = 1, \ldots, K$, the eigenvectors of $\boldsymbol{N}_k$ are equal to the eigenvectors of $\mathbf{A}^H\mathbf{A}$, and hence do not depend on k. Now, if we let $\mathbf{Q}\boldsymbol{L}\mathbf{Q}^H$ be the eigenvalue decomposition of $\mathbf{A}^H\mathbf{A}$, where $\boldsymbol{L} = \mathrm{diag}(a_1, \ldots, a_K)$ has the eigenvalues of $\mathbf{A}^H\mathbf{A}$ on the diagonal, and $\mathbf{Q} = [\mathbf{q}_1, \ldots, \mathbf{q}_N]$ is a unitary matrix with the unit-norm eigenvectors of $\mathbf{A}^H\mathbf{A}$ as columns, we have the following result: Let $\boldsymbol{S}^* = [\boldsymbol{s}_1^*, \ldots, \boldsymbol{s}_K^*] = [\mathbf{q}_1, \ldots, \mathbf{q}_K]$, where $\mathbf{q}_1, \ldots, \mathbf{q}_K$ are the eigenvectors of $\mathbf{A}^H\mathbf{A}$ corresponding to the K largest eigenvalues. Then, the Nash equilibria for the proposed non-cooperative game are all the permutations of the columns of $\boldsymbol{S}^*$.

A couple of remarks are now in order. First, in order to minimize his own MSE_k, each user will try to get the maximum eigenvalue eigenvector of $\mathbf{A}^H\mathbf{A}$. However, this selfish behavior could result in more users sharing the same spreading code, which is not a Nash equilibrium for the proposed game. This circumstance can be avoided by ordering the players and making the rule that spreading codes are to be chosen according to this order. However, in the considered non-cooperative scenario, the ordering can not be decided by the users themselves, but by a higher hierarchical entity, such as the relay. We remark that the interaction between the multiple access users is still totally non-cooperative, but each players is motivated to respect the ordering fixed by the relay, because he knows that otherwise he would get the same spreading code as another user, thus increasing his own MSE.

Second, applying the above strategy makes it possible to perform resource allocation without actually running (5.9). Indeed, ordering the users, also fixes a permutation of the columns of $\boldsymbol{S}^*$. Then, once the order is known, the users will non-cooperatively compute the corresponding Nash equilibrium without running (5.9). This also implies that by choosing the proper order, the relay can induce the users to play the Nash equilibrium that optimizes his own utility function, as explained in the following.

Relay Matrix Design. In this part, we turn to the problem of optimum relay matrix design. Since it is reasonable to assume that the relay is interested in opti-

mizing the global performance of the system, a logical choice for the relay's utility function is the Total Mean Square Error (TMSE), defined as $\text{TMSE} = \sum_{k=1}^{K} \text{MSE}_k$. Substituting the expression of the MMSE filter into the TMSE expression, and summing over k, we get $\text{TMSE} = K - \sum_{k=1}^{K} d_k^2 g_k^2 \boldsymbol{s}_k^H \left(\boldsymbol{S}\boldsymbol{D}_k\boldsymbol{S}^H + \boldsymbol{N}_k\right)^{-1} \boldsymbol{s}_k$. An important observation is that even if the relay chooses the matrix $\mathbf{A}$ before spreading code optimization is performed, he knows that after spreading code optimization, a fixed point of (5.9) will be reached. Hence, the expression of the TMSE can be further simplified to $\text{TMSE} = K - \sum_{k=1}^{K} \frac{d_k^2 g_k^2}{g_k^2 \lambda_k + \sigma^2 (g_k^2 + \frac{1}{a_k})}$, and we see that we need to optimize with respect to only the eigenvalues of $\mathbf{A}^H\mathbf{A}$, and not with respect to the whole matrix $\mathbf{A}$. Moreover, since only the K largest a_k affect the TMSE, we can set the other $N - K$ eigenvalues to zero, allocating all the available power only to the directions of interest. Finally, since $\lambda_k = d_k^2$, we can formulate the relay matrix design problem as

$$\begin{cases} \arg \min\limits_{a_1,\ldots,a_K} K - \sum\limits_{k=1}^{K} \dfrac{d_k^2 g_k^2 a_k}{a_k g_k^2 (d_k^2 + \sigma^2) + \sigma^2} \\ \text{s.t.} \quad \sum\limits_{k=1}^{K} a_k = N^2 \\ a_k \geq 0 \quad \forall k = 1, \ldots, K \end{cases} . \tag{5.10}$$

This problem is a convex one. Indeed, the constraint functions are affine, while the objective function is convex, because the function $1 - \frac{d_k^2 g_k^2 a_k}{a_k g_k^2 (d_k^2+\sigma^2)+\sigma^2}$ is convex with respect to a_k, and the sum of convex functions is convex [77]. Defining a multiplier β for the equality constraint, multipliers $\delta_1, \ldots, \delta_K$ for the inequality constraints, and applying standard Lagrangian techniques, problem (5.10) can be shown to admit the following water filling solution

$$a_k = \frac{1}{g_k^2 (d_k^2 + \sigma^2)} \left(\frac{\sigma d_k g_k}{\sqrt{\beta - \delta_k}} - \sigma^2 \right)^+ \qquad \text{for} \quad k = 1, \ldots, K \tag{5.11}$$

where the Lagrange multipliers are to be chosen so as to fulfill the constraints.

A remark is now in order. Before we claimed that the relay can choose the permutation of the columns of $\boldsymbol{S}^*$ so as to optimize his own utility function. Well, we claim that the TMSE minimizing permutation is the one obtained by ordering the users in non-increasing order according the eigenvalues $\{a_k\}_{k=1}^K$. To see this, recall that due to the multiple access users' selfish behavior, the first user will choose the largest a_k, the second user will choose the second largest a_k, and so on. Now, according to (5.11), the TMSE is minimized if for all $k = 1, \ldots, K$, user k chooses as his spreading code the unit-norm eigenvector of $\mathbf{A}^H\mathbf{A}$ corresponding to the eigenvalue a_k, which is achieved exactly if we order the users in non-increasing order according the eigenvalues $\{a_k\}_{k=1}^K$.

Numerical Results. In this part we present numerical results to confirm the merits of the proposed resource allocation policies. In our simulations we considered a DS/CDMA system with processing gain $N = 32$, and we compared three different systems

- A system with linear MMSE reception, spreading code optimization, and relay matrix optimization.

- A system with linear MMSE reception, spreading code optimization, and relay matrix set to $\mathbf{A} = \sqrt{N}\boldsymbol{I}_N$.

- A system with linear MMSE reception, random spreading codes, and relay matrix set to $\mathbf{A} = \sqrt{N}\boldsymbol{I}_N$.

The SAPHYRE gain, defined as the difference between the non-sharing scenario and the proposed scheme, requires to consider a fair comparison in terms of throughput gain for fixed transmit power. In future work, the performance measure TMSE needs to be replaced by a rate-based utiliy function and the SAPHYRE gain will be assessed.

The users' transmit powers have been randomly generated in the interval $[0; P_{max}]$, with P_{max} being the maximum feasible transmit power for all users, and we defined the Signal to Noise Ratio (SNR) as SNR $= \frac{P_{max}}{\sigma^2}$. Then, denoting by H and G the random variables modeling the channel complex gains from the transmitters to the relay, and from the relay to the receivers, respectively, we define the ratio $\alpha^2 = E[\frac{|G|^2}{|H|^2}]$. Note that having $\alpha \leq 1$ means that the relay is closer to the transmitters than to the receivers, whereas having $\alpha \geq 1$ means the opposite. In our simulations, we set $\alpha = 10^{-2}$, which means that the average distances from the receivers to the relay have been assumed to be ten times larger than the transmitters'.

In Fig. 5.8 and 5.9 we consider a system with $K = 12$ and $K = 22$ users respectively, and we plot the system's TMSE normalized with respect to the number of users, versus the SNR. As expected, comparing the system with spreading code optimization and that with random spreading codes, we see that a large gain is obtained when $K = 22$. Indeed, in this case we have a high network load, and therefore the system employing random spreading codes is impaired by a large multiuser interference, whereas in the system employing optimized spreading codes multiuser interference is completely suppressed thanks to the orthonormality among codes. Obviously, when the load of the network is lower, spreading code optimization achieves a lower gain with respect to the case of random spreading codes. On the other hand, contrasting the system with optimum relay matrix choice, to that without relay optimization, we get an opposite behavior. This is also expected, since setting the relay matrix to the identity means that we are giving the same amount of power to all of the N eigenvalues of $\mathbf{A}$, whereas the TMSE is affected by only the K largest eigenvalues of $\mathbf{A}$. Therefore, the lower K is, the more power is wasted by setting $\mathbf{A} = \sqrt{N}\boldsymbol{I}_N$.

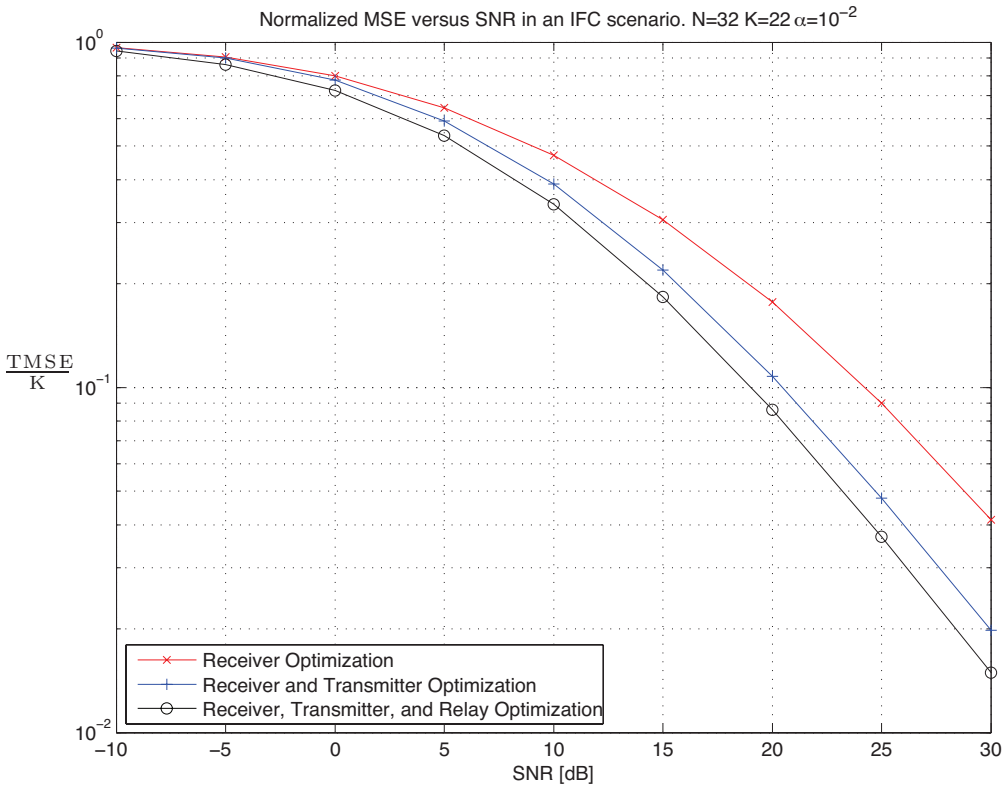

Figure 5.8: Normalized TMSE versus SNR in an IC scenario. System parameters: $N = 32$, $\alpha = 10^{-2}$, $K = 22$

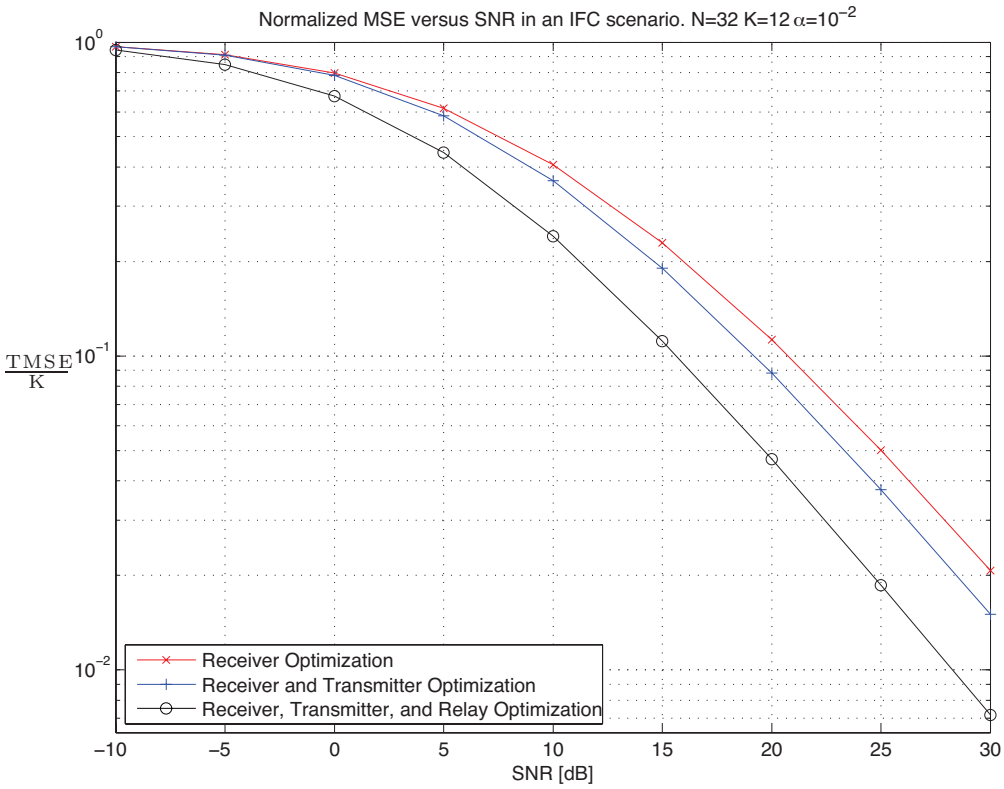

Figure 5.9: Normalized TMSE versus SNR in an IC scenario. System parameters: $N = 32$, $\alpha = 10^{-2}$, $K = 12$

Conclusions. In this work, resource allocation for MSE minimization in a DS/CDMA relay-assisted IC have been studied. The interaction between the relay and the multiple access users has been modeled as a two-level Stackelberg game, with the relay as the leader, and the multiple access users as followers. First, the best response dynamics and the Nash Equilibria for the non-cooperative game played by the followers have been derived, given the relay matrix. Then, optimum relay matrix design has been dealt with. Finally, numerical simulation corroborating the theoretical results have been provided, showing the merits of the proposed resource allocation techniques.

5.3 Relaying Techniques for Two-Way Relay Channel

5.3.1 Projection Based Separation of Multiple Operators in Two-Way Relaying

Introduction

In this section, we present a relay-assisted resource sharing scenario in which multiple communication partners (belonging to different operators) use one relay (possibly owned by another operator / virtual operator) to bidirectionally exchange information using the same spectrum. The relay has multiple antennas and operate in half-duplex mode. We propose sub-optimal algorithms for computing the relay amplification matrix at the relay as well as transmit and receive beamforming matrices at the UTs.

Data Model

The scenario under investigation is shown in Figure 5.10. Pairs of users belonging to L different operators want to communicate with each other. However, due to the poor quality of the direct channel between pairs of users, they can only communicate with the help of the relay. The kth user of the ℓth operator has $M_k^{(\ell)}$ antennas ($k \in \{1,2\}$ for users, $\ell \in \{1,\ldots,L\}$ for operators). The relay is equipped with M_{R} antennas. We assume that the channel is flat fading. The channel between the kth user of the ℓth operator and the relay is denoted by $\boldsymbol{H}_k^{(\ell)} \in \mathbb{C}^{M_{\mathrm{R}} \times M_k^{(\ell)}}$. Furthermore, we assume $\boldsymbol{H}_k^{(\ell)}$ is a full rank matrix which implies $\mathrm{rank}\{\boldsymbol{H}_k^{(\ell)}\} = \min\{M_{\mathrm{R}}, M_k^{(\ell)}\}$.

The two-way AF relaying protocol consists of two transmission phases: in the first phase, which could be also called MAC (Multiple Access) phase, all the user terminals transmit their data simultaneously to the relay. Let the kth user of the ℓth operator transmit the data vector $\boldsymbol{d}_k^{(\ell)} \in \mathbb{C}^{r_k^{(\ell)}}$ with transmit beamforming matrix $\boldsymbol{W}_k^{(\ell)} \in \mathbb{C}^{M_k^{(\ell)} \times r_k^{(\ell)}}$ ($r_k^{(\ell)}$ is the number of transmitted data streams of the correspond-

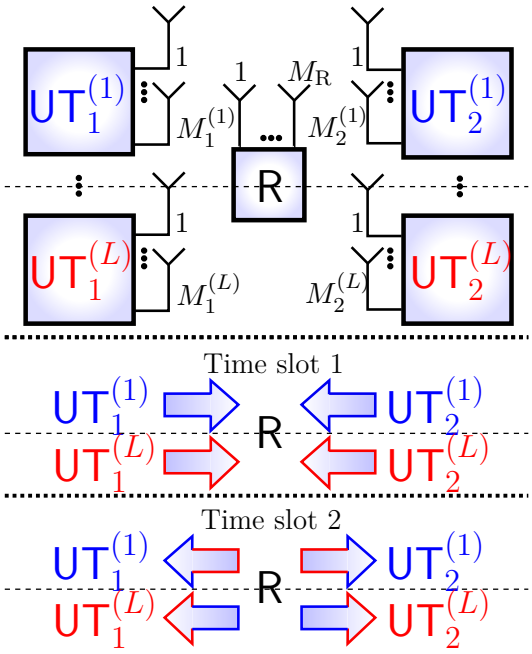

Figure 5.10: Multi-operator two-way relaying system model. The k-th terminal belonging to the ℓ-th operator has $M_k^{(\ell)}$ antennas and the relay station is equipped with $^{\mathrm{MR}}$ antennas.

ing user.). Then its transmitted signal vector $\boldsymbol{x}_k^{(\ell)}$ can be written as

$$\boldsymbol{x}_k^{(\ell)} = \boldsymbol{W}_k^{(\ell)} \boldsymbol{d}_k^{(\ell)}, \tag{5.12}$$

with the transmit power constraint $\mathbb{E}\left\{\|\boldsymbol{x}_k^{(\ell)}\|^2\right\} \leq P_k^{(\ell)}$. The elements of the input data vectors $\boldsymbol{d}_k^{(\ell)}$ are independently distributed with zero mean and unit variance. We further define the concatenated overall transmit beamforming matrix as $\boldsymbol{W} = \mathrm{blkdiag}\{\boldsymbol{W}_1^{(1)}, \boldsymbol{W}_2^{(1)}, \cdots, \boldsymbol{W}_1^{(L)}, \boldsymbol{W}_2^{(L)}\}$.

The received signal vector at the relay is then

$$\boldsymbol{r} = \sum_{\ell=1}^{L} \sum_{k=1}^{2} \boldsymbol{H}_k^{(\ell)} \boldsymbol{x}_k^{(\ell)} + \boldsymbol{n}_{\mathrm{R}} \in \mathbb{C}^{M_{\mathrm{R}}} \tag{5.13}$$

where $\boldsymbol{n}_{\mathrm{R}} \in \mathbb{C}^{M_{\mathrm{R}}}$ is zero-mean circularly symmetric complex Gaussian (ZMCSCG) noise and $\mathbb{E}\{\boldsymbol{n}_{\mathrm{R}} \boldsymbol{n}_{\mathrm{R}}^{\mathrm{H}}\} = \sigma_{\mathrm{R}}^2 \boldsymbol{I}_{M_{\mathrm{R}}}$.

In the second phase, which could be also called BC (Broadcast) phase, the relay amplifies the received signal and then forwards it to all the terminals simultaneously. The signal transmitted by the relay can be expressed as

$$\bar{\boldsymbol{r}} = \boldsymbol{G} \cdot \boldsymbol{r}. \tag{5.14}$$

where $\boldsymbol{G} \in \mathbb{C}^{M_{\mathrm{R}} \times M_{\mathrm{R}}}$ is the relay amplification matrix. The transmit power constraint at the relay should be fulfilled such that $\mathbb{E}\{\|\bar{\boldsymbol{r}}\|^2\} \leq P_{\mathrm{R}}$, where P_{R} denotes the total power at the base station.

For notational simplicity, we assume that the reciprocity assumption between the first- and second- phase channels is valid. This assumption is fulfilled in a TDD system if identical RF chains are applied.[1] The received signal vector $\boldsymbol{y}_k^{(\ell)}$ at the kth user of the ℓth operator can be written as

$$\begin{aligned}\boldsymbol{y}_k^{(\ell)} &= \boldsymbol{H}_k^{(\ell)^{\mathrm{T}}} \bar{\boldsymbol{r}} + \boldsymbol{n}_k^{(\ell)} \\ &= \underbrace{\boldsymbol{H}_k^{(\ell)^{\mathrm{T}}} \boldsymbol{G} \boldsymbol{H}_{3-k}^{(\ell)} \boldsymbol{x}_{3-k}^{(\ell)}}_{\text{desired signal}} + \underbrace{\boldsymbol{H}_k^{(\ell)^{\mathrm{T}}} \boldsymbol{G} \boldsymbol{H}_k^{(\ell)} \boldsymbol{x}_k^{(\ell)}}_{\text{self-interference}} \\ &\quad + \underbrace{\sum_{\substack{\bar{\ell} \neq \ell \\ \bar{k} \neq k}} \boldsymbol{H}_k^{(\ell)^{\mathrm{T}}} \boldsymbol{G} \boldsymbol{H}_{\bar{k}}^{(\bar{\ell})} \boldsymbol{x}_{\bar{k}}^{(\bar{\ell})}}_{\text{inter-operator interference}} \\ &\quad + \underbrace{\boldsymbol{H}_k^{(\ell)^{\mathrm{T}}} \boldsymbol{G} \boldsymbol{n}_{\mathrm{R}} + \boldsymbol{n}_k^{(\ell)}}_{\text{effective noise}} \in \mathbb{C}^{M_k^{(\ell)}}\end{aligned} \tag{5.15}$$

where $\boldsymbol{n}_k^{(\ell)} \in \mathbb{C}^{M_k^{(\ell)}}$ is ZMCSCG noise and $\mathbb{E}\left\{\boldsymbol{n}_k^{(\ell)} \boldsymbol{n}_k^{(\ell)^{\mathrm{H}}}\right\} = {\sigma_k^{(\ell)}}^2 \boldsymbol{I}_{M_k^{(\ell)}}$. Then the receive beamforming matrix $\boldsymbol{F}_k^{(\ell)} \in \mathbb{C}^{\bar{r}_k^{(\ell)} \times M_k^{(\ell)}}$ ($\bar{r}_k^{(\ell)}$ is the number of received data streams of the corresponding user.) will be used to convert the received signal $\boldsymbol{y}_k^{(\ell)}$ into an estimate of the original transmitted data

$$\hat{\boldsymbol{d}}_k^{(\ell)} = \boldsymbol{F}_k^{(\ell)} \boldsymbol{y}_k^{(\ell)} \tag{5.16}$$

Again, the concatenated overall receive beamforming matrix is defined as $\boldsymbol{F} = \mathrm{blkdiag}\{\boldsymbol{F}_1^{(1)}, \boldsymbol{F}_2^{(1)}, \cdots, \boldsymbol{F}_1^{(L)}, \boldsymbol{F}_2^{(L)}\}$.

The overall sum rate of the system could be written as

$$R_{\mathrm{sum}} = \frac{1}{2} \sum_{\ell=1}^{L} \sum_{k=1}^{2} \sum_{i=1}^{\bar{r}_k^{(\ell)}} \log_2(1 + \eta_{k,i}^{(\ell)}) \tag{5.17}$$

where $\eta_{k,i}^{(\ell)}$ is the SINR per stream at each user and the pre-factor 1/2 is due to the two channel uses (half duplex). The optimization problem to find the relay amplification matrix structure which maximizes (5.17) subject to transmit power constrains at the relay is non-convex. To avoid the non-tractable optimization problem, we resort to efficient linear algorithms instead.

Furthermore, we assume that one successful communication consists of training phase and data phase. This means that in the first phase each UT only transmits

[1] Our method is not limited to the reciprocity assumption.

N_p training symbols. These training symbols are used for channel estimation as well as the calculation of the $\boldsymbol{G}$ matrix at the relay. They are also used for channel estimation as well as the calculation of beamforming matrices at the terminals. The proposed algorithms are all executed in the training phase. In the data phase, each user terminal transmits and receives data sequences using the transmit and receive beamforming vectors computed from the training phase. The amplification matrix $\boldsymbol{G}$ at the relay remains unchanged during the data phase. Note that training signals are also parts of transmitted data. Thus, the throughput of each user will be reduced depending on the number of training symbols.

Projection Based Separation of Multiple Operators (ProBaSeMo)

As can be seen from (5.15), if we could null the inter-operator interference but leave the self-interference at first, the system will be decoupled into L parallel independent three-nodes (single-operator) two-way relaying sub-systems. Then, in the second step, arbitrary transmission techniques for single-operator two-way relaying can be applied separately on each sub-system. However, the traditional SDMA based interference nulling will sacrifice the degree of freedoms of the system. One simple solution to reserve enough degree of freedoms for each sub-system is to artificially increase the spatial dimensions, e.g., using projection matrices in our work. To fulfill the requirement of our proposed projection based separation of multiple operators (ProBaSeMo) approach, we need to decompose the relay amplification matrix $\boldsymbol{G}$ into

$$\boldsymbol{G} = \boldsymbol{G}_\mathrm{T} \cdot \boldsymbol{G}_\mathrm{S} \cdot \boldsymbol{G}_\mathrm{R} \in \mathbb{C}^{M_\mathrm{R} \times M_\mathrm{R}} \tag{5.18}$$

where $\boldsymbol{G}_\mathrm{R} \in \mathbb{C}^{LM_\mathrm{R} \times M_\mathrm{R}}$ and $\boldsymbol{G}_\mathrm{T} \in \mathbb{C}^{M_\mathrm{R} \times LM_\mathrm{R}}$ are filters designed to suppress the inter-operator interference during the MAC phase and BC phase, respectively. The matrix $\boldsymbol{G}_\mathrm{S} \in \mathbb{C}^{LM_\mathrm{R} \times LM_\mathrm{R}}$ is constructed via

$$\boldsymbol{G}_\mathrm{S} = \gamma_0 \cdot \begin{bmatrix} w^{(1)}\boldsymbol{G}_\mathrm{S}^{(1)} & \cdots & \boldsymbol{0}_{M_\mathrm{R} \times M_\mathrm{R}} \\ \vdots & \ddots & \vdots \\ \boldsymbol{0}_{M_\mathrm{R} \times M_\mathrm{R}} & \cdots & w^{(L)}\boldsymbol{G}_\mathrm{S}^{(L)} \end{bmatrix}, \tag{5.19}$$

where $w^{(1)}\boldsymbol{G}_\mathrm{S}^{(1)}, \ldots, w^{(L)}\boldsymbol{G}_\mathrm{S}^{(L)} \in \mathbb{C}^{M_\mathrm{R} \times M_\mathrm{R}}$ are the relay amplification matrices for each sub-system and $w^{(\ell)} \in \mathbb{R}^+$ is the weighting factor for the power allocated to the ℓth operator at the relay. The parameter $\gamma_0 \in \mathbb{R}^+$ is chosen such that the transmit power constraint at the relay is fulfilled. Note that $\boldsymbol{G}_\mathrm{S}$ is block diagonal since it represents the processing performed in the individual subsystems.

The overall transmit and receive filter matrices $\boldsymbol{G}_\mathrm{T}$ and $\boldsymbol{G}_\mathrm{R}$ can also be partitioned as

$$\boldsymbol{G}_\mathrm{T} = \left[\boldsymbol{G}_\mathrm{T}^{(1)}, \ \ldots, \ \boldsymbol{G}_\mathrm{T}^{(L)}\right], \ \ \boldsymbol{G}_\mathrm{R} = \left[\boldsymbol{G}_\mathrm{R}^{(1)^\mathrm{T}}, \ \ldots, \ \boldsymbol{G}_\mathrm{R}^{(L)^\mathrm{T}}\right]^\mathrm{T} \tag{5.20}$$

where $\boldsymbol{G}_\mathrm{T}^{(\ell)} \in \mathbb{C}^{M_\mathrm{R} \times M_\mathrm{R}}$ and $\boldsymbol{G}_\mathrm{R}^{(\ell)} \in \mathbb{C}^{M_\mathrm{R} \times M_\mathrm{R}}$. Now we focus on the question how to choose the matrices $\boldsymbol{G}_\mathrm{T}^{(\ell)}$, $\boldsymbol{G}_\mathrm{S}^{(\ell)}$, and $\boldsymbol{G}_\mathrm{R}^{(\ell)}$ for each operator separately.

A. Block-diagonalization at the Relay

As mentioned before, to eliminate the inter-operator interference but leave the intra-operator interference to the users themselves as in single-operator two-way relaying, one choice would be to adapt the block diagonalization (BD) technique of [60] to design the projection matrix $\boldsymbol{G}_{\mathrm{T}}^{(\ell)}$ and $\boldsymbol{G}_{\mathrm{R}}^{(\ell)}$.

Assume that we want to design $\boldsymbol{G}_{\mathrm{T}}^{(\ell)}$, $\boldsymbol{G}_{\mathrm{S}}^{(\ell)}$, $\boldsymbol{G}_{\mathrm{R}}^{(\ell)}$ for the ℓth operator, in the MAC phase, let us define the combined channel matrix $\tilde{\boldsymbol{H}}^{(\ell)}$ for all UTs except for the UTs of the ℓth operator as

$$\tilde{\boldsymbol{H}}^{(\ell)} = \left[\boldsymbol{H}^{(1)} \ \ldots \ \boldsymbol{H}^{(\ell-1)} \ \boldsymbol{H}^{(\ell+1)} \ \ldots \ \boldsymbol{H}^{(L)}\right], \tag{5.21}$$

where $\boldsymbol{H}^{(\ell)} = \left[\boldsymbol{H}_1^{(\ell)} \ \boldsymbol{H}_2^{(\ell)}\right]$ is the users' concatenated uplink channel matrix of the ℓth operator. Then the receive filter matrix $\boldsymbol{G}_{\mathrm{R}}^{(\ell)}$ should lie in the null space of $\tilde{\boldsymbol{H}}^{(\ell)}$ so that the signal of the ℓth operator will not cause interference to all the other operators. Let $\tilde{L}^{(\ell)} = \mathrm{rank}\{\tilde{\boldsymbol{H}}^{(\ell)}\}$ and define the singular value decomposition (SVD)

$$\tilde{\boldsymbol{H}}^{(\ell)} = [\,\tilde{\boldsymbol{U}}_{\mathrm{s}}^{(\ell)} \ \tilde{\boldsymbol{U}}_{\mathrm{n}}^{(\ell)}\,]\tilde{\boldsymbol{\Sigma}}^{(\ell)}\tilde{\boldsymbol{V}}^{(\ell)^{\mathrm{H}}}. \tag{5.22}$$

where $\tilde{\boldsymbol{U}}_{\mathrm{n}}^{(\ell)}$ contains the last $(M_{\mathrm{R}} - \tilde{L}^{(\ell)})$ left singular vectors. Thus, $\tilde{\boldsymbol{U}}_{\mathrm{n}}^{(\ell)}$ forms an orthogonal basis for the null space of $\tilde{\boldsymbol{H}}^{(\ell)}$ such that $\tilde{\boldsymbol{U}}_{\mathrm{n}}^{(\ell)^{\mathrm{H}}}\tilde{\boldsymbol{H}}^{(\ell)} = 0$. Then the columns of $\tilde{\boldsymbol{U}}_{\mathrm{n}}^{(\ell)^{\mathrm{H}}}$ are the candidate for the receive filter $\boldsymbol{G}_{\mathrm{R}}^{(\ell)}$. Unlike the work in [78] and [79], here we choose

$$\boldsymbol{G}_{\mathrm{R}}^{(\ell)} = \tilde{\boldsymbol{U}}_{\mathrm{n}}^{(\ell)}\tilde{\boldsymbol{U}}_{\mathrm{n}}^{(\ell)^{\mathrm{H}}} \in \mathbb{C}^{M_{\mathrm{R}} \times M_{\mathrm{R}}}. \tag{5.23}$$

It can be easily seen that the $\boldsymbol{G}_{\mathrm{R}}^{(\ell)}$ in (5.23) is a projection matrix which projects any matrix onto the null space of $\tilde{\boldsymbol{H}}^{(\ell)}$.

In the BC phase, due to the reciprocity of the channel and the usage of BD, the transmit filter $\boldsymbol{G}_{\mathrm{T}}^{(\ell)}$ and receive filter $\boldsymbol{G}_{\mathrm{R}}^{(\ell)}$ are also reciprocal, so that we get

$$\boldsymbol{G}_{\mathrm{T}}^{(\ell)} = \boldsymbol{G}_{\mathrm{R}}^{(\ell)^{\mathrm{T}}}. \tag{5.24}$$

Although BD could null the inter-operator interference completely, it is restricted by the dimensionality constraint, i.e., the null space of $\tilde{\boldsymbol{H}}^{(\ell)}$ cannot be empty. That means, in our case, the dimensionality constraint $M_{\mathrm{R}} > \max_{\ell} \sum_{\substack{\bar{\ell}=1 \\ \bar{\ell}\neq\ell}}^{L} \sum_{k=1}^{2} M_k^{(\bar{\ell})}$ has to be fulfilled.

B. Regularized Block-Diagonalization at the Relay

One algorithm which is not limited by the dimensionality constraint is the so called regularized block diagonalization (RBD) algorithm [61]. It allows a residual amount

of inter-operator interference in order to balance it with the noise enhancement. It is also proved in [80] that the performance of RBD converges to BD in the high SNR regime. Now we adopt the RBD design for our scenario.

In the MAC phase, the cost function of RBD can be written as

$$J(\boldsymbol{G}_{\mathrm{R}}) = \arg\min_{\boldsymbol{G}_{\mathrm{R}}} \mathbb{E}\{\|\boldsymbol{x} - \boldsymbol{G}_{\mathrm{R}}\boldsymbol{r}\|^2\} \tag{5.25}$$

where $\boldsymbol{x} = [\boldsymbol{x}_1^{(1)^{\mathrm{T}}}, \boldsymbol{x}_2^{(1)^{\mathrm{T}}}, \ \ldots \boldsymbol{x}_1^{(L)^{\mathrm{T}}}, \boldsymbol{x}_2^{(L)^{\mathrm{T}}}]^{\mathrm{T}}$ is the concatenated transmitted signal vectors of all the terminals.

With the help of (5.13) and (5.20), the cost function can be further expanded as

$$\begin{aligned} J(\boldsymbol{G}_{\mathrm{R}}) &= \arg\min_{\boldsymbol{G}_{\mathrm{R}}} \mathbb{E}\{\|\boldsymbol{x} - \boldsymbol{G}_{\mathrm{R}}\boldsymbol{H}\boldsymbol{x} - \boldsymbol{G}_{\mathrm{R}}\boldsymbol{n}_{\mathrm{R}}\|^2\} \\ &= \arg\min_{\boldsymbol{G}_{\mathrm{R}}} \mathbb{E}\{\|(\boldsymbol{I} - \boldsymbol{G}_{\mathrm{R}}\boldsymbol{H})\boldsymbol{x}\|^2 + \|\boldsymbol{G}_{\mathrm{R}}\boldsymbol{n}_{\mathrm{R}}\|^2\} \end{aligned} \tag{5.26}$$

where the equivalent combined channel matrix of all the operators $\boldsymbol{G}_{\mathrm{R}}\boldsymbol{H}$ is equal to

$$\boldsymbol{G}_{\mathrm{R}}\boldsymbol{H} = \begin{bmatrix} \boldsymbol{G}_{\mathrm{R}}^{(1)}\boldsymbol{H}^{(1)} & \boldsymbol{G}_{\mathrm{R}}^{(1)}\boldsymbol{H}^{(2)} & \ldots & \boldsymbol{G}_{\mathrm{R}}^{(1)}\boldsymbol{H}^{(L)} \\ \boldsymbol{G}_{\mathrm{R}}^{(2)}\boldsymbol{H}^{(1)} & \boldsymbol{G}_{\mathrm{R}}^{(2)}\boldsymbol{H}^{(2)} & \ldots & \boldsymbol{G}_{\mathrm{R}}^{(2)}\boldsymbol{H}^{(L)} \\ \vdots & \vdots & \ddots & \vdots \\ \boldsymbol{G}_{\mathrm{R}}^{(L)}\boldsymbol{H}^{(1)} & \boldsymbol{G}_{\mathrm{R}}^{(L)}\boldsymbol{H}^{(2)} & \ldots & \boldsymbol{G}_{\mathrm{R}}^{(L)}\boldsymbol{H}^{(L)} \end{bmatrix} \tag{5.27}$$

with the same definition of the interference channel $\tilde{\boldsymbol{H}}^{(\ell)}$ as in (5.21), the ℓth operator's effective channel is given by $\boldsymbol{G}_{\mathrm{R}}^{(\ell)}\boldsymbol{H}^{(\ell)}$ and the interference caused by the other operators is determined by $\boldsymbol{G}_{\mathrm{R}}^{(\ell)}\tilde{\boldsymbol{H}}^{(\ell)}$. If we ignore the optimization of the block matrices on the main diagonal of (5.27), the matrix $\boldsymbol{G}_{\mathrm{R}}$ is designed to minimize the interference plus noise power. Thus, the optimization criterion can be rewritten as

$$\boldsymbol{G}_{\mathrm{R}} = \arg\min_{\boldsymbol{G}_{\mathrm{R}}} \mathbb{E}\left\{ \sum_{\ell=1}^{L} \left\| \boldsymbol{G}_{\mathrm{R}}^{(\ell)}\tilde{\boldsymbol{H}}^{(\ell)}\tilde{\boldsymbol{x}}^{(\ell)} \right\|^2 + \|\boldsymbol{G}_{\mathrm{R}}\boldsymbol{n}_{\mathrm{R}}\|^2 \right\}, \tag{5.28}$$

where $\tilde{\boldsymbol{x}}^{(\ell)} = \left[\boldsymbol{x}^{(1)^{\mathrm{T}}} \ \ldots \ \boldsymbol{x}^{(\ell-1)^{\mathrm{T}}} \boldsymbol{x}^{(\ell+1)^{\mathrm{T}}} \ \ldots \ \boldsymbol{x}^{(L)^{\mathrm{T}}}\right]^{\mathrm{T}}$ with $\boldsymbol{x}^{(\ell)} = \left[\boldsymbol{x}_1^{(\ell)^{\mathrm{T}}} \ \boldsymbol{x}_2^{(\ell)^{\mathrm{T}}}\right]^{\mathrm{T}}$ and $\mathbb{E}\{\|\boldsymbol{x}^{(\ell)}\|^2\} = 2P_k^{(\ell)}$.

Let us again compute the SVD of $\tilde{\boldsymbol{H}}^{(\ell)}$ as

$$\tilde{\boldsymbol{H}}^{(\ell)} = \tilde{\boldsymbol{U}}^{(\ell)}\tilde{\boldsymbol{\Sigma}}^{(\ell)}\tilde{\boldsymbol{V}}^{(\ell)^{\mathrm{H}}}. \tag{5.29}$$

Following the similar procedure as in [61], the solution to (5.28) can be obtained as

$$\boldsymbol{G}_{\mathrm{R}}^{(\ell)} = \left\{ \frac{P_k^{(\ell)}}{M_{\mathrm{U}}} \tilde{\boldsymbol{\Sigma}}^{(\ell)}\tilde{\boldsymbol{\Sigma}}^{(\ell)^{\mathrm{H}}} + \delta_{\mathrm{R}}^2 \boldsymbol{I}_{M_{\mathrm{R}}} \right\}^{-1/2} \tilde{\boldsymbol{U}}^{(\ell)^{\mathrm{H}}}. \tag{5.30}$$

In the BC phase, the design of the transmit filter matrices $\boldsymbol{G}_{\mathrm{T}}$ could follow the same way. The major difference is that in this case we define the interference generated to the other operator as $\tilde{\boldsymbol{H}}^{(\ell)^{\mathrm{T}}}\boldsymbol{G}_{\mathrm{T}}^{(\ell)}$.[2] Then, the optimization criterion becomes

$$\boldsymbol{G}_{\mathrm{T}} = \arg\min_{\boldsymbol{G}_{\mathrm{T}}} \mathbb{E}\left\{ \sum_{\ell=1}^{L} \left\| \tilde{\boldsymbol{H}}^{(\ell)^{\mathrm{T}}} \boldsymbol{G}_{\mathrm{T}}^{(\ell)} \tilde{\boldsymbol{x}}^{(\ell)} \right\|^2 + \left\| \boldsymbol{n}^{(\ell)} \right\|^2 \right\}, \tag{5.31}$$

where $\mathbb{E}\left\{ \boldsymbol{n}^{(\ell)} \boldsymbol{n}^{(\ell)^{\mathrm{H}}} \right\} = \delta_k^{(\ell)^2} \boldsymbol{I}_{2M_k^{(\ell)}}$. After following the optimization procedure in [61] and utilizing the SVD definition in (5.29) , $\boldsymbol{G}_{\mathrm{T}}^{(\ell)}$ can be obtained as

$$\boldsymbol{G}_{\mathrm{T}}^{(\ell)} = \tilde{\boldsymbol{U}}^{(\ell)^*} \left\{ \tilde{\boldsymbol{\Sigma}}^{(\ell)^*} \tilde{\boldsymbol{\Sigma}}^{(\ell)^{\mathrm{T}}} + 2LM_k^{(\ell)} \delta_k^{(\ell)^2} \boldsymbol{I}_{M_{\mathrm{R}}} / P_{\mathrm{R}} \right\}^{-1/2}. \tag{5.32}$$

C. Relay Amplification Matrix for Each Sub-System

After applying the receive filter $\boldsymbol{G}_{\mathrm{R}}$ and the transmit filter $\boldsymbol{G}_{\mathrm{T}}$, we get L independent single-operator TWR systems when BD is used or at high SNR regime when RBD is used. Thus, each sub-matrix $\boldsymbol{G}_{\mathrm{S}}^{(\ell)}$ can be derived separately. In general, any arbitrary design of $\boldsymbol{G}_{\mathrm{S}}^{(\ell)}$ can be applied. However, in our work, we use the algebraic norm-maximizing (ANOMAX) transmit strategy [57] and its derivative rank-restored ANOMAX [81]. The received signal vectors (5.15) at the users of the ℓth operator can be further expanded as

$$\begin{aligned} \boldsymbol{y}_1^{(\ell)} &= \boldsymbol{H}_{1,1}^{(\ell)} \boldsymbol{x}_1^{(\ell)} + \boldsymbol{H}_{1,2}^{(\ell)} \boldsymbol{x}_2^{(\ell)} + \tilde{\boldsymbol{n}}_1^{(\ell)} \\ \boldsymbol{y}_2^{(\ell)} &= \boldsymbol{H}_{2,2}^{(\ell)} \boldsymbol{x}_2^{(\ell)} + \boldsymbol{H}_{2,1}^{(\ell)} \boldsymbol{x}_1^{(\ell)} + \tilde{\boldsymbol{n}}_2^{(\ell)}, \end{aligned} \tag{5.33}$$

where $\tilde{\boldsymbol{n}}_1^{(\ell)}$ and $\tilde{\boldsymbol{n}}_2^{(\ell)}$ denote the effective noise terms which consists of the terminals' own noise and the forwarded relay noise contribution.

Moreover, the effective channel $\boldsymbol{H}_{k,m}^{(\ell)}$ between the source and destination is defined as

$$\boldsymbol{H}_{k,m}^{(\ell)} = \boldsymbol{H}_k^{(\ell)^{\mathrm{T}}} \boldsymbol{G}_{\mathrm{T}}^{(\ell)} \boldsymbol{G}_{\mathrm{S}}^{(\ell)} \boldsymbol{G}_{\mathrm{R}}^{(\ell)} \boldsymbol{H}_m^{(\ell)}, \tag{5.34}$$

where $m \in \{1, 2\}$. Observe from (5.33) that the first term represents the self-interference which can be subtracted from the received signal if channel knowledge is available. The second term contains the desired signal. The ANOMAX solves the following cost function [57]

$$\begin{aligned} &\arg\max_{\boldsymbol{G}_{\mathrm{S}}^{(\ell)}} \beta^2 \left\| \boldsymbol{H}_{1,2}^{(\ell)} \right\|_{\mathrm{F}}^2 + (1-\beta)^2 \left\| \boldsymbol{H}_{2,1}^{(\ell)} \right\|_{\mathrm{F}}^2 \\ &\qquad s.t. \left\| \boldsymbol{G}_{\mathrm{S}}^{(\ell)} \right\|_{\mathrm{F}} = 1, \end{aligned} \tag{5.35}$$

[2] $\{\cdot\}^{\mathrm{T}}$ comes from the reciprocity assumption.

where $\beta \in [0,1]$ is a weighting factor. Now we introduce the definitions $\boldsymbol{g}^{(\ell)} = \text{vec}\{\boldsymbol{G}_{\text{S}}^{(\ell)}\}$ and

$$\begin{aligned}\boldsymbol{K}_{\beta}^{(\ell)} = \big[&\beta((\boldsymbol{G}_{\text{R}}^{(\ell)}\boldsymbol{H}_{2}^{(\ell)}) \otimes (\boldsymbol{G}_{\text{T}}^{(\ell)^{\text{T}}}\boldsymbol{H}_{1}^{(\ell)})),\\ &(1-\beta)((\boldsymbol{G}_{\text{R}}^{(\ell)}\boldsymbol{H}_{1}^{(\ell)}) \otimes (\boldsymbol{G}_{\text{T}}^{(\ell)^{\text{T}}}\boldsymbol{H}_{2}^{(\ell)}))\big].\end{aligned} \tag{5.36}$$

We compute the SVD of $\boldsymbol{K}_{\beta}^{(\ell)}$ as $\boldsymbol{K}_{\beta}^{(\ell)} = \boldsymbol{U}_{\beta}^{(\ell)}\boldsymbol{\Sigma}_{\beta}^{(\ell)}\boldsymbol{V}_{\beta}^{(\ell)^{\text{H}}}$. Then, following the same procedure in [57], the optimal $\boldsymbol{g}^{(\ell)}$ is given by $\boldsymbol{g}^{(\ell)} = \boldsymbol{u}_{\beta,1}^{(\ell)^{*}}$, where $\boldsymbol{u}_{\beta,1}^{(\ell)}$ is the first column of $\boldsymbol{U}_{\beta}^{(\ell)}$, i.e., the dominant left singular vector of $\boldsymbol{K}_{\beta}^{(\ell)}$. Finally, the optimal matrix $\boldsymbol{G}_{\text{S}}^{(\ell)}$ is computed via

$$\boldsymbol{G}_{\text{S}}^{(\ell)} = \text{unvec}_{M_{\text{R}}\times M_{\text{R}}}\{\boldsymbol{u}_{\beta,1}^{(\ell)^{*}}\}. \tag{5.37}$$

However, as discussed in [81], the ANOMAX scheme yields a low rank relay amplification matrix and therefore cannot reach the full multiplexing gain for high SNRs especially when multiple antennas are deployed at the terminals. Therefore, one alternate low complexity scheme which is called water filling rank-restored ANOMAX (WF RR-ANOMAX) is proposed in the same paper. The name comes from the fact that RR-ANOMAX restores the rank of the relay amplification matrix $\boldsymbol{G}_{\text{S}}^{(\ell)}$ via an optimization inspired by the water filling algorithm over the profile of the singular values.

That means, if we define the SVD of the matrix $\boldsymbol{G}_{\text{S}}^{(\ell)}$ which is obtained via ANOMAX as

$$\boldsymbol{G}_{\text{S}}^{(\ell)} = \boldsymbol{U}_{\text{S}}^{(\ell)} \cdot \text{diag}\{\boldsymbol{\sigma}\} \cdot \boldsymbol{V}_{\text{S}}^{(\ell)^{\text{H}}}, \tag{5.38}$$

where the vector $\boldsymbol{\sigma} = [\sigma_1, \sigma_2, \cdots, \sigma_{M_{\text{R}}}]$ denotes the singular value profile. Compared to ANOMAX, the WF RR-ANOMAX solution adjusts the $\boldsymbol{\sigma}$ using the water filling algorithm [81].

D. Transmit and Receive Beamforming Matrices at the Terminals

When terminals are equipped with multiple antennas, it is beneficial to use beamforming to either exploit the multiplexing gain or the diversity gain. Such beamforming designs have also been addressed in [82]. The beamforming schemes used in [82] are based on the amount of channel state information (CSI) available at the terminals. Moreover, the design of the beamforming vectors only utilizes the intermediate CSI $\boldsymbol{H}_{k}^{(\ell)}$ and aims mainly at single-stream transmission. As we know, the source and destination nodes in this scenario are the pair of users which would like to communicate with each other. Therefore, a better strategy is to design the transmit and receive beamforming vectors according to the equivalent channel matrices between the source and the destination.

Sine the destination (or source) is also the source (or destination) at the same time, the transmit and receive beamforming of the same user are based on different equivalent channels. Let us define two kinds of equivalent channels. The first one which we refer to as the equivalent forward channel means the effective channel from the source to the destination. And the second one which we refer to as the equivalent backward channel means the effective channel measured at the destination from the source. Take user terminals of the ℓth operator as an example, the equivalent forward channel of its 1st user is $\boldsymbol{H}_2^{(\ell)^{\mathrm{T}}}\boldsymbol{G}\boldsymbol{H}_1^{(\ell)}$ and its corresponding equivalent backward channel is $\boldsymbol{H}_1^{(\ell)^{\mathrm{T}}}\boldsymbol{G}\boldsymbol{H}_2^{(\ell)}$.

Finally, in our work, the transmit beamforming matrix $\boldsymbol{W}_k^{(\ell)}$ of each UT is calculated according to its equivalent forward channel while its receive beamforming vectors $\boldsymbol{F}_k^{(\ell)}$ is calculated based on its equivalent backward channel. Furthermore, we employ two beamforming schemes.

- **Dominant eigenmode transmission (DET)**: The transmit and receive beamforming vectors of the kth user of the ℓth operator are defined as the right dominant singular vector of its effective forward channel and the left dominant singular vector of its effective backward channel, respectively. DET maximizes the receive SNR at the receiver of the point-to-point MIMO communication system and yields single-stream transmission.
- **Spatial multiplexing with water-filling algorithm (WF)**: It is well known that for point-to-point MIMO communication system with CSI at the transmitter the capacity maximizing spatial multiplexing strategy is the water-filling algorithm [41]. Therefore, it is chosen in our work as the beamforming strategy for multiple-stream transmission. The details of water-filling algorithms can be found in many MIMO textbooks, e.g., [41].

E. Power Control at the Relay

In the previous sub-sections, we have described how to design the matrices $\boldsymbol{G}_{\mathrm{T}}$, $\boldsymbol{G}_{\mathrm{R}}$ and $\boldsymbol{G}_{\mathrm{S}}$. However, how to calculate the relay amplification factor γ_0 to fulfill the transmit power constraint at the relay has not been discussed yet.

In general, the relay amplification factor γ_0 shall be calculated as

$$\begin{aligned}\gamma_0 &= \sqrt{\frac{P_{\mathrm{R}}}{\mathbb{E}\{\|\bar{\boldsymbol{r}}\|^2\}}} \\ &= \sqrt{\frac{P_{\mathrm{R}}}{\mathrm{tr}\left\{\left\{\boldsymbol{G}\left(\sum_{k,\ell} P_k^{(\ell)}\boldsymbol{Q}_k^{(\ell)} + \delta_{\mathrm{R}}^2\boldsymbol{I}_{M_{\mathrm{R}}}\right)\boldsymbol{G}^{\mathrm{H}}\right\}\right\}}},\end{aligned} \tag{5.39}$$

with $\boldsymbol{Q}_k^{(\ell)} = \boldsymbol{H}_k^{(\ell)}\boldsymbol{R}_{\boldsymbol{x}_k^{(\ell)}\boldsymbol{x}_k^{(\ell)}}\boldsymbol{H}_k^{(\ell)^{\mathrm{H}}}$. The transmit covariance matrix of the kth user of

Table 5.1: Iterative Power Control at the Relay

Initialization step: set $\gamma_0^{(0)} = 1$, $\boldsymbol{G}^{(0)} = \boldsymbol{G}$,
maximum iteration number $N_{\max}$ and the threshold value ϵ.

Main step:
for $p = 0$ to $N_{\max} - 1$ **do**
Calculate $\boldsymbol{R}^{(p)}_{\boldsymbol{x}_k^{(\ell)}\boldsymbol{x}_k^{(\ell)}}$ using waterpouring algorithm in [41]
$P^{(p)} = \mathrm{tr}\left\{\boldsymbol{G}^{(p)}\left(\sum_{k,\ell} P_k^{(\ell)}\boldsymbol{Q}_k^{(\ell)} + \delta_{\mathrm{R}}^2\boldsymbol{I}_{M_{\mathrm{R}}}\right)\boldsymbol{G}^{(p)\mathrm{H}}\right\}$
$\gamma_0^{(p+1)} = \gamma_0^{(p)} \cdot \sqrt{\frac{P_{\mathrm{R}}}{P^{(p)}}}$
$\boldsymbol{G}^{(p+1)} = \gamma_0^{(p+1)}\boldsymbol{G}^{(p)}$
if $\left|\log_{10}\left(\frac{\gamma_0^{(p+1)}}{\gamma_0^{(p)}}\right)\right| < \epsilon$ **then**
break
end if
end for

the ℓth operator is defined as $\boldsymbol{R}_{\boldsymbol{x}_k^{(\ell)}\boldsymbol{x}_k^{(\ell)}} = \mathbb{E}\left\{\boldsymbol{x}_k^{(\ell)}\boldsymbol{x}_k^{(\ell)\mathrm{H}}\right\}$.

In case of single stream transmission (in our case single-antenna at each UT or DET beamforming), the transmit covariance matrix $\boldsymbol{R}_{\boldsymbol{x}_k^{(\ell)}\boldsymbol{x}_k^{(\ell)}}$ is just a scalar and therefore equation (5.39) is the closed-form solution to the power constraint at the relay. However, when each UT has multiple antennas and spatial multiplexing with the water-filling strategy is applied, the problem becomes complex since water-filling algorithm is SNR dependent and γ_0 scales the SNR. This means $\boldsymbol{R}_{\boldsymbol{x}_k^{(\ell)}\boldsymbol{x}_k^{(\ell)}}$ and γ_0 are completely coupled. A closed-form solution to find these two parameters jointly is intractable. However, if we assume the beamforming algorithms are known at the relay, we could relax the problem and utilize an iterative solution to find the two parameters.

The developed iterative algorithm can be presented as in Table 5.1.

Remarks

Remark 1. As shown in [57], if the weighting factor β is set to 0.5, we will have $\boldsymbol{G}_{\mathrm{S}}^{(\ell)} = \boldsymbol{G}_{\mathrm{S}}^{(\ell)^{\mathrm{T}}}$. Furthermore, if BD is applied or RBD is applied at the high regime, we will get $\boldsymbol{G} = \boldsymbol{G}^{\mathrm{T}}$. Such feature could help to avoid the use of channel feedback or backhauling when channel reciprocity exists. Thus it further reduces the complexity of the system.

Table 5.2: Comparison of Relay Amplification Schemes

Algorithm	$\boldsymbol{G}_{\mathrm{T}}$	$\boldsymbol{G}_{\mathrm{S}}$	$\boldsymbol{G}_{\mathrm{R}}$
ZF	$(\boldsymbol{F}\boldsymbol{H}^{\mathrm{T}})^{\mathrm{H}}\left((\boldsymbol{F}\boldsymbol{H}^{\mathrm{T}})(\boldsymbol{F}\boldsymbol{H}^{\mathrm{T}})^{\mathrm{H}}\right)^{-1}$	$\boldsymbol{I}_L \otimes \left(\boldsymbol{\Pi}_2 \otimes \boldsymbol{I}_{M_k^{(\ell)}}\right)$	$\left((\boldsymbol{H}\boldsymbol{W})^{\mathrm{H}}(\boldsymbol{H}\boldsymbol{W})\right)^{-1}(\boldsymbol{H}\boldsymbol{W})^{\mathrm{H}}$
MMSE	$\left(\boldsymbol{H}^{\mathrm{H}^{\mathrm{T}}}\boldsymbol{F}^{\mathrm{H}}\boldsymbol{F}\boldsymbol{H}^{\mathrm{T}} + 2L\delta_k^{(\ell)^2}\boldsymbol{I}_{M_{\mathrm{R}}}/P_{\mathrm{R}}\right)^{-1}\boldsymbol{H}^{\mathrm{H}^{\mathrm{T}}}\boldsymbol{F}^{\mathrm{H}}$	$\boldsymbol{I}_L \otimes \left(\boldsymbol{\Pi}_2 \otimes \boldsymbol{I}_{M_k^{(\ell)}}\right)$	$\boldsymbol{W}^{\mathrm{H}}\boldsymbol{H}^{\mathrm{H}}\left(\boldsymbol{H}\boldsymbol{W}\boldsymbol{W}^{\mathrm{H}}\boldsymbol{H}^{\mathrm{T}} + \delta_{\mathrm{R}}^2\boldsymbol{I}_{M_{\mathrm{R}}}/P_k^{(\ell)}\right)^{-1}$
BD	$\boldsymbol{G}_{\mathrm{R}}^{\mathrm{T}}$	Arbitrary	$\tilde{\boldsymbol{U}}_{\mathrm{n}}^{(\ell)}\tilde{\boldsymbol{U}}_{\mathrm{n}}^{(\ell)^{\mathrm{H}}}\forall\ell$
RBD	$\tilde{\boldsymbol{U}}^{(\ell)^*}\left\{\tilde{\boldsymbol{\Sigma}}^{(\ell)^*}\tilde{\boldsymbol{\Sigma}}^{(\ell)^{\mathrm{T}}} + 2LM_k^{(\ell)}\delta_k^{(\ell)^2}\boldsymbol{I}_{M_{\mathrm{R}}}/P_{\mathrm{R}}\right\}^{-1/2}, \forall\ell$	Arbitrary	$\left\{\frac{P_k^{(\ell)}}{M_{\mathrm{U}}}\tilde{\boldsymbol{\Sigma}}^{(\ell)}\tilde{\boldsymbol{\Sigma}}^{(\ell)^{\mathrm{H}}} + \delta_{\mathrm{R}}^2\boldsymbol{I}_{M_{\mathrm{R}}}\right\}^{-1/2}\tilde{\boldsymbol{U}}^{(\ell)^{\mathrm{H}}}, \forall\ell$

Remark 2. The ZF and MMSE solution in [82] can be also re-interpreted using our two-step approach. Moreover, since in these cases all the channels are equalized, the matrix $\boldsymbol{G}_{\mathrm{S}}^{(\ell)} = \boldsymbol{\Pi}_2 \otimes \boldsymbol{I}_{M_k^{(\ell)}}$ is the permutation matrix where $\boldsymbol{\Pi}_2 = \left[\begin{smallmatrix} 0 & 1 \\ 1 & 0 \end{smallmatrix}\right]$ is the row exchange matrix which ensures that the user will not receive its own transmitted data. A detailed comparison can be found in Table 5.2.

Simulation Results

In this section, the performance of the designed systems are evaluated via Monte Carlo simulations. The system sum rate is calculated via (5.17). The system BER is defined as the BER averaged over the users. In the first set of simulation, only a single antenna is equipped at each UT and the performance of the proposed resource-sharing algorithm is evaluated and compared to the non-sharing case as well as the algorithm in [82] and [79]. In the second set of simulation, multiple antennas are equipped at each terminal and the performance of proposed algorithm is evaluated in the same way as in the first set. Here, "uXX" stands for the beamforming strategy at each UT and "rXX" stands for the transmit strategy at the relay. In the last set of simulation, the effects of CSI imperfections are evaluated and discussed.

The simulated MIMO flat fading channels $\boldsymbol{H}_k^{(\ell)}$ are uncorrelated Rayleigh channels. The channel $\boldsymbol{H}_k^{(\ell)}$ is fixed during the training phase and data phase. The transmit power at each user terminal and relay are identical and $P_k^{(\ell)} = P_{\mathrm{R}} = 1$. The SNR at each user terminal and at the relay are also identical. It is defined as $\mathrm{SNR} = 1/\sigma_{\mathrm{R}}^2 = 1/\sigma_k^{(\ell)^2}$, $\forall k, \ell$. The weighting factor $w^{(\ell)}$ is set to 1 for all ℓ. Moreover, the weighting factor β is set to 0.5 in all simulations. All the simulation results are obtained by averaging over 1000 channel realizations.

The non-sharing case performance is labeled by "excl" which stands for exclusively. In our work, it means that the relay as well as the frequency spectrum are exclusively used by users of operators in a TDMA fashion. In particular, in the first two time slots, only one pair of users of one operator is served. In the next two time slots, the pair of users of another operator will be served and so on.

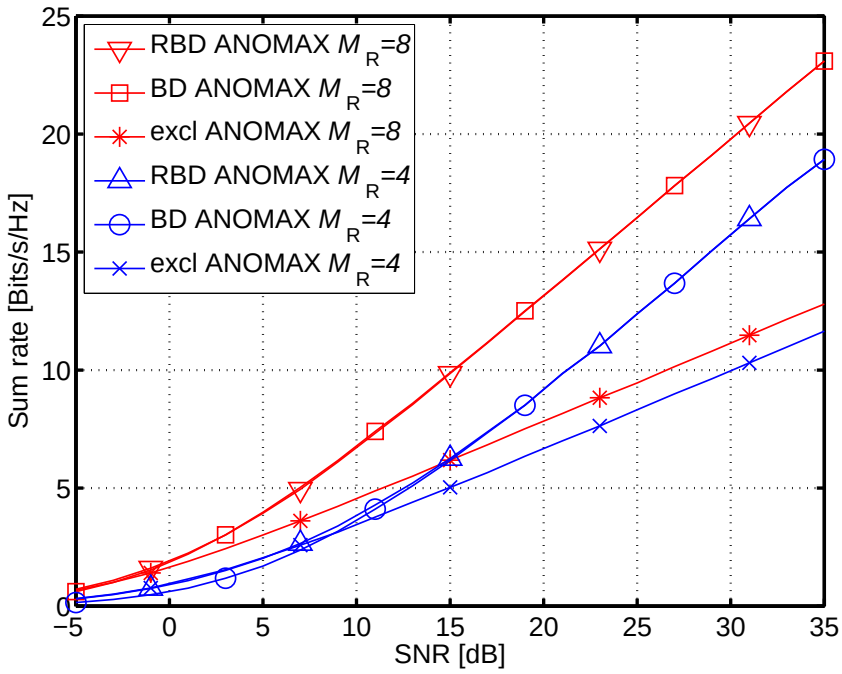

Figure 5.11: Sum rate comparison of exclusive approach and proposed approaches for $M_k^{(\ell)} = 1$ and $L = 2$.

A. Single Antenna at Each User Terminal

Figure 5.11 shows the system sum rate obtained from the simulation when $M_k^{(\ell)} = 1$ and $L = 2$. The performance of the proposed BD ("BD ANOMAX") and RBD ("RBD ANOMAX") outperforms the exclusive approach ("excl ANOMAX") for large value of M_{R} as well as moderate to high SNR values. Especially in the high SNR regime, the sharing gain is nearly two-fold. The result also implies that in the low SNR regime and with few number of antennas at the relay, we do not gain from the relay sharing.

In Figure 5.12, we compare the performance of various multi-operator two-way relaying approaches for $M_k^{(\ell)} = 1$, $M_{\mathrm{R}} = 8$ and $L = 2$. The "ZF" and "MMSE" methods are the single antenna version of algorithms proposed in [82]. "Erhan" stands for the algorithm proposed in [79]. As the result suggests, the proposed pairing aware algorithms (BD and RBD) methods give the best performance especially from moderate to high SNR regime. Due to the sufficient number of degree of freedoms under this configuration, non-pairing aware algorithms (ZF and MMSE) almost approach the performance of pairing aware algorithms with less than 1 dB difference. The Erhan method gives approximately 10 dB worse performance compared to the proposed BD and RBD methods at the high SNRs. This implies that ANOMAX offers the performance enhancement. However, all the curves have the same slope in the high SNR regime which means that they yield the same multiplexing gain.

Figure 5.13 shows the sum rate as a function of the number of antennas at the

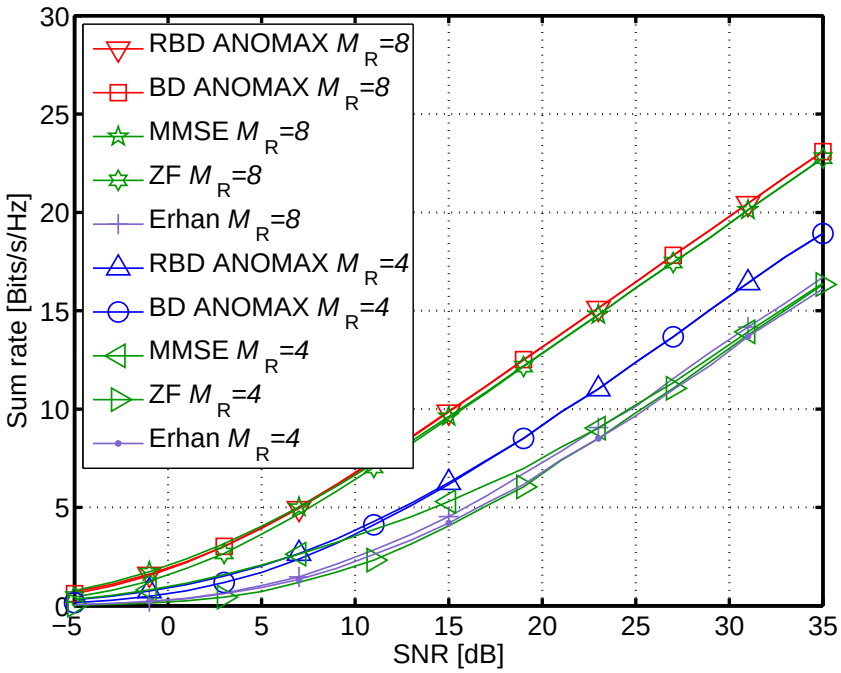

Figure 5.12: Sum rate comparison of different multi-operator two-way relaying approaches for $M_k^{(\ell)} = 1$ and $L = 2$.

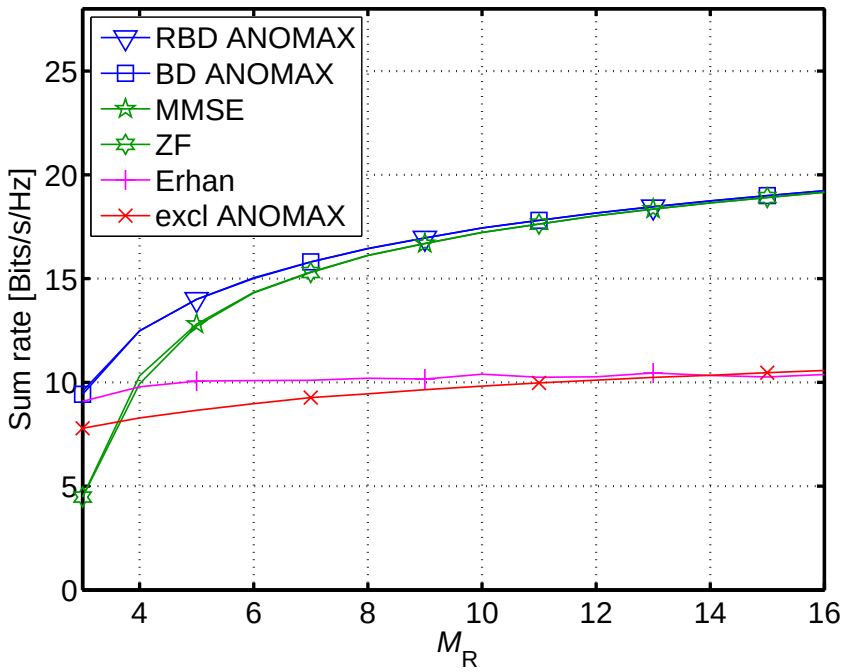

Figure 5.13: Sum rate comparison of different multi-operator two-way relaying approaches for $M_k^{(\ell)} = 1$, SNR= 25 dB and $L = 2$.

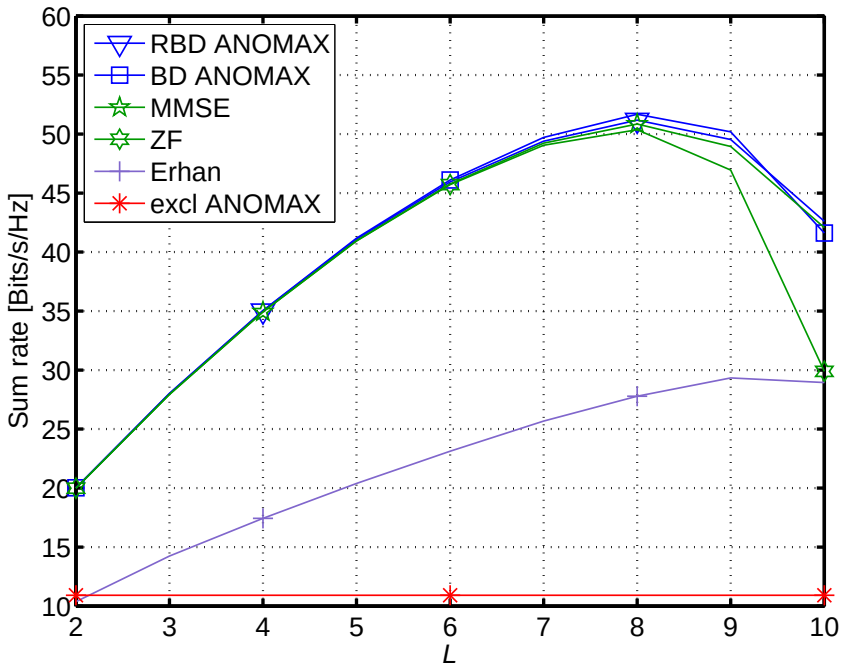

Figure 5.14: Sum rate comparison of different multi-operator two-way relaying approaches for $M_k^{(\ell)} = 1$, SNR= 25 dB, and $M_{\mathrm{R}} = 20$.

relay when the SNR is 25 dB. The sharing gain of paring aware schemes (BD and RBD) as well as non-paring aware schemes (ZF and MMSE) increases as the array size at the relay increases. BD and RBD outperforms ZF and MMSE especially when only few antennas are deployed at the relay. For example, When the relay has only 3 antennas, the sum rate of BD and RBD are two-times higher than ZF and MMSE. This is because the ZF and MMSE algorithms cannot used under this configuration. It can be also seen that the exclusive approach has better or equal performance compared to sharing approaches when the relay has a few antennas (e.g., 3 antennas). Again, the performance of the Erhan approach implies that the ANOMAX algorithm decides the gain obtained in BD and RBD schemes.

Figure 5.14 demonstrates the system sum rate performance when the relay has 20 antennas and the SNR is 25 dB. It shows that increasing the number of pairs (operators) which share the spectrum and the relay will increase the sharing gain. However, due to the dimensionality constraint of the SDMA based approach, there is an inflexion point after which increasing number of operators will decrease the system sum rate.

B. Two Antennas at Each User Terminal

Figure 5.15 shows the comparison of different transmit strategies when each UT has 2 antennas. Three beamforming approaches, namely, “uWF (water-filling algorithm in 5.3.1)", “uDET (dominant eigenmode transmission in 5.3.1)" and

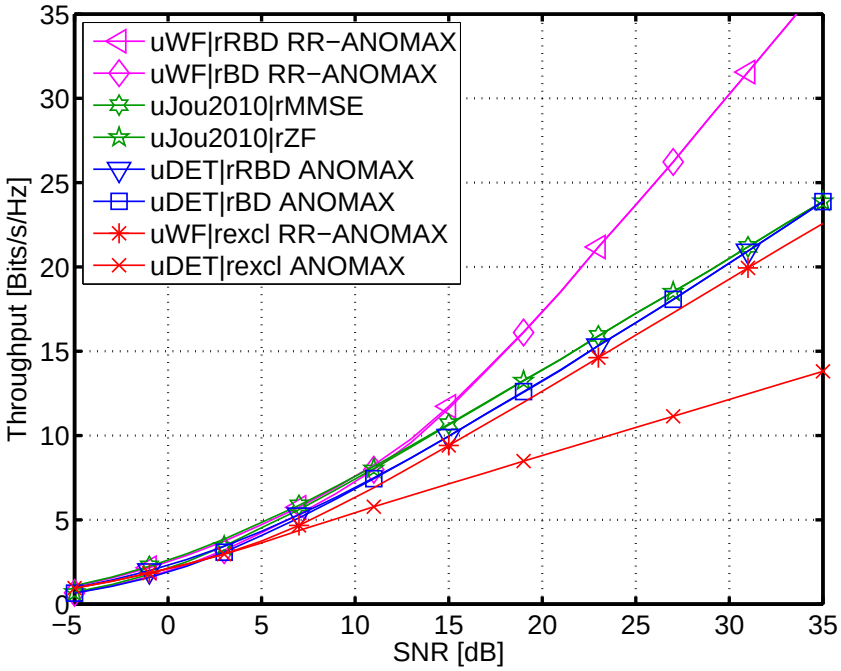

Figure 5.15: Sum rate comparison of different multi-operator two-way relaying transmit strategies for $M_k^{(\ell)} = 2$, $M_{\mathrm{R}} = 8$ and $L = 2$.

"uJou2010 (eigen beamforming in [82])", are used in this simulation. Since multiple stream transmission is possible, it is necessary to use the rank-restored solution "RR-ANOMAX". As could be seen, compared to the exclusive approach "uWF|rexcl RR-ANOMAX" (multiple-stream transmission) and "uDET|rexcl ANOMAX" (single-stream transmission), all proposed approaches ("uWF|rRBD RR-ANOMAX" / "uWF|rBD RR-ANOMAX" and "uDET|rRBD ANOMAX" / "uDET|rBD ANOMAX") could obtain almost two-fold sharing gain in terms of sum rate in the high SNR regime. Similar to the single antenna case, the BD and the RBD strategy only differ in the low SNR regime. Compared to the transmit strategies ("uJin2010|rZF" and "uJin2010|rMMSE") which are proposed in [82], proposed single stream transmission strategies ("uDET|rRBD ANOMAX" and "uDET|rBD ANOMAX") are worse from low to moderate SNRs.

In Figure 5.16, the sum rate performance as a function of the number of antennas at the relay at high SNR (25 dB) is shown. As the number of antennas increases, the slope of the proposed algorithms is higher compared to the exclusive approach, respectively. This means that larger sharing gains are obtained when the relay has more antennas. However, it could be still observed that when the relay has only 5 antennas, the exclusive approach outperforms the proposed approach because the interference suppression sacrifices the degree of freedoms. As can be also seen, the algorithms proposed in [82] also outperforms the proposed multi-stream transmission approaches when relay has only 5 antennas. Moreover, they always outperform the proposed single-stream transmission algorithms in this simulation.

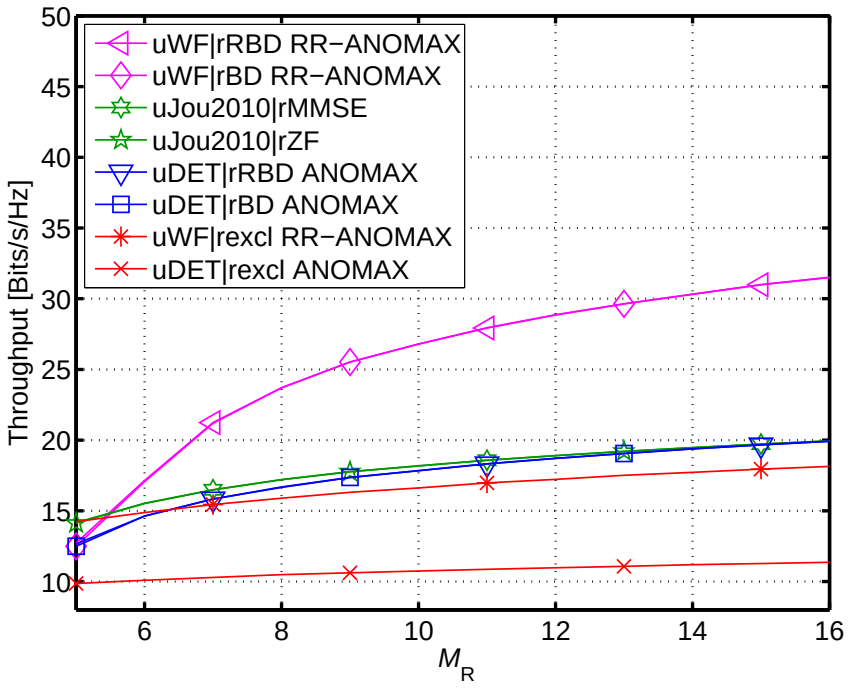

Figure 5.16: Sum rate comparison of different multi-operator two-way relaying approaches for $M_k^{(\ell)} = 2$, SNR= 25 dB and $L = 2$.

Conclusions

In this section, we investigate a relay sharing model where the relay and the spectrum are shared between multiple operators. We demonstrate that all operators can serve their users by using multiple antennas at the relay via the proposed projection based separation of multiple operators (ProBaSeMo) inspired by BD and RBD methods. This ProBaSeMo strategy can be applied for both single- and multi- antenna systems. Transmit- and receive- beamforming aimed at single-stream and multi-stream transmission are also proposed, respectively. In a two-operator case, the proposed strategy can provide a two-fold sharing gain with many antennas at the relay or in the high SNR regime regardless of single stream transmission or multiple stream transmission at the UTs. For fixed number of antennas at the relay, higher sharing gain can be obtained if the number of operators increases. The proposed pairing aware method has less dimensionality constraint compared to the non-pairing aware methods in [82].

5.3.2 Two-Way Relaying with Multiple Relays

The case in which multiple relays assist the unidirectional communication between two terminals is studied extensively in the literature. [83] proposes the AF cooperative transmission with multiple relays using phase feedback in single antenna terminals. MIMO terminals communicate over disjunct sets of relays in [84] using

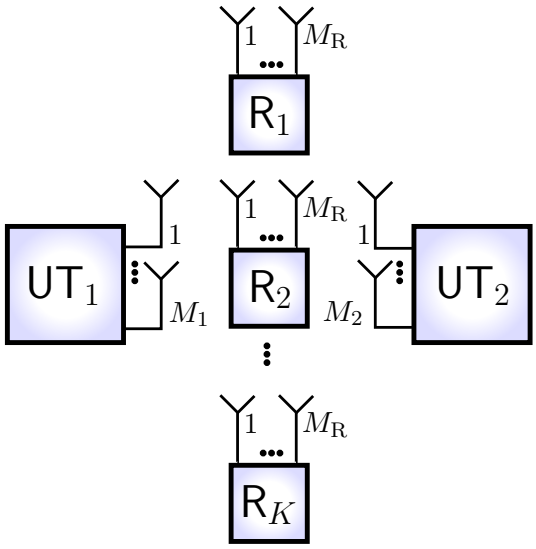

Figure 5.17: Two-way relaying system model with multiple relays: Two user terminals equipped with M_1 and M_2 antennas communicate with a set of K relay stations that have M_{R} antennas. There are two transmission phases.

transmit beamforming. The relay selection for single antenna terminals is studied in [85]. The exact outage analysis of cooperative communication with multiple amplify and forward relays is given in [86] and the diversity-multiplexing tradeoff for multiple terminal pairs and multiple relays is studied in [87] and [88].

The case in which multiple relays assist the bidirectional communication is studied less often. In [58], the diversity multiplexing tradeoff is characterized using dual matching matrices at the relays.

The basic system model is shown in Figure 5.17: The relay stations are equipped with $^{\mathrm{MR}}$ antennas and the terminals possess M_1 and M_2 antennas, respectively. Assuming quasi-static block fading channels as well as frequency-flat fading, the received signal at the k-th relay during the first time slot can be expressed as

$$\tilde{\boldsymbol{y}}_k = \boldsymbol{H}_{1,k}^{(\mathrm{f})} \boldsymbol{Q}_1^{1/2} \boldsymbol{d}_1 + \boldsymbol{H}_{2,k}^{(\mathrm{f})} \boldsymbol{Q}_2^{1/2} \boldsymbol{d}_2 + \tilde{\boldsymbol{n}}_k, \tag{5.40}$$

where $\boldsymbol{H}_{1,k}^{(\mathrm{f})} \in \mathbb{C}^{^{\mathrm{MR}} \times M_1}$ and $\boldsymbol{H}_{2,k}^{(\mathrm{f})} \in \mathbb{C}^{^{\mathrm{MR}} \times M_2}$ represent the forward MIMO channel matrices between the terminals and the k-th relay, $\boldsymbol{d}_1 \in \mathbb{C}^{\mathrm{rank}(\boldsymbol{Q}_1)\times 1}$ and $\boldsymbol{d}_2 \in \mathbb{C}^{\mathrm{rank}(\boldsymbol{Q}_2)\times 1}$ denote the data transmitted by the terminals, $\boldsymbol{Q}_1$ and $\boldsymbol{Q}_2$ are the transmit covariance matrices at the terminals and $\tilde{\boldsymbol{n}}_k$ represents the additive noise component at the relay. We assume a noise covariance matrix $\sigma^2 \boldsymbol{I}_{M_{\mathrm{R}}}$.

The transmit vector at relay k in phase two is given by

$$\tilde{\boldsymbol{x}}_k = \boldsymbol{A}_k \tilde{\boldsymbol{y}}_k = \boldsymbol{A}_k \boldsymbol{H}_{1,k}^{(\mathrm{f})} \boldsymbol{Q}_1^{1/2} \boldsymbol{d}_1 + \boldsymbol{A}_k \boldsymbol{H}_{2,k}^{(\mathrm{f})} \boldsymbol{Q}_2^{1/2} \boldsymbol{d}_2 + \boldsymbol{A}_k \tilde{\boldsymbol{n}}_k, \tag{5.41}$$

with relay amplification matrix $\boldsymbol{A}_k$ and the corresponding transmit power at the relay k averaged over transmit symbols $\boldsymbol{d}_1, \boldsymbol{d}_2$ and noise realizations at the relay $\tilde{\boldsymbol{n}}_k$ is given by

$$p_{R_k} = \mathbb{E}\{\mathrm{tr}\{\tilde{\boldsymbol{x}}_k \tilde{\boldsymbol{x}}_k^H\}\} = \mathrm{tr}\left\{\boldsymbol{A}_k \boldsymbol{H}_{1,k}^{(\mathrm{f})} \boldsymbol{Q}_1 \boldsymbol{H}_{1,k}^{(\mathrm{f})^{\mathrm{H}}} \boldsymbol{A}_k^H\right\} + \mathrm{tr}\left\{\boldsymbol{A}_k \boldsymbol{H}_{2,k}^{(\mathrm{f})} \boldsymbol{Q}_2 \boldsymbol{H}_{2,k}^{(\mathrm{f})^{\mathrm{H}}} \boldsymbol{A}_k^H\right\} + \sigma^2 \mathrm{tr}\left\{\boldsymbol{A}_k \boldsymbol{A}_k^H\right\}. \tag{5.42}$$

The normalized transmit vector at relay k is $\boldsymbol{x}_k = \frac{\tilde{\boldsymbol{x}}_k}{\sqrt{\gamma_k}}\sqrt{P_k}$, where γ_k is used to satisfy certain average or short-term power constraints.

When comparing different relaying strategies it is important to normalize the transmit power at the relays by γ_k. We observe in (5.42) that the relay power p_{R_k} depends on both transmit covariance matrices $\boldsymbol{Q}_1, \boldsymbol{Q}_2$ in a complex way via the forward channels $\boldsymbol{H}_{1,k}^{(\mathrm{f})}, \boldsymbol{H}_{2,k}^{(\mathrm{f})}$ and the relay amplification matrices $\boldsymbol{A}_k$. Usually there are two power constraints, the short-term (instantaneous) power constraint on p_{R_k} or the long-term (average) power constraint on $\mathbb{E}\{p_{R_k}\}$.

The received vector at terminal one in phase two is given by

$$\boldsymbol{y}_1 = \sum_{k=1}^{K} \boldsymbol{H}_{1,k}^{(\mathrm{b})} \boldsymbol{x}_k + \boldsymbol{n}_1 \tag{5.43}$$

with AWGN $\boldsymbol{n}_1 \sim CN(0, \sigma^2 \boldsymbol{I}_{M_1})$. For convenience, we assume that the noise variance at the relay and the terminals is equal to σ^2. The extension to different noise variances is straightforward. Terminal one subtracts the self interference (analog network coding) and obtains

$$\hat{\boldsymbol{y}}_1 = \sum_{k=1}^{K} \sqrt{\frac{P_k}{\gamma_k}} \boldsymbol{H}_{1,k}^{(\mathrm{b})} \boldsymbol{A}_k \boldsymbol{H}_{2,k}^{(\mathrm{f})} \boldsymbol{Q}_2^{1/2} \boldsymbol{d}_2 + \sum_{k=1}^{K} \sqrt{\frac{P_k}{\gamma_k}} \boldsymbol{H}_{1,k}^{(\mathrm{b})} \boldsymbol{A}_k \tilde{\boldsymbol{n}}_k + \boldsymbol{n}_1. \tag{5.44}$$

Define the matrices $\tilde{\boldsymbol{H}}_{2:1} = \sum_{k=1}^{K} \sqrt{\frac{P_k}{\gamma_k}} \boldsymbol{H}_{1,k}^{(\mathrm{b})} \boldsymbol{A}_k \boldsymbol{H}_{2,k}^{(\mathrm{f})}$ and $\tilde{\boldsymbol{H}}_{1:2} = \sum_{k=1}^{K} \sqrt{\frac{P_k}{\gamma_k}} \boldsymbol{H}_{2,k}^{(\mathrm{b})} \boldsymbol{A}_k \boldsymbol{H}_{1,k}^{(\mathrm{f})}$ as the effective channels seen by terminal one and two. The noise covariance matrix at terminal one is given by

$$\tilde{\boldsymbol{Z}}_1 = \sigma^2 \boldsymbol{I}_{M_1} + \sigma^2 \sum_{k=1}^{K} \frac{P_k}{\gamma_k} \boldsymbol{H}_{1,k}^{(\mathrm{b})} \boldsymbol{A}_k \boldsymbol{A}_k^H \boldsymbol{H}_{1,k}^{(\mathrm{b})^{\mathrm{H}}}. \tag{5.45}$$

Observe that the colored noise matrix $\tilde{\boldsymbol{Z}}_1$ depends indirectly on the transmit strategies $\boldsymbol{Q}_1$ and $\boldsymbol{Q}_2$ via γ_k. This fact complicates the analysis and design of optimal relaying strategies.

Before we discuss suboptimal relay approaches, the performance measures need to be described. The achievable rate of the transmission from terminal one to terminal two is given by

$$R_1(\boldsymbol{Q}_1, \boldsymbol{Q}_2, \boldsymbol{A}_1, ..., \boldsymbol{A}_K) = \log\det\left(\boldsymbol{I}_{M_1} + \tilde{\boldsymbol{Z}}_1^{-1} \tilde{\boldsymbol{H}}_{1:2} \boldsymbol{Q}_1 \tilde{\boldsymbol{H}}_{1:2}^H\right) \tag{5.46}$$

where the effective channel $\tilde{\boldsymbol{H}}_{1:2}$ seen by terminal one depends on the relay amplification matrices $\boldsymbol{A}_1, ..., \boldsymbol{A}_K$. The colored noise matrix $\tilde{\boldsymbol{Z}}_1$ is defined in (5.45). The achievable rate of the transmission from terminal two to terminal one is denoted by R_2 and also a function of the transmit covariance matrices $\boldsymbol{Q}_1$ and $\boldsymbol{Q}_2$ and the relay amplification matrices $\boldsymbol{A}_1, ..., \boldsymbol{A}_K$.

The objectives R_1 and R_2 can be maximized by choosing the relay AF matrices $\boldsymbol{A}_1, ..., \boldsymbol{A}_K$ and the two transmit covariance matrices $\boldsymbol{Q}_1$ and $\boldsymbol{Q}_2$. These should be optimized *jointly*. However, if the transmit covariance matrices $\boldsymbol{Q}_1$ and $\boldsymbol{Q}_2$ change, this usually changes the AF matrices $\boldsymbol{A}_k$ and their transmit power p_{R_k} in (5.42) as discussed before. For the one-way channel, a complete solution can be found in [89]. In [90], an approximation of the relay power was applied for large number of relays. Up to now, no complete characterization of the optimal AF matrices and covariance matrices at the nodes for the two-way relay channel is available.

Therefore, we relax the power constraints at the relay and allow for average power constraints there, i.e., average with respect to channel realizations $\mathbb{E}\{p_{R_k}\} \leq P_k$ for all $k, 1 \leq k \leq K$ and consider three different relay strategies:

1. The relay AF matrices are chosen fixed as *DFT matrices* of size $M_{\mathrm{R}} \times M_{\mathrm{R}}$, $\boldsymbol{A}_k^D = \boldsymbol{D}_{n_k}$. For this scheme no channel information is needed at the relay and the processing can be efficiently implemented.

2. The relay AF matrices are chosen according to the *dual channel matching* scheme (recently proposed in [58]) as follows

$$\boldsymbol{A}_k^M = \boldsymbol{H}_{2,k}^{(\mathrm{b})^{\mathrm{H}}} \boldsymbol{H}_{1,k}^{(\mathrm{f})^{\mathrm{H}}} + \boldsymbol{H}_{1,k}^{(\mathrm{b})^{\mathrm{H}}} \boldsymbol{H}_{2,k}^{(\mathrm{f})^{\mathrm{H}}}. \tag{5.47}$$

   Note that dual channel matching can only be used if $M_1 = M_2$. Otherwise, a dimension reduction must be performed.

3. The relay AF matrices are chosen by *ANOMAX* [57] as $\mathrm{vec}(\boldsymbol{A}_k^A) = \boldsymbol{u}_k^*$ where $\boldsymbol{u}_k$ is the dominant left singular vector of the matrix

$$\boldsymbol{K}_k = [\boldsymbol{H}_{2,k}^{(\mathrm{f})^{\mathrm{T}}} \otimes \boldsymbol{H}_{1,k}^{(\mathrm{b})}; \boldsymbol{H}_{1,k}^{(\mathrm{f})^{\mathrm{T}}} \otimes \boldsymbol{H}_{2,k}^{(\mathrm{b})}].$$

   This follows with $\beta = \frac{1}{2}$.

For a given relay strategy $\boldsymbol{A}_k^D, \boldsymbol{A}_k^M$ or $\boldsymbol{A}_k^A$, the remaining problem statement is as follows: The optimal transmit covariance matrices $\boldsymbol{Q}_1$ and $\boldsymbol{Q}_2$ solve the sum rate maximization problem given by

$$\max_{\boldsymbol{Q}_1 \succeq 0, \mathrm{tr}\{\boldsymbol{Q}_1\} \leq P_A} \max_{\boldsymbol{Q}_2 \succeq 0, \mathrm{tr}\{\boldsymbol{Q}_2\} \leq P_B} R_1 + R_2. \tag{5.48}$$

First, the average transmit power at relay k needs to be computed as a function of the transmit covariance matrices in order to solve (5.48). The less coupling between $\boldsymbol{Q}_1$ and $\boldsymbol{Q}_2$ and the relay transmit power the simpler is the remaining optimization.

Result 1: Using DFT relay amplification matrices $\boldsymbol{A}_k^D$, the average transmit power at the relay k is given by

$$P_D^r = \mathbb{E}\{p_k\} = \mathrm{tr}\left\{\left(\mathbb{E}\left\{\boldsymbol{H}_{1,k}^{(\mathrm{f})^{\mathrm{H}}}\boldsymbol{H}_{1,k}^{(\mathrm{f})}\right\}\boldsymbol{Q}_A\right)\right\} + \mathrm{tr}\left\{\left(\mathbb{E}\left\{\boldsymbol{H}_{2,k}^{(\mathrm{f})^{\mathrm{H}}}\boldsymbol{H}_{2,k}^{(\mathrm{f})}\right\}\boldsymbol{Q}_B\right)\right\} + \sigma^2\mathrm{tr}\left\{\boldsymbol{I}_{M_{\mathrm{R}}}\right\}. \quad (5.49)$$

For independent and spatially uncorrelated fading the average transmit power is

$$P_D^r = M_{\mathrm{R}}\mathrm{tr}\left\{(\boldsymbol{Q}_A + \boldsymbol{Q}_B)\right\} + \sigma^2 M_{\mathrm{R}}. \quad (5.50)$$

Remark: Observe that this result also holds for the identity AF matrices $\boldsymbol{A}_k^I = \boldsymbol{I}_{M_{\mathrm{R}}}$. The nice observation in (5.50) is that the average relay power does only depend on the transmit power of the nodes $\mathrm{tr}\{\boldsymbol{Q}_A\}$ and $\mathrm{tr}\{\boldsymbol{Q}_B\}$, respectively.

Result 2: Using the dual channel matching matrices in (5.47), the average transmit power at the relay k is characterized by

$$P_M^r = \mathbb{E}\{p_{R_k}\} = c_k\mathrm{tr}\left\{\boldsymbol{Q}_A + \boldsymbol{Q}_B\right\} + 3\sigma^2 M_{\mathrm{R},k}. \quad (5.51)$$

The constant c_k depends on the number of antennas at the nodes and at the relay (more details can be found in [91]).

Remark: Observe that the average power depends on the transmit covariance matrices via only the trace again. This implies that for fixed trace constraint on $\boldsymbol{Q}_A$ and $\boldsymbol{Q}_B$, the average power at the relay does not vary. Therefore, the optimization in (5.48) decouples into single-user optimization problems.

Denote the effective channel including the colored noise at terminal one by

$$\boldsymbol{C}_{2:1} = \tilde{\boldsymbol{Z}}_1^{-1/2}\tilde{\boldsymbol{H}}_{2:1}$$

and its singular value decomposition by $\boldsymbol{C}_{2:1} = \boldsymbol{U}_{2:1}\boldsymbol{\Lambda}_{2:1}\boldsymbol{V}_{2:1}^{\mathrm{H}}$.

Result 3: Under individual average relay power constraints, the optimal transmit covariance matrix $\boldsymbol{Q}_2 = \boldsymbol{U}_{Q_2}\boldsymbol{\Lambda}_{Q_2}\boldsymbol{U}_{Q_2}^{\mathrm{H}}$ is given by $\boldsymbol{U}_{Q_2} = \boldsymbol{V}_{2:1}$. The power allocation in $\boldsymbol{\Lambda}_{Q_2} = \mathrm{diag}\left\{\lambda_{Q_2,1}, ..., \lambda_{Q_2,M_2}\right\}$ is given by

$$\lambda_{Q_2,k} = \left(\frac{1}{\nu} - \frac{\sigma^2}{\lambda_{2:1,k}}\right)^+ \quad (5.52)$$

where $(\cdot)^+ = \max(\cdot, 0)$ and ν is chosen such that $\sum\lambda_{Q_2,k}$ satisfies the transmit power constraint. Indeed, (5.52) is the waterfilling solution for the effective channel seen by terminal two.

Adding more relays to assist two-way communication increases the transmission rates while increasing the overhead costs due to channel estimation and signalling. In Figure 5.18, the average sum rate for a two-way link between two two-antenna

terminals and two to six two-antenna relays is shown over the transmit SNR. We average over 100.000 channel realizations. We compare equal power allocation (EPA) without transmit precoding and optimal transmit covariance matrix optimization at the terminals (Opt). For the simulations, we assumed reciprocal channels, e.g., in a half-duplex time division relaying protocol in which identical RF chains are applied, i.e., the backward channels are the transpose forward channels

$$\boldsymbol{H}_{1,k}^{(\mathrm{f})^{\mathrm{T}}} = \boldsymbol{H}_{1,k}^{(\mathrm{b})} \quad \boldsymbol{H}_{2,k}^{(\mathrm{f})^{\mathrm{T}}} = \boldsymbol{H}_{2,k}^{(\mathrm{b})} \quad \text{for all } k = 1...K.$$

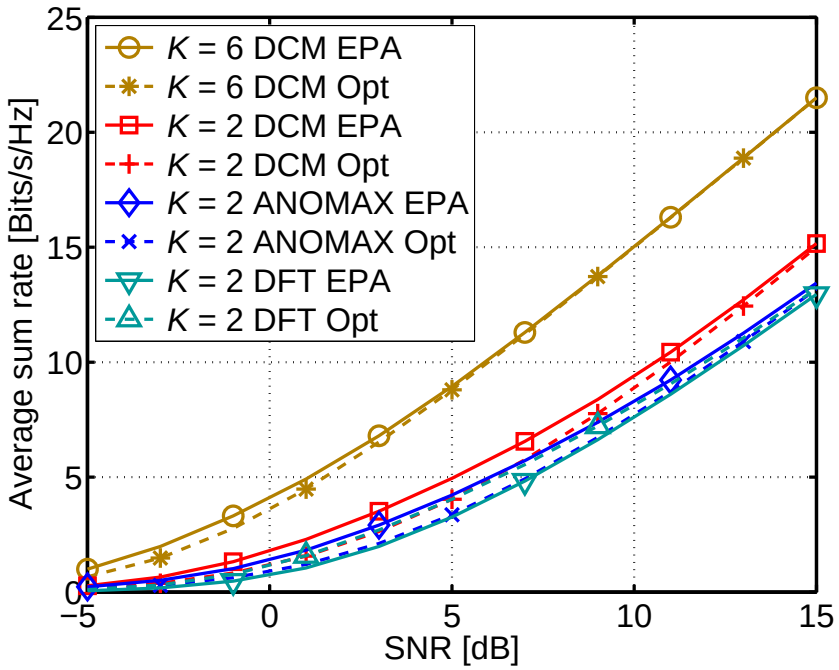

Figure 5.18: Average sum rate for $2 \times 2 \times 2$ relay assisted two-way channel with $K = 2, 6$ relays for different relaying and transmit strategies.

In Figure 5.18, the gain of having multiple relays can be observed. The sum rate curve is shifted to the left by adding more relays. Channel aware dual channel matching increases the sum rate in the medium SNR regime. The power normalization is chosen such that the average relay transmit power is equal for all three relaying strategies. It turns out that the original version of ANOMAX performs worse than DFT AF. This was observed and an improved version of ANOMAX is proposed in [81] which is close to maximum sum rate performance in single relay systems. Furthermore, it can be observed that for $K = 6$ multiple relays, the DCM clearly outperforms the fixed DFT relaying.

When DFT relaying, ANOMAX, and DCM are compared, it is important to observe the tradeoff between performance (here the average sum rate), the control overhead, the complexity, and the restrictions. DFT is less complex and requires no channel information at the relays at all. DCM requires information at the relay k on its own channels $\boldsymbol{H}_{1,k}$ and $\boldsymbol{H}_{2,k}$ and has the additional restriction that $M_1 = M_2$.

ANOMAX requires also information at the relay on its own channels but can be applied to asymmetric channels as well.

The two way amplify-and-forward relaying with multiple relays contains important and interesting open research problems. This section presents the state-of-the-art and gives some directions for future research. The system model is easily extended to the multiple relay scenario. However, the optimal choice of transmit strategies and relaying matrices is a difficult coupled programming problem. The choice of the transmit strategies influences the transmit power at the relays. This complicates the optimization additionaly. Under average transmit power constraints at the relays and certain amplify and forward strategies it is possible to simplify the transmit optimization problem. Without channel state information at the relay, we propose to use the DFT matrix and with channel state information on the own channels, we propose to apply the dual channel matching approach. Both relaying techniques lead to a simple dependency of the relays' transmit power on the transmit covariance matrices. The transmit covariance matrix optimization reduces to single-user problems which are solved by single-user waterfilling. Numerical results illustrate the gain by using transmit optimization and different relaying strategies.

The optimal AF relaying strategy for MIMO two-way channels with multiple relays is thus still unknown. The section presents one approach to compare recently proposed AF strategies with optimal node precoding under a fair average relay power constraint. When a single relay is applied the fixed AF strategy using a DFT matrix performs reasonable well. However, with multiple relays the channel aware DCM outperforms DFT significantly. Further gains in sum rate can be achieved by node optimization. Multiple relays improve the sum rate performance and reduce the impact of the transmit strategies at the nodes.

In future work, a comparison of the exclusive use of the relays will be performed and the SAPHYRE gain will be assessed.

5.4 Signal Processing for WNC Based Relay Sharing

This section identifies areas of the WNC with various strategies (e.g. HDF) which are affected or directly depend on the signal processing. Actual analysis and synthesis of the particular algorithms is planned for later project stages. At the current stage, we need only to *identify* the critical points.

WNC strategies based on interim decision at relays (xDF) achieve the sharing gain by a proper construction of the multi-source codebooks, a proper design of the decoding algorithms at relays and destinations (e.g. decisions on hierarchical symbols in HDF strategy). The actual impact of signal processing is only secondary. For example the synchronization related matters. However the situation in the WNC system offers a number of additional options to the classical synchronization and channel state estimation problems. Namely, the *distributed* synchronization and

estimation algorithms utilizing various forms of available (soft) side information on *hierarchical* data can be effectively used. The non-availability of direct source data at the relay when using HDF strategy puts the data (soft or decision) aided synchronization algorithms under strongly different position. There is also a significant distinguishing fact that the received signal is affected by the channel parameters of multiple incoming signals but the hierarchical symbol/codeword decoding process usually requires only some compound form of the channel state. As an example, consider the reception of 2-source HXC coded signals for HDF strategy at relay each with channel transfer h_a, h_b. However, the hierarchical decoder requires not the individual transfers but a compound one h_a/h_b.

WNC strategies with various forms of *compression* strategies (e.g. HCF) rely jointly on the cooperative/sharing codebook construction (as in the WNC/xDF case) and, on top of it, on soft decoding metric compression technique. The latter topic can be seen from both information theory (decoding) and signal processing perspective. Since, as an example, the soft-decoding metric can be relayed by an analog communication technique.

A consideration will also be given to hybrid decode & forward and amplify & forward techniques including comparisons of possible gains achievable by those two.

Given the discussion above, we identify the critical areas of the signal processing for WNC based relay sharing. The following algorithms will be developed at the later stages of the project:

- Synchronization and channel state estimation of the compound multi-source channel state suited for hierarchical relay decoder,
- Distributed and hierarchical symbol (soft) information aided forms of the above algorithms,
- Signal processing for soft relay decoding metric transfer,
- Making a connection between A&F based technique and HDF technique for a comparison purposes,
- Hybrid approaches with HDF coding technique helped by analog preprocessing (on both Tx and Rx side).

6 Conclusions

This report describes initial signal processing techniques to handle the new interference that is created in the sharing scenarios of SAPHYRE. We have presented the sharing scenarios that are investigated in SAPHYRE, and have introduced the new approaches that have been developed in the SAPHYRE project. Moreover, we have demonstrated the SAPHYRE gain, which is defined as the system rate of the simultaneous sharing scenario compared to the time-shared case of the spectrum and infrastructure by the operators.

For the interference channel, all the proposed algorithms can achieve a significant SAPHYRE gain. Specially the following results are shown.

- in Section 3.2 it can be observed that the K-users MISO interference channel, shown in Figure 3.1, is mainly noise limited for low SNR. The best strategies then are maximum ratio transmission (MRT) at the transmitters. In this case, the relative gain grows with the number of users K. For very high SNRs, the system becomes interference limited and the SAPHYRE gain shrinks down to 0. The impact of the number of transmit antennas is also investigated for medium SNRs. Increasing the number of transmit antennas leads to new spatial degrees of freedom and the region looks more convex. Thereby, the fairness of the resource allocation (for sum rate maximization) is increased. However, the SAPHYRE gain has not changed significantly.
- in Section 3.3 the beamforming algorithm, which is based on balancing the egoistic and the altruistic behavior with the aim of maximizing the sum rate, exhibits the same optimal rate scaling (when the SNR grows) shown by recent iterative interference-alignment based methods. The proposed beamforming algorithm achieves almost the same performance as the optimal sum rate maximization method [39] without additional pricing feedbacks from the users and outperform interference alignment based methods in terms of sum rate in asymmetric networks. A large SAPHYRE gain is observed for the asymmetric channels and it increases with increasing SNR.
- in Chapter 4 the proposed cooperative algorithm achieves an operating point which is almost Pareto optimal. The final solution is in all cases better than the Nash equilibrium (NE), which would be the outcome if there was no cooperation. The novel element of the proposed algorithm is the use of the generated interference level as bargaining value. The algorithm is equally applicable to the case of instantaneous and statistical CSI. The SAPHYRE gain increases with increasing SNR for the scenarios of instantaneous CSI and statistical CSI with low-rank matrices.

For the relay-assisted communications, several novel relay sharing models are presented and investigated. By evaluating the proposed methods, we have the following conclusions.

- in Section 5.2.1 the linear precoding design for the interference relay channel is studied. The proposed flexible coordinated beamforming for the interference relay channel (IRC FlexCoBF) algorithm at the BSs achieves a better sum rate performance compared to coordinated zero-forcing (CoZF) [56] as well as eigen-beamforming [56]. IRC FlexCoBF is also more robust to the interference. Last but not least, the sum rate performance of the interference relay channel (IRC) is compared to the relay channel (RC) and there exists a large sharing gain, which strongly supports the use of a shared relay instead of operating in the time multiplexing mode.
- in Section 5.2.2 the resource allocation for MSE minimization in a DS/CDMA relay-assisted IC has been studied. The interaction between the relay and the multiple access users has been modeled as a two-level Stackelberg game, with the relay as the leader, and the multiple access users as followers. Numerical simulation corroborating the theoretical results have been provided, showing the merits of the proposed resource allocation techniques.
- in Section 5.3.1 it is demonstrate that all L operators ($L > 1$) can serve their users by using multiple antennas at a shared relay via a sub-optimal transmit strategy inspired by the BD [60] and RBD [61] algorithms using the two-way relaying principle. This proposed projection based separation of multiple operators (ProBaSeMO) in two-way relaying can be applied for both single and multiple antenna systems at the user terminals. Transmit and receive concepts using single-stream and multi-stream transmission are also proposed. In the two-operator case ($L = 2$), the proposed ProBaSeMo strategy can provide a two-fold sharing gain with many antennas at the relay or in the high SNR regime regardless of the number of the transmitted data streams at the UTs. For a fixed number of antennas at the relay, higher sharing gains can be obtained if the number of operators L increases. The proposed pairing aware method has less dimensionality constraints compared to the non-pairing aware methods in [82].
- in Section 5.3.2 one approach to compare recently proposed AF strategies with optimal node precoding under a fair average relay power constraint is presented. When a single relay is applied, the fixed AF strategy using a DFT matrix performs reasonably well. However, with multiple relays the channel aware DCM outperforms the DFT matrix significantly. Further gains in sum rate can be achieved by node optimization. Multiple relays improve the sum rate performance and reduce the impact of the transmit strategies at the nodes.

This deliverable has summarized various practical approaches to deal with the new interference in the sharing scenarios. Some of these approaches are further evaluated

via the system level simulation in WP4 and via a demonstrator implementation in WP6.

A Appendix

Proof of Lemma 3.3

Define the Lagrangian of the sum rate maximization problem for Tx i to be $\mathcal{L}(\mathbf{w}_i, \mu) = \bar{R} - \mu_{max}(\mathbf{w}_i^H \mathbf{w}_i - 1)$. The neccessary condition of Lagrangian $\frac{\partial}{\partial \mathbf{w}_i^H}\mathcal{L}(\mathbf{w}_i, \mu) = 0$ gives: $\frac{\partial}{\partial \mathbf{w}_i^H} R_i + \sum_{j\neq i}^{N_c} \frac{\partial}{\partial \mathbf{w}_i^H} R_j = \mu_{max}\mathbf{w}_i$. With elementary matrix calculus,

$$\frac{\partial}{\partial \mathbf{w}_i^H} R_i = \frac{P}{\sum_{k=1}^{N_c} |\mathbf{v}_i^H \mathbf{H}_{ik}\mathbf{w}_k|^2 P + \sigma_i^2}\mathbf{E}_i \mathbf{w}_i \tag{A.1}$$

$$\frac{\partial}{\partial \mathbf{w}_i^H} R_j = -\frac{|\mathbf{v}_j^H \mathbf{H}_{jj}\mathbf{w}_j|^2 P}{\sum_{k=1}^{N_c} |\mathbf{v}_j^H \mathbf{H}_{jk}\mathbf{w}_k|^2 P + \sigma_j^2}$$
$$\frac{P}{\sum_{k\neq j}^{N_c} |\mathbf{v}_j^H \mathbf{H}_{jk}\mathbf{w}_k|^2 P + \sigma_j^2}\mathbf{A}_j \mathbf{w}_i \tag{A.2}$$

where λ_{ji}^{opt} is a function of all channel states information and beamformer feedback:

$$\lambda_{ji}^{opt} = -\frac{S_{jj}}{\sum_{k=1}^{N_c} S_{jk} + \sigma_j^2} \frac{\sum_{k=1}^{N_c} S_{ik} + \sigma_i^2}{\sum_{k\neq j}^{N_c} S_{jk} + \sigma_j^2} \tag{A.3}$$

where $S_{jk} = |\mathbf{v}_j^H \mathbf{H}_{jk}\mathbf{w}_k|^2 P$. Thus, the gradient is zero for any $\mathbf{w}_i$ eigenvector of the matrix shown on the L.H.S. of (3.14). Among all stable points, the global maximum of the cost function is reached by selecting the dominant eigenvector of $E_i + \sum_{j\neq i} \lambda_{ji} A_{ji}$.

Proof of Theorem 3.5

To prove that interference alignment forms a convergence set of *DBA*, we will prove that if *DBA* achieves interference alignment, *DBA* will not deviate from the solution (stable point).

Assumed interference alignment is reached and let $(\mathbf{w}_1^{IA}, \ldots, \mathbf{w}_{N_c}^{IA}) \in \mathcal{IA}^{DL}$ and $(\mathbf{v}_1^{IA}, \ldots, \mathbf{v}_{N_c}^{IA}) \in \mathcal{IA}^{UL}$. Let $\mathbf{Q}_i^{DL} = \sum_{k\neq i}^{N_c} \mathbf{H}_{ik}\mathbf{w}_k^{IA}\mathbf{w}_k^{IA,H}\mathbf{H}_{ik}^H$ and $\mathbf{Q}_i^{UL} = \sum_{k\neq i}^{N_c} \mathbf{H}_{ki}^H \mathbf{v}_k^{IA}\mathbf{v}_k^{IA,H}\mathbf{H}_{ki}$.

Given receivers $(\mathbf{v}_1^{IA}, \ldots, \mathbf{v}_{N_c}^{IA})$, we compute new transport beamformers. In high SNR regime, $\lambda_{ji} \to -\infty$ and *DBA* gives $\mathbf{w}_i = V^{min}(\mathbf{Q}_i^{UL})$ (3.16). By (3.26), $\mathbf{Q}_i^{UL}$ is low rank and thus $\mathbf{w}_i$ is in the null space of $\mathbf{Q}_i^{UL}$. In direct consequence, the conditions of interference alignment (3.28) are satisfied. Thus, $(\mathbf{w}_1, \ldots, \mathbf{w}_{N_c}) \in \mathcal{IA}^{DL}$.

Given transmitters $(\mathbf{w}_1^{IA}, \ldots, \mathbf{w}_{N_c}^{IA})$, we compute new receive beamformers. The receive beamformer is defined as $\mathbf{v}_i = \arg\max \frac{\mathbf{v}_i^H \mathbf{H}_{ii} \mathbf{w}_i^{IA} \mathbf{w}_i^{IA,H} \mathbf{H}_{ii}^H \mathbf{v}_i}{\mathbf{v}_i^H \mathbf{Q}_i^{DL} \mathbf{v}_i}$. Since $\mathbf{Q}_i^{DL}$ is low rank, the optimal $\mathbf{v}_i$ is in the null space of $\mathbf{Q}_i^{DL}$. Hence, $\mathbf{v}_i \in \mathcal{IA}^{UL}$.

Since both $\mathbf{w}_i$ and $\mathbf{v}_i$ stays within $\mathcal{IA}^{DL}$ and $\mathcal{IA}^{UL}$, interference alignment is a convergence point of *DBA* in high SNR.

Bibliography

[1] T. S. Rappaport, *Wireless Communications*. Prentice Hall, 1996.

[2] K. H. Teo, Z. Tao, and J. Zhang, "The mobile broadband WiMAX standard [standards in a nutshell]," *IEEE Signal Processing Magazine*, Sep. 2007.

[3] M. Bennis and J. Lilleberg, "Inter-Operator Resource Sharing for 3G Systems and Beyond," in *IEEE Ninth International Symposium on Spread Spectrum Techniques and Applications*, 2006.

[4] V. Heinonen, P. Pirinen, and J. Iinatti, "Capacity gains through inter-operator resource sharing in a cellular network," in *Proc. IEEE WPMC*, 2008.

[5] SAPHYRE, "D3.3a, SAPHYRE reference scenarios and interference models," December 2010.

[6] R. Stankiewicz, "Analytical Models of Selected DiffServ Network Elements Supporting Assured Forwarding," Ph.D. dissertation, AGH University of Science and Technology, 2007.

[7] J. Heinanen and R. Guerin, "A single rate three color marker," RFC2697 IETF, September 1999.

[8] J. Heinanen, T. Finland, and R. Guerin, "A two rate three color marker," IETF RFC2698, September 1999.

[9] J. Kidambi, D. Ghosal, and B. Mukherjee, "Dynamic token bucket (DTB): a fair bandwidth allocation algorithm for high-speed networks," in *Proc. Eight Int Computer Communications and Networks Conf*, 1999, pp. 24–29.

[10] E.-C. Park and C.-H. Choi, "Adaptive token bucket algorithm for fair bandwidth allocation in DiffServ networks," in *Proc. IEEE Global Telecommunications Conf. GLOBECOM '03*, vol. 6, 2003, pp. 3176–3180.

[11] W. Fang, N. Seddigh, and B. Nandy, "A time sliding window three colour marker (TSWTCM)," IETF RFC2859, June 2000.

[12] S. Floyd and V. Jacobson, "Random Early Detection (RED) gateways for Congestion Avoidance," *IEEE/ACM Transactions on Networking*, vol. 1(4), pp. 397–413, 1993.

[13] O. Elloumi and H. Afifi, "RED algorithm in ATM networks," in *Proc. IEEE ATM Workshop 1997*, 1997, pp. 312–319.

[14] T. J. Ott, T. V. Lakshman, and L. H. Wong, "SRED: stabilized RED," in *Proc. IEEE Eighteenth Annual Joint Conf. of the IEEE Computer and Communications Societies INFOCOM '99*, vol. 3, 1999, pp. 1346–1355.

[15] B. Zheng and M. Atiquzzaman, "DSRED: an active queue management scheme for next generation networks," in *Proc. 25th Annual IEEE Conf. LCN 2000*, 2000, pp. 242–251.

[16] W. K. Wong, H. Y. Tang, and V. C. M. Leung, "Token bank fair queuing: a new scheduling algorithm for wireless multimedia services," *Int. J. Commun. Syst.*, vol. 17, pp. 591–614, August 2004. [Online]. Available: http://portal.acm.org/citation.cfm?id=1067899.1067905

[17] H. S. Kim, E.-C. Park, and S. Weon, "A Token-Bucket Based Rate Control Algorithm with Maximum and Minimum Rate Constraints," *IEICE Transactions on Communications*, vol. E91-B, 2008.

[18] F. A. Bokhari, W. K. Wong, and H. Yanikomeroglu, "Adaptive Token Bank Fair Queuing Scheduling in the Downlink of 4G Wireless Multicarrier Networks," in *Proc. IEEE Vehicular Technology Conf. VTC Spring 2008*, 2008, pp. 1995–2000.

[19] W. K. Wong, H. Zhu, and V. C. M. Leung, "Soft QoS provisioning using the token bank fair queuing scheduling algorithm," *IEEE Wireless Communications Magazine*, vol. 10, no. 3, pp. 8–16, 2003.

[20] M. J. Fischer, D. A. Garbin, and D. M. B. Masi, "An Analytic Model for Static and Dynamic Token Buckets," *The Telecommunications Review, Noblis Publications*, vol. 4, pp. 27–32, 2008.

[21] G. Bolch, S. Greiner, H. de Meer, and K. S. Trivedi, *Queueing Networks and Markov Chains: Modeling and Performance Evaluation with Computer Science Applications*, 2nd ed. WileyBlackwell, May 2006. [Online]. Available: http://www.amazon.com/exec/obidos/redirect?tag=citeulike07-20\&path=ASIN/0471565253

[22] M. Viitanen, "Migrating from HSPA to HSPA+ and LTE," Mobile Broadband Outlook for the Americas, April 2010.

[23] RAD Data Communications, "Carrier ethernet: Service level agreement support tools," February 2009.

[24] P. Marshall, "Getting mobile backhaul to measure up," Sunrise Telecom, 2010. [Online]. Available: \url{http://www.sunrisetelecom.com/support/article_mibile_backhaul.php}

[25] R. Ahlswede, "The capacity region of a channel with two senders and two receivers," *Ann. Prob.*, vol. 2, pp. 805–814, 1974.

[26] A. Carleial, "Interference channel," *IEEE Trans. Inf. Theory*, vol. 24, pp. 60–70, Jan. 1978.

[27] T. S. Han and K. Kobayashi, "A new achievable rate region for the interference channel," *IEEE Transaction on Infomation Theory*, vol. 27, no. 1, pp. 49–60, January 1981.

[28] M. H. M. Costa, "On the Gaussian interference channel," *IEEE Trans. on Inf. Theory*, vol. 31, pp. 607–615, 1985.

[29] X. Shang, B. Chen, and M. J. Gans, "On the achievable sum rate for MIMO interference channels," *IEEE Trans. on Inf. Theory*, vol. 52, pp. 4313–4320, 2006.

[30] R. H. Etkin, D. N. C. Tse, and H. Wang, "Gaussian interference channel capacity to within one bit: the general case," *Proc. IEEE ISIT*, 2007.

[31] E. A. Jorswieck, E. G. Larsson, and D. Danev, "Complete characterization of the pareto boundary for the MISO interference channel," *IEEE Trans. Signal Process.*, vol. 56, pp. 5292–5296, Oct. 2008.

[32] R. Mochaourab and E. A. Jorswieck, "Optimal beamforming in interference networks with perfect local channel information," *IEEE Trans. on Signal Processing*, 2011, will appear.

[33] E. G. Larsson and E. A. Jorswieck, "The MISO interference channel: Competition versus collaboration," in *Proc. Allerton Conference on Communication, Control and Computing*, September 2007.

[34] J. Lindblom, E. G. Larsson, and E. A. Jorswieck, "Parametrization of the MISO IFC rate region: The case of partial channel state information," *IEEE Trans. Wireless Commun.*, vol. 9, pp. 500–504, Feb. 2010.

[35] M. A. Maddah-Ali, A. S. Motahari, and A. K. Khandani, "Communication over MIMO X channels: Interference alignmnet, decomposition and performance analysis," *IEEE Transactions on Information Theory*, vol. 54, no. 8, August 2008.

[36] K. S. Gomadam, V. R. Cadambe, and S. A. Jafar, "Approaching the capacity of wireless networks through distributed interference alignment," in *submitted to IEEE Transaction of Information Theory*, 2008, available at http://arxiv.org/pdf/0803.3816.

[37] S. W. Peters and R. W. Heath, "Cooperative algorithms for mimo interference channels," *submitted to IEEE Transactions on Vehicular Technology*, December 2009, available at http://arxiv.org/pdf/1002.0424v1.

[38] S. Ye and R. S. Blum, "Optimized signaling for MIMO interference systems with feedback," *IEEE Transactions on Signal Processing*, vol. 51, no. 11, Nov,2003.

[39] C. X. Shi, D. A. Schmidt, R. A. Berry, M. L. Honig, and W. Utschick, "Distributed interference pricing for the MIMO interference channel," in *IEEE ICC*, 2009.

[40] D. Gesbert, S. Hanly, H. Huang, S. Shamai, O. Simeone, and W. Yu, "Multi-cell MIMO cooperative networks: A new look at interference," *IEEE Journal on Selected Areas in Communications*, 2010, submitted in Jan 2010.

[41] A. Paulraj, R. Nabar, and D. Gore, *Introduction to Space-Time Wireless Communications*. Cambridge University Press, 2003.

[42] A. F. Molisch, *Wireless Communications*. IEEE, 2005.

[43] E. G. Larsson, E. A. Jorswieck, J. Lindblom, and R. Mochaourab, "Game theory and the flat fading gaussian interference channel," *IEEE Signal Process. Mag.*, vol. 26, pp. 18–27, Sep. 2009.

[44] J. Lindblom, E. Karipidis, and E. G. Larsson, "Selfishness and altruism on the MISO interference channel: The case of partial transmitter CSI," *IEEE Commun. Lett.*, vol. 13, pp. 667–669, Sep. 2009.

[45] E. Karipidis, A. Gründinger, J. Lindblom, and E. G. Larsson, "Pareto-optimal beamforming for the MISO interference channel with partial CSI," in *Proc. IEEE Int. Workshop on Computational Advances in Multi-Sensor Adaptive Proces. (CAMSAP)*, Aruba, Dec. 2009, pp. 13–16.

[46] Z. Ho and D. Gesbert, "Spectrum sharing in multiple antenna channels: A distributed cooperative game theoretic approach," in *Proc. IEEE Internat. Symp. on Personal, Indoor and Mobile Radio Communications (PIMRC)*, Cannes, France, Sep. 2008, pp. 1–5.

[47] R. Zakhour and D. Gesbert, "Coordination on the MISO interference channel using the virtual SINR framework," in *Proc. ITG Workshop on Smart Antennas (WSA)*, Berlin, Germany, Feb. 2009, pp. 16–18.

[48] R. Zakhour, Z. Ho, and D. Gesbert, "Spectrum sharing in multiple antenna channels: A distributed cooperative game theoretic approach," in *Proc. IEEE Vehicular Techn. Conf. (VTC)*, Barcelona, Spain, Apr. 2009, pp. 1–5.

[49] Y. Huang and D. P. Palomar, "Rank-constrained separable semidefinite programming with applications to optimal beamforming," *IEEE Trans. Signal Process.*, vol. 58, pp. 664–678, Feb. 2010.

[50] S. Saunders, S. Carlaw, A. Giustina, R. R. Bhat, V. S. Rao, and R. Siegberg, *Femtocells: Opportunities and Challenges for Business and Technology*. Wiley, 2009.

[51] P. Jiang, J. Bigham, and J. Wu, "Self-organizing relay stations in relay based cellular networks," *Comput. Commun.*, vol. 31, no. 13, pp. 2937–2945, 2008.

[52] A. Nosratinia, T. Hunter, and A. Hedayat, "Cooperative communication in wireless networks," *IEEE communications Magazine*, vol. 42, no. 10, pp. 74–80, 2004.

[53] A. Sendonaris, E. Erkip, and B. Aazhang, "User cooperation diversity. part i. system description," *IEEE Transactions on Communications*, vol. 51, no. 11, pp. 1927–1938, 2003.

[54] T. Cover and A. E. Gamal, "Capacity theorems for the relay channel," *IEEE Trans. Inf. Theory*, vol. IT-27, pp. 572–584, Sep. 1979.

[55] B. Song, F. Roemer, and M. Haardt, "Flexible Coordinated Beamforming (FlexCoBF) Algorithm for the Downlink of Multi-User MIMO Systems," in *Proc. ITG Workshop on Smart Antennas (WSA'10)*, Bremen, Germany, Feb. 2010, pp. 414–420.

[56] C. B. Chae, I. Hwang, R. W. Heath, and V. Tarokh, "Interference Aware-Coordinated Beamforming System in a Two-Cell Environment," *submitted to IEEE J. Sel. Areas Commun.*, 2009.

[57] F. Roemer and M. Haardt, "Algebraic Norm-Maximizing (ANOMAX) transmit strategy for Two-Way relaying with MIMO amplify and forward relays," *IEEE Sig. Proc. Lett.*, vol. 16, Oct. 2009.

[58] R. Vaze and R. W. H. Jr, "On the Capacity and Diversity Multiplexing Tradeoff of the Two-Way Relay channel," *submitted to IEEE Trans. Inf. Theory*, Oct. 2008.

[59] T. Unger and A. Klein, "Duplex schemes in multiple antenna two-hop relaying," *EURASIP Journal on Advanced Signal Process*, 2008.

[60] Q. H. Spencer, A. L. Swindlehurst, and M. Haardt, "Zero-forcing methods for downlink spatial multiplexing in multi-user mimo channels," *IEEE Transactions on Signal Processing*, vol. 52, pp. 461–471, Feb. 2004.

[61] V. Stankovic and M. Haardt, "Generalized design of multi-user mimo precoding matrices," *IEEE Transactions on Wireless Communications*, vol. 7, pp. 953–961, Mar. 2008.

[62] C. Jaeweon and Z. J. Haas, "On the throughput enhancement of the downstream channel in cellular radio networks through multihop relaying," *IEEE Journal on Selected Areas in Communications*, vol. 22, no. 7, pp. 1206–1219, September 2004.

[63] J. N. Laneman, D. N. C. Tse, and G. W. Wornell, "Cooperative diversity in wireless networks: Efficient protocols and outage behavior," *IEEE Transactions on Information Theory*, vol. 50, pp. 3062–3080, 2004.

[64] A. Sendonaris, E. Erkip, and B. Aazhang, "User cooperation diversity. part ii. implementation aspects and performance analysis," *IEEE Transactions on Communications*, vol. 51, no. 11, pp. 1939–1948, 2003.

[65] Y. Cao and B. Vojcic, "Mmse multiuser detection for cooperative diversity cdma systems," in *2004 IEEE Wireless Communications and Networking Conference, 2004. WCNC*, vol. 1, 2004.

[66] L. Venturino, X. Wang, and M. Lops, "Multiuser detection for cooperative networks and performance analysis," *IEEE Transactions on Signal Processing*, vol. 54, no. 9, pp. 3315–3329, 2006.

[67] M. Yang and P. Chong, "Uplink capacity analysis for multihop tdd-cdma cellular system," *IEEE Transactions on Communications*, vol. 57, no. 2, pp. 509–519, 2009.

[68] D. Gregoratti and X. Mestre, "Random DS/CDMA for the amplify and forward relay channel," *IEEE Transactions on Wireless CommunicationsCommunications*, vol. 8, no. 2, pp. 1017–1027, February 2009.

[69] R. Nabar, H. Bolcskei, and F. Kneubuhler, "Fading relay channels: Performance limits and space-time signal design," *IEEE Journal on Selected Areas in Communications*, vol. 22, no. 6, pp. 1099–1109, 2004.

[70] T. Ng, W. Yu *et al.*, "Joint optimization of relay strategies and resource allocations in cooperative cellular networks," *IEEE Journal on Selected Areas in Communications*, vol. 25, no. 2, p. 328, 2007.

[71] E. Calvo, J. Vidal, and J. R. Fonollosa, "Optimal resource allocation in relay-assisted cellular networks with partial csi," *IEEE Transactions on Signal Processing*, vol. 57, no. 7, pp. 2809–2823, July 2009.

[72] T. Basar and G. J. Olsder, *Dynamic Noncooperative Game Theory*, 2nd ed., ser. Classics In Applied Mathematics. SIAM, 1999.

[73] R. Myerson, *Game theory: analysis of conflict*. Harvard Univ Pr, 1997.

[74] S.Ulukus and R.D.Yates, "Iterative construction of optimum signature sequence sets in synchronous CDMA systems," *IEEE Transactions on Information Theory*, vol. 47, no. 5, pp. 1989–1998, July 2001.

[75] C. Rose, S. Ulukus, and R. Yates, "Wireless systems and interference avoidance," *IEEE Transactions on Wireless Communications*, vol. 1, no. 3, pp. 415–428, 2002.

[76] P. Anigstein and V. Anantharam, "Ensuring convergence of the MMSE iteration for interference avoidance to the global optimum," *IEEE Transactions on Information Theory*, vol. 9, no. 4, pp. 873–885, April 2003.

[77] S. Boyd and L. Vandenberghe, *Convex optimization*. Cambridge Univ Pr, 2004.

[78] A. U. T. Amah and A. Klein, "Pair-aware transceive beamforming for non-regenerative multi-user two-way relaying," in *Proc. IEEE Int. Conf. on Acoustics, Speech, and Signal Processing (ICASSP)*, Dallas, TX, Mar. 2010.

[79] E. Yilmaz, R. Zakhour, D. Gesbert, and R. Knopp, "Multi-pair two-way relay channel with multiple antenna relay station," in *Proc. IEEE Int. Conf. on Communications (ICC 2010)*, Cape Town, South Africa, May 2010.

[80] B. Song and M. Haardt, "Achievable throughput approximation for rbd precoding at high snrs," in *Proc. IEEE Int. Conf. on Acoustics, Speech, and Signal Processing (ICASSP)*, Taipei, Taiwan, Apr. 2009.

[81] F. Roemer and M. Haardt, "A low-complexity relay transmit strategy for two-way relaying with MIMO amplify and forward relays," in *Proc. IEEE Int. Conf. Acoustics, Speech and Sig. Proc. (ICASSP 2010)*, Dallas, TX, Mar. 2010.

[82] J. Joung and A. H. Sayed, "Multiuser two-way amplify-and-forward relay processing and power control methods for beamforming systems," *IEEE Transactions on Signal Processing*, vol. 58, pp. 1833–1846, Mar. 2010.

[83] D. Lee, Y. S. Jung, and J. H. Lee, "Amplify-and-forward cooperative transmission with multiple relays using phase feedback," in *Proc. VTC-2006 Fall Vehicular Technology Conference 2006 IEEE 64th*, Sep. 25–28, 2006, pp. 1–5.

[84] E. Yilmaz and M. O. Sunay, "Amplify-and-forward capacity with transmit beamforming for MIMO multiple-relay channels," in *Proc. IEEE Global Telecommunications Conference GLOBECOM '07*, Nov. 26–30, 2007, pp. 3873–3877.

[85] I. Krikidis, J. Thompson, S. Mclaughlin, and N. Goertz, "Max-min relay selection for legacy amplify-and-forward systems with interference," *IEEE Journal on Wireless Communications*, vol. 8, no. 6, pp. 3016–3027, Jun. 2009.

[86] A. Bletsas, H. Shin, and M. Z. Win, "Outage analysis for co-operative communication with multiple amplify-and-forward relays," *Electronics Letters*, vol. 43, no. 6, pp. 51–52, Mar. 2007.

[87] S. O. Gharan, A. Bayesteh, and A. K. Khandani, "Diversity-multiplexing tradeoff in multiple-relay network - Part I: Proposed scheme and single-antenna networks," in *Proc. Allerton*, 2008.

[88] ——, "Diversity-multiplexing tradeoff in multiple-relay network - Part II: Multiple-antenna networks," in *Proc. Allerton*, 2008.

[89] X. Tang and Y. Hua, "Optimal design of non-regenerative MIMO wireless relays," *IEEE Transactions on Wireless Communications*, vol. 6, pp. 1398–1407, 2007.

[90] W. Guan, H. Luo, and W. Chen, "Linear relaying scheme for MIMO relay system with QoS requirements," *IEEE Signal Processing Letters*, vol. 15, pp. 697–700, 2008.

[91] E. Jorswieck and A. Sezgin, "Transmit strategies for the MIMO two-way amplify-forward channel with multiple relays and MMSE receiver," in *Proc. IEEE Int. Conf. Acoustics, Speech and Sig. Proc. (ICASSP 2010)*, Dallas, TX, 2010.